

MASTER

APAE NO. 54

Copy No. 21

AEC Research and
Development Report
UC-81, Reactors-Power
(Special Distribution)

SM-2 CRITICAL EXPERIMENTS

CE-1



ALCO PRODUCTS, INC.

NUCLEAR POWER ENGINEERING DEPARTMENT
P. O. BOX 414, SCHENECTADY 1, N. Y.

DISCLAIMER

This report was prepared as an account of work sponsored by an agency of the United States Government. Neither the United States Government nor any agency Thereof, nor any of their employees, makes any warranty, express or implied, or assumes any legal liability or responsibility for the accuracy, completeness, or usefulness of any information, apparatus, product, or process disclosed, or represents that its use would not infringe privately owned rights. Reference herein to any specific commercial product, process, or service by trade name, trademark, manufacturer, or otherwise does not necessarily constitute or imply its endorsement, recommendation, or favoring by the United States Government or any agency thereof. The views and opinions of authors expressed herein do not necessarily state or reflect those of the United States Government or any agency thereof.

DISCLAIMER

Portions of this document may be illegible in electronic image products. Images are produced from the best available original document.

APAE NO. 54
Copy No. 21
AEC Research and
Development Report
UC-81, Reactor-Power
(Special Distribution)

SM-2 CRITICAL EXPERIMENTS

CE-1

J. W. Noaks
W. J. McCool
R. A. Robinson
E. W. Schrader
S. H. Weiss

Approved by: J. W. Noaks, Supv., Criticality Facility

Issued: November 30, 1959

Contract No. AT(30-3)-326

With U. S. Atomic Energy Commission

New York Operations Office

ALCO PRODUCTS, INC.
Post Office Box 414
Schenectady 1, N. Y.

AEC LEGAL NOTICE

This report was prepared as an account of Government sponsored work. Neither the United States, nor the Commission, nor any person acting on behalf of the Commission:

A. Makes any warranty or representation, expressed or implied, with respect to the accuracy, completeness, or usefulness of the information contained in this report, or that the use of any information, apparatus, method, or process disclosed in this report may not infringe privately owned rights: or

B. Assumes any liabilities with respect to the use of, or for damages resulting from the use of any information, apparatus, method, or process disclosed in this report.

As used in the above, "person acting on behalf of the Commission" includes any employee or contractor of the Commission, or employee of such contractor, to the extent that such employee or contractor of the Commission, or employee of such contractor prepares, disseminates, or provides access to, any information pursuant to this employment or contract with the Commission, or his employment with such contractor.

ALCO LEGAL NOTICE

This report was prepared by Alco Products, Incorporated in the course of work under, or in connection with, Contract No. AT(30-3)-326, issued by U. S. Atomic Energy Commission, New York Operations Office and subject only to the rights of the United States, under the provisions of this contract, Alco Products, Incorporated makes no warranty or representation, express or implied, and shall have no liability with respect to this report or any of its contents or with respect to the use thereof or with respect to whether any such use will infringe the rights of others.

DISTRIBUTION

COPIES

1 - 2

New York Operations Office
U. S. Atomic Energy Commission
376 Hudson Street
New York 14, N. Y.

Attention: Chief, Army Reactor Branch

3 - 5

U. S. Atomic Energy Commission
Army Reactors Branch
Division of Reactor Development
Washington 25, D. C.

Attention: Chief, Water Systems Project Branch
Office Asstt. Director (Army Reactors)

6

U. S. Atomic Energy Commission
Chief, Patents Branch
Washington 25, D. C.

Attention: Roland A. Anderson

7

U. S. Atomic Energy Commission
Chief, New York Patent Group
Brookhaven National Laboratory
Upton, N. Y.

Attention: Harmon Potter

8

U. S. Atomic Energy Commission
Idaho Operations Office
Phillips Petroleum Company, NRTS
Technical Library
P. O. Box 1250
Idaho Falls, Idaho

Attention: Technical Liaison Officer,
Army Reactors

9 - 11

Nuclear Power Field Office
USAERDL
Fort Belvoir, Virginia

Attention: Chief, Nuclear Power Field Office

DISTRIBUTION (Cont'd)

COPIES

12 Union Carbide Nuclear Corporation
Oak Ridge National Laboratory
Y-12 Building 9704-1
P. O. Box "Y"
Oak Ridge, Tennessee

Attention: A. L. Boch

13 District Engineer, Alaska District
U. S. Army Corps of Engineers
P. O. Box 7002
Anchorage, Alaska

Attention: NPAVO-N

14 The Martin Company
P. O. Box 5042
Middle River, Maryland

Attention: AEC Contract Document Custodian

15 Combustion Engineering, Inc.
P. O. Box 2558
Idaho Falls, Idaho

Attention: Mr. W. B. Allred, Project Mgr. SL-1

16 - 41 U. S. Atomic Energy Commission
Reference Branch
Technical Information Service Extension
P. O. Box 62
Oak Ridge, Tennessee

42 - 80 ALCO PRODUCTS, INC.
Post Office Box 414
Schenectady, N. Y.

Attention:

43 K. Kasschau

44 - 45 J. W. Noaks

DISTRIBUTION (Cont'd)

COPIES

| | |
|---------|-----------------|
| 46 | W. J. McCool |
| 47 | E. Schrader |
| 48 | R. A. Robinson |
| 49 | S. Weiss |
| 50 | J. G. Gallagher |
| 51 | P. Bohe |
| 52 | B. Byrne |
| 53 - 80 | File |

THIS PAGE
WAS INTENTIONALLY
LEFT BLANK

ABSTRACT

Critical experiment studies were performed, varying the parameters U^{235} , B^{10} and metal to water ratio, in the SM-2 7 x 7 core configuration with 38 stationary elements and seven control rods of the SM-1 (APPR-1) type.

An experimental mock-up of the SM-1 was assembled using the basic SM-2 fuel plates. Excellent agreement between the SM-1 boron loading, determined by chemical analysis, and the SM-1 mock-up boron loading, for equivalent bank positions, was noted.

Several SM-2 mock-ups, cold clean and midlife, were assembled and studied with regard to reflector effects, flow divider effects, relative control rod array worths, critical rod configurations, and relative power distributions.

The results of these experiments indicate as satisfactory a U^{235} loading of 36.4 K_g and a B^{10} loading of 63.4 grams for the SM-2. Attention is drawn to numerous power peaks present in the active core. The open seven control rod array has a slight reactivity advantage over the closed seven array and consequent minor disadvantage with respect to "stuck rod" criteria.

THIS PAGE
WAS INTENTIONALLY
LEFT BLANK

TABLE OF CONTENTS

| | <u>PAGE</u> |
|--|-------------|
| ABSTRACT ----- | vii |
| SUMMARY ----- | 1 |
| INTRODUCTION ----- | 3 |
| CHAPTER 1 - SYSTEM DESCRIPTION | |
| 1.1 Introduction ----- | 5 |
| 1.2 Experimental Assembly ----- | 5 |
| 1.2.1 Core Support Assembly ----- | 5 |
| 1.2.2 Control Rod Assembly ----- | 5 |
| 1.2.3 Fuel Element Structure ----- | 13 |
| 1.2.4 Steel Reflector Assembly ----- | 13 |
| 1.3 Experimental Techniques ----- | 13 |
| 1.3.1 Method of Loading Uniform Burnable Poison - | 13 |
| 1.3.2 Reactivity Coefficients of Uranium ----- | 21 |
| 1.4 Nomenclature and Explanations ----- | 21 |
| 1.5 Criticality Safety Data ----- | 25 |
| CHAPTER 2 - PARAMETER STUDIES | |
| 2.1 Introduction ----- | 25 |
| 2.2 Experimental Techniques ----- | 25 |
| 2.2.1 Procedure ----- | 25 |
| 2.2.2 Fuel Plate Arrangements ----- | 25 |
| 2.2.3 Metal to Water Ratio ----- | 27 |
| 2.2.4 Boron Loadings ----- | 27 |
| 2.3 Seven Rod Bank vs. Mass of U^{235} and Worth ----- | 31 |
| 2.3.1 Seven Rod Bank vs Mass of U^{235} ----- | 31 |
| 2.3.2 Seven Rod Bank Calibration ----- | 35 |

TABLE OF CONTENTS (Cont'd)

| | <u>PAGE</u> |
|---|-------------|
| 2.4 Excess K (ΔK_E) - - - - - | 51 |
| 2.4.1 Integration of Calibration Curves - - - - - | 51 |
| 2.4.2 ΔK_E Versus Mass of U^{235} in Active Core - - | 51 |
| 2.4.3 ΔK_E Versus Mass of B^{10} in Active Core for SM-2 Configuration - - - - - | 51 |
| 2.5 Data Evaluation - - - - - | 51 |
| 2.5.1 ΔK_E Versus Mass of B^{10} in Active Core for SM-2 Configuration - - - - - | 51 |
| 2.5.2 Final SM-2 Mockup - - - - - | 57 |

CHAPTER 3 - SM-1 MOCKUP EXPERIMENTS

| | |
|---|----|
| 3.1 Introduction - - - - - | 59 |
| 3.2 Preliminary SM-1 Mockup - - - - - | 60 |
| 3.3 Final SM-1 Mockup - - - - - | 60 |
| 3.3.1 Reactivity Evaluation - - - - - | 60 |
| 3.3.2 Uranium Worth Measurements - - - - - | 60 |
| 3.3.3 Boron Worth Measurements - - - - - | 65 |
| 3.3.4 Substitution Measurements - - - - - | 66 |
| 3.4 Experimental Technique Evaluation - - - - - | 66 |
| 3.4.1 Heterogeneity Measurements - - - - - | 66 |
| 3.4.2 Boron Standard - - - - - | 67 |
| 3.5 Experimental Evaluation of Boron in SM-1 Core I - - - | 67 |
| 3.5.1 Procedure - - - - - | 67 |
| 3.5.2 Data Compilation - - - - - | 73 |
| 3.5.3 Comparison of Results with Chemical Analysis | 73 |

CHAPTER 4 - SM-2 MOCKUP REACTIVITY EXPERIMENTS

| | |
|------------------------------------|----|
| 4.1 Introduction - - - - - | 75 |
| 4.1.1 Preliminary Mockup - - - - - | 75 |
| 4.1.2 Final Mockup - - - - - | 75 |

TABLE OF CONTENTS (Cont'd)

| | <u>PAGE</u> |
|--|-------------|
| 4.2 Seven Rod Bank Evaluation - - - - - | 79 |
| 4.2.1 Bank Calibration - - - - - | 79 |
| 4.2.2 Integral Worth - - - - - | 79 |
| 4.2.3 Data Evaluation - - - - - | 79 |
| 4.3 Temperature Coefficients - - - - - | 89 |
| 4.3.1 Experimental Technique - - - - - | 89 |
| 4.3.2 Experimental Data - - - - - | 90 |
| 4.3.3 Discussion of Results - - - - - | 92 |
| 4.4 Core Material Coefficients - - - - - | 99 |
| 4.4.1 Experimental Technique - - - - - | 99 |
| 4.4.2 Boron Reactivity Coefficients - - - - - | 105 |
| 4.4.3 Uranium Reactivity Coefficients - - - - - | 105 |
| 4.4.4 Polystyrene Measurements - - - - - | 106 |
| 4.4.5 Conclusions - - - - - | 106 |
| 4.5 Reflector Measurements - - - - - | 106 |
| 4.5.1 Preliminary Mockup - Open 7 and Closed 7 Array | 106 |
| 4.5.2 Final Mockup - Open 7 Array - - - - - | 107 |
| 4.6 Control Rod Array Evaluation - - - - - | 113 |
| 4.7 Critical Control Rod Configurations - - - - - | 114 |
| 4.8 Miscellaneous Reactivity Measurements - - - - - | 115 |
| 4.8.1 Effect of Rotating Elements - - - - - | 115 |
| 4.8.2 Effect of Substituting Stationary Elements for Control Rods - - - - - | 115 |
| CHAPTER 5 - SM-2 MOCKUP NEUTRON FLUX MEASUREMENTS | |
| 5.1 Introduction - - - - - | 117 |
| 5.2 Axial Traverses - - - - - | 123 |
| 5.2.1 Water Reflected - - - - - | 123 |
| 5.2.2 Steel Reflected - - - - - | 123 |

TABLE OF CONTENTS (Cont'd)

| | <u>PAGE</u> |
|---|-------------|
| 5.3 Core Average - - - - - | 123 |
| 5.4 Local Flux Distributions - - - - - | 153 |
| 5.4.1 Water Reflection - - - - - | 153 |
| 5.4.2 Laminated Steel Reflection - - - - - | 153 |
| 5.5 Core-Reflector Interface Flux Distribution - - - - - | 153 |
| 5.6 Conclusions - - - - - | 153 |
| CHAPTER 6 - SM-2 MIDLIFE MOCKUP EXPERIMENTS | |
| 6.1 Introduction - - - - - | 165 |
| 6.2 Preliminary SM-2 Midlife Mockup - - - - - | 165 |
| 6.2.1 Flow Divider - - - - - | 166 |
| 6.2.2 Reflector Measurements - - - - - | 166 |
| 6.2.3 Critical Rod Configurations - - - - - | 173 |
| 6.2.4 Flux Measurements - - - - - | 174 |
| 6.3 Final SM-2 Midlife Mockup - - - - - | 175 |
| 6.3.1 Critical Rod Configurations - - - - - | 175 |
| REFERENCES - - - - - | 177 |
| APPENDIX A - CORE LOADING COMPOSITIONS - - - - - | A-1 |
| APPENDIX B - CHEMICAL ANALYSIS OF CORE MATERIALS - - - - - | B-1 |
| APPENDIX C - PROBABLE ERROR ANALYSIS - - - - - | C-1 |
| APPENDIX D - EFFECT OF DELAYED NEUTRON UNCERTAINTIES ON REACTIVITY REPORTED IN DOLLARS AND CENTS - - - - - | D-1 |

LIST OF FIGURES

| FIGURE | TITLE | PAGE |
|--------|--|------|
| 1. 1 | Core Support Structure - - - - - | 7 |
| 1. 2 | SM-2 Core in Reactor Tank - - - - - | 9 |
| 1. 3 | Control Rod Assembly - - - - - | 11 |
| 1. 4 | Stationary Fuel Element - - - - - | 15 |
| 1. 5 | Control Rod Fuel Element - - - - - | 17 |
| 1. 6 | Boron Tape Applicator - - - - - | 19 |
| 2. 1 | Metal to Water Ratio vs. Loaded U^{235} - - - - - | 29 |
| 2. 2 | Seven Rod Bank Critical Position vs. Mass of U^{235} in Active Core - - - - - | 33 |
| 2. 3 | Seven Rod Bank Calibration - 0.0 gm B^{10} per $K_E U^{235}$ - - - - - | 37 |
| 2. 4 | Seven Rod Bank Calibration - 1.305 gm B^{10} per $K_E U^{235}$ - - - - - | 41 |
| 2. 5 | Seven Rod Bank Calibration - 2.610 gm B^{10} per $K_E U^{235}$ - - - - - | 45 |
| 2. 6 | Seven Rod Bank Calibration - 0.456 gm B^{10} per $K_E U^{235}$ - - - - - | 49 |
| 2. 7 | ΔK_E vs. Mass of U^{235} in Active Core - - - - - | 53 |
| 2. 8 | ΔK_E vs. Mass of B^{10} in Active Core for SM-2 Configura- tion - - - - - | 55 |
| 3. 1 | SM-1 Five Rod Bank Calibration - - - - - | 61 |
| 3. 2 | Integral SM-1 Five Rod Bank Worth vs. Bank Position - - - - - | 63 |
| 3. 3 | ΔK_E vs. Number of Fuel Bundles - - - - - | 69 |
| 3. 4 | Areal Density of B^{10} vs. Reactivity in Cents - - - - - | 71 |
| 4. 1 | Full Reflector of SM-2 Mockup - - - - - | 77 |
| 4. 2 | Composite 7 Rod Bank Calibration - - - - - | 81 |
| 4. 3 | Seven Rod Bank Calibration with Aluminum - - - - - | 83 |
| 4. 4 | Integral 7 Rod Bank Worth - - - - - | 85 |
| 4. 5 | ΔK_E versus Mass of B^{10} in Active Core - - - - - | 87 |
| 4. 6 | Seven Rod Bank Critical Position vs. Heating Temperature - - - - - | 93 |
| 4. 7 | Seven Rod Bank Critical Position vs. Aluminum Equivalent Temperature at 2000 psia - - - - - | 95 |
| 4. 8 | ΔK_E versus Temperature - - - - - | 97 |
| 4. 9 | ΔK_E versus Equivalent Temperature at 2000 psi - - - - - | 101 |
| 4. 10 | ΔK_E versus Void Volume Fraction in Core - - - - - | 103 |
| 4. 11 | Laminated Steel Reflector Assembly - - - - - | 109 |
| 4. 12 | ΔK_E vs. Laminated Steel Reflector Thickness - - - - - | 111 |
| 5. 1 | Instrumented Fuel Plate - - - - - | 119 |
| 5. 2 | Location of Radial Planes - - - - - | 121 |
| 5. 3 | Axial Bare Gold Traverse with Infinite Water Reflector - - - - - | 129 |
| 5. 4 | Axial Bare Gold Traverse with Infinite Water Reflector - - - - - | 131 |
| 5. 5 | Axial Traverses with Laminated Steel Reflector - - - - - | 141 |
| 5. 6 | Axial Traverses with Laminated Steel Reflector - - - - - | 143 |
| 5. 7 | Axial Cadmium Covered Uranium Traverses with Laminated Steel Reflector - - - - - | 145 |

LIST OF FIGURES (Cont'd)

| <u>FIGURE</u> | <u>TITLE</u> | <u>PAGE</u> |
|---------------|---|-------------|
| 5.8 | Fuel Element Mapping - - - - - | 147 |
| 5.9 | Element Averages - Water Reflector - - - - - | 149 |
| 5.10 | Element Averages - Laminated Steel Reflector - - - - - | 151 |
| 5.11 | Radial Bare Uranium Traverses with Water Reflector - - - - - | 155 |
| 5.12 | Radial Bare Uranium Traverses with Laminated Steel Reflector - - - - - | 157 |
| 5.13 | Girdle Neutron Flux - Water Reflected - - - - - | 159 |
| 5.14 | Girdle Neutron Flux - 1/8 inch Skirt - - - - - | 161 |
| 5.15 | Girdle Neutron Flux - 1/4 inch Skirt - - - - - | 163 |
| 6.1 | Flow Divider Location - - - - - | 167 |
| 6.2 | ΔK_E vs. Flow Divider Thickness - - - - - | 169 |
| 6.3 | ΔK_E vs. Laminated Steel Reflector Thickness - - - | 171 |

LIST OF TABLES

| TABLE | TITLE | PAGE |
|-------|--|------|
| 2. 1 | Stationary Fuel Plate Arrangement in Parameter Studies - - - - - | 26 |
| 2. 2 | Control Rod Fuel Plate Arrangement in Parameter Studies - - - - - | 26 |
| 2. 3 | Variation of Metal to Water Ratio with Loaded U ²³⁵ Mass - - - - - | 27 |
| 2. 4 | Boron Loadings - - - - - | 31 |
| 2. 5 | Seven Rod Bank Critical Position vs. Mass of U ²³⁵ in Active Core - - - - - | 31 |
| 2. 6 | Seven Rod Bank Position vs. Seven Rod Bank Worth for 0. 0 gm B ¹⁰ per Kg U ²³⁵ - - - - - | 35 |
| 2. 7 | Seven Rod Bank Position vs. Seven Rod Bank Worth for 1. 305 gm B ¹⁰ per Kg U ²³⁵ - - - - - | 39 |
| 2. 8 | Seven Rod Bank Position vs. Seven Rod Bank Worth for 2. 610 gm B ¹⁰ per Kg U ²³⁵ - - - - - | 43 |
| 2. 9 | Seven Rod Bank Position vs. Seven Rod Bank Worth for 0. 456 gm B ¹⁰ per Kg U ²³⁵ - - - - - | 47 |
| 3. 1 | Summary of SM-1 Experiments at ALCO - - - - - | 59 |
| 3. 2 | U ²³⁵ Worth for Various Element Positions - - - - - | 65 |
| 3. 3 | B ¹⁰ Worth for Various Element Positions - - - - - | 66 |
| 3. 4 | Mylar Tape Loadings - - - - - | 67 |
| 3. 5 | Factors in Boron Determination - - - - - | 73 |
| 4. 1 | Heating Measurements - - - - - | 90 |
| 4. 2 | Aluminum Measurements - - - - - | 91 |
| 4. 3 | Seven Rod Bank Calibration - - - - - | 92 |
| 4. 4 | Temperature Coefficients - - - - - | 99 |
| 4. 5 | Reactivity Coefficients of Boron 10 - - - - - | 105 |
| 4. 6 | Reactivity Coefficients of U ²³⁵ - - - - - | 106 |
| 4. 7 | Reflector Effects vs. Control Rod Array - - - - - | 107 |
| 4. 8 | Effect of Varying Reflector Thickness for the Open 7 Control Rod Array - - - - - | 113 |
| 4. 9 | Critical Bank Position vs. Control Rod Array - - - - - | 113 |
| 4. 10 | Critical Rod Configurations - Open 7 Array - - - - - | 114 |
| 4. 11 | Critical Rod Configurations - Closed 7 Array - - - - - | 114 |
| 4. 12 | Effect of Substituting Stationary Fuel Elements for Control Rods - - - - - | 115 |
| 5. 1 | Axial Flux Traverses with Water Reflector -Bare Gold Activity - - - - - | 124 |
| 5. 2 | Axial Flux Traverses with Water Reflector - Bare Gold Activity - - - - - | 124 |

LIST OF TABLES (Cont'd)

| <u>TABLE</u> | <u>TITLE</u> | <u>PAGE</u> |
|--------------|--|-------------|
| 5. 3 | Axial Flux Traverses with Water Reflector - Bare Gold Activity - - - - - | 125 |
| 5. 4 | Axial Flux Traverses with Water Reflector - Element 42 - - | 125 |
| 5. 5 | Axial Flux Traverses with Water Reflector - Element 43 - - | 126 |
| 5. 6 | Axial Flux Traverses with Water Reflector Bare Uranium in Element 43 - - - - - | 126 |
| 5. 7 | Axial Flux Traverses with Water Reflector - Bare Uranium Foils in Control Rod C - - - - - | 127 |
| 5. 8 | Neutron Flux Measurements with Water Reflector - Bare Uranium Foils in 5 inch Axial Plane - - - - - | 128 |
| 5. 9 | Axial Flux Traverses with Laminated Steel Reflector - - - - | 133 |
| 5. 10 | Axial Flux Traverses with Laminated Steel Reflector - - - - | 134 |
| 5. 11 | Axial Flux Traverses with Laminated Steel Reflector - - - - | 135 |
| 5. 12 | Axial Flux Traverses with Laminated Steel Reflector - Element 42 - - - - - | 137 |
| 5. 13 | Axial Flux Traverses with Laminated Steel Reflector - Element 43 - - - - - | 139 |
| 5. 14 | Axial Flux Traverses with Laminated Steel Reflector - Control Rod C - - - - - | 140 |
| 6. 1 | Seven Rod Bank Calibration - - - - - | 165 |
| 6. 2 | Flow Divider Measurements - - - - - | 166 |
| 6. 3 | ΔK_E for Various Laminated Steel Reflectors - - - - - | 173 |
| 6. 4 | Preliminary SM-2 Midlife Critical Rod Configurations - - - - | 174 |
| 6. 5 | SM-2 Midlife Final Mockup Critical Rod Configurations - - - - | 175 |
| 6. 6 | Calibration of Control Rods - - - - - | 176 |

SUMMARY

The cold clean water-reflected final SM-2 mockup containing 33.2 kilograms U^{235} and 55.6 grams B^{10} distributed uniformly in the active core maintained criticality after a seven rod bank withdrawal of 7.142 inches and has an "excess K" (ΔK_E) of 1520 cents. A flow divider and an infinite steel-water laminated reflector respectively are worth approximately -96. and \neq 85 cents. The measured reactivity coefficient, @ 2000 psi, ranges from -1.15 cents/ $^{\circ}F$ @ 150 $^{\circ}F$ to -5.20 cents/ $^{\circ}F$ @ 510 $^{\circ}F$. The integral reactivity effect of raising the SM-2 core water temperature from 103 $^{\circ}F$ to 510 $^{\circ}F$ @ 2000 psi and the water in the reflector coolant graph from 103 $^{\circ}F$ to 477 $^{\circ}F$ @ 2000 psi is -889.7 cents. The average measured material coefficients for U^{235} and B^{10} are 0.157 cents/gm and 42.54 cents/gm respectively. Without the benefit of flux suppressors the maximum to average power ratio of 7.28 occurs at the top of the fuel section of control rod C (withdrawn to 7.14 inches), and a ratio of 5.28 occurs at the bottom of stationary element 43 and symmetric elements. The open seven control rod array controls slightly more reactivity than the closed seven and consequently is at a slight disadvantage in meeting "stuck rod" criteria.

At room conditions a minimum loading of 7.5 grams of B^{10} uniformly distributed in the active SM-2 core is required to maintain a subcritical condition with the open 7 control rod array fully inserted.

An estimated loading of 15.84 \pm 0.38 grams of B^{10} in the SM-1 Core I was obtained by substitution methods utilizing an assembly of known composition. This represents a boron loss of 22.0 \pm 1.9% from the specified 20.29 grams.

THIS PAGE
WAS INTENTIONALLY
LEFT BLANK

INTRODUCTION

The critical experiments described in this report were required as part of the SM-2 Core and Vessel Development Program performed under AEC Contract No. AT (30-3)-326. Initially, these experiments consisted of a series of parametric studies designed to define some critical characteristics of stainless steel-UO₂ matrix fuel plates and to verify the analytically determined uranium and boron burnable-poison loadings for the SM-2 core. Detailed mock-ups of the SM-1 core were then assembled to study the reliability of the experimental and assembly techniques and concurrently to provide an estimate of the actual SM-1 boron loading. The final experiments were performed on mockups of the SM-2 midlife and initial core compositions for the purpose of investigating the power producing and control characteristics of the reactor.

This report includes the results of all these critical experiments, originally proposed as Tasks 7.0 and 9.0 of the SM-2 Core and Vessel Development Program. The body of the report presents tabulated reduced data and numerous graphs. All data points are associated with core reference loading numbers which define the core compositions for each specific experiment. An extensive description of core composition corresponding to each core reference loading number is presented in Appendix A to permit an exact analytic duplication of all cores studied.

Wherever possible an error analysis has been performed to define the limits of reliability of core composition and experimental data.

THIS PAGE
WAS INTENTIONALLY
LEFT BLANK

CHAPTER 1 - SYSTEM DESCRIPTION

1.1 Introduction

The SM-2 critical experiments were conducted at the Alco Products, Inc., Criticality Facility ⁽¹⁾ in Schenectady, N. Y. A detailed description of the experimental assembly and its relationships to this Facility is presented in the Hazards Summary Report for the SM-2 Critical Experiments ⁽²⁾ together with descriptions of the basic experimental techniques.

The content of this chapter includes a general description of the experimental techniques and core assembly and a summary of preliminary criticality safety data. System nomenclature is also defined for the reader's convenience.

1.2 Experimental Assembly

1.2.1 Core Support Assembly

The core support assembly consists of a three-tiered stainless steel table located over the center of the reactor tank floor at the Facility. Structural support, alignment, and position of the assembly are assured by tie rods and spacers as shown in Figure 1.1.

The core support has the potential of accommodating reactor cores with a total of 89 fuel elements and control rods, although a maximum of only 38 fuel elements and seven control rods were required for the 7 x 7 SM-2 array. Figure 1.2 shows the assembled SM-2 in place in the reactor tank with associated nuclear instrumentation.

1.2.2 Control Rod Assembly

Reactor control is maintained by the insertion or withdrawal of control rod assemblies, Figure 1.3, containing both nuclear fuel and box type boron absorbers. The control rod assemblies are driven by overhead drives and drop by gravity on scram. Guide rods and dashpot plungers to act as guides and decelerative devices respectively are attached to the ends of the control rod baskets.

THIS PAGE
WAS INTENTIONALLY
LEFT BLANK



7

THIS PAGE
WAS INTENTIONALLY
LEFT BLANK

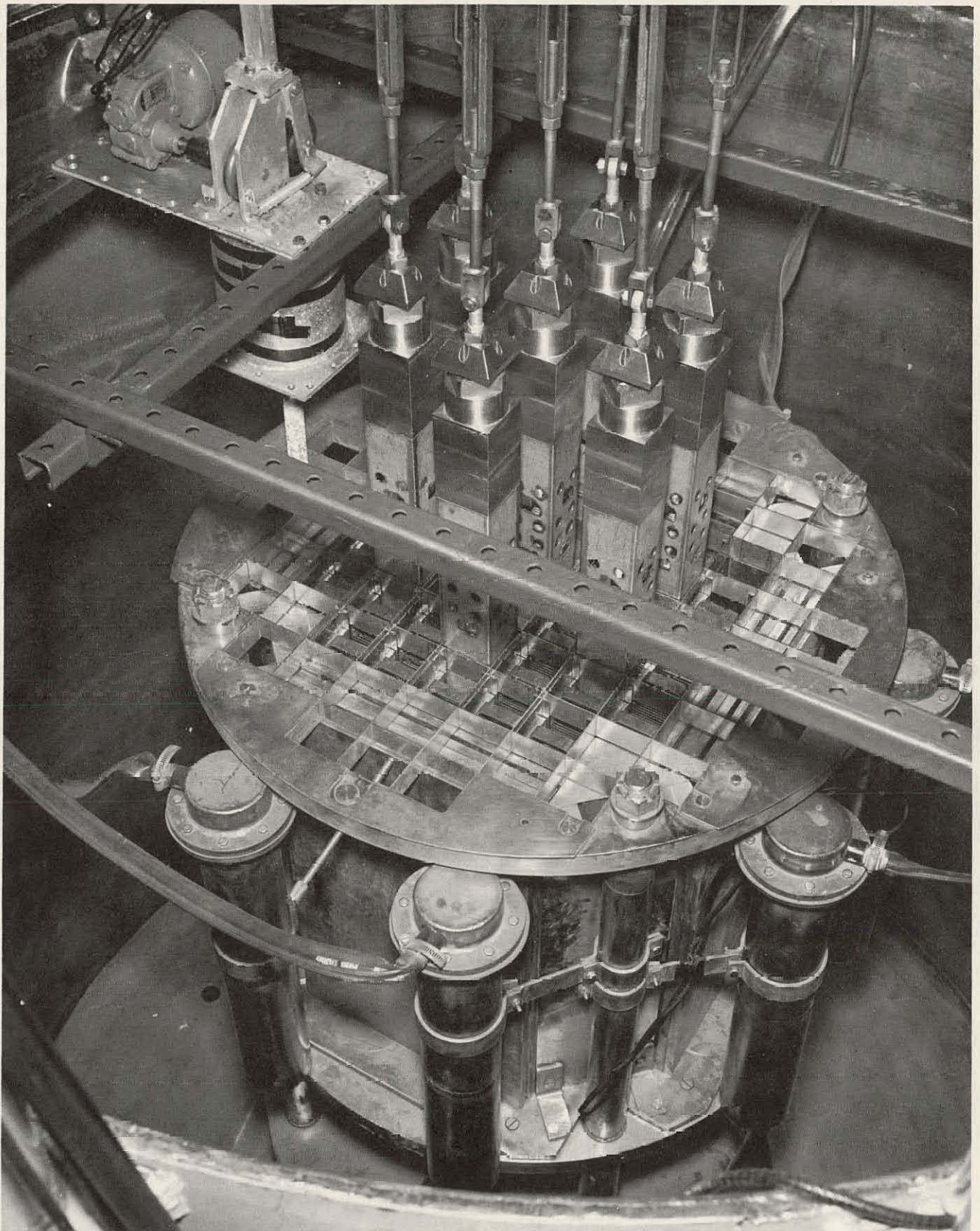


FIG. 1.2 - SM-2 CORE IN REACTOR TANK

THIS PAGE
WAS INTENTIONALLY
LEFT BLANK

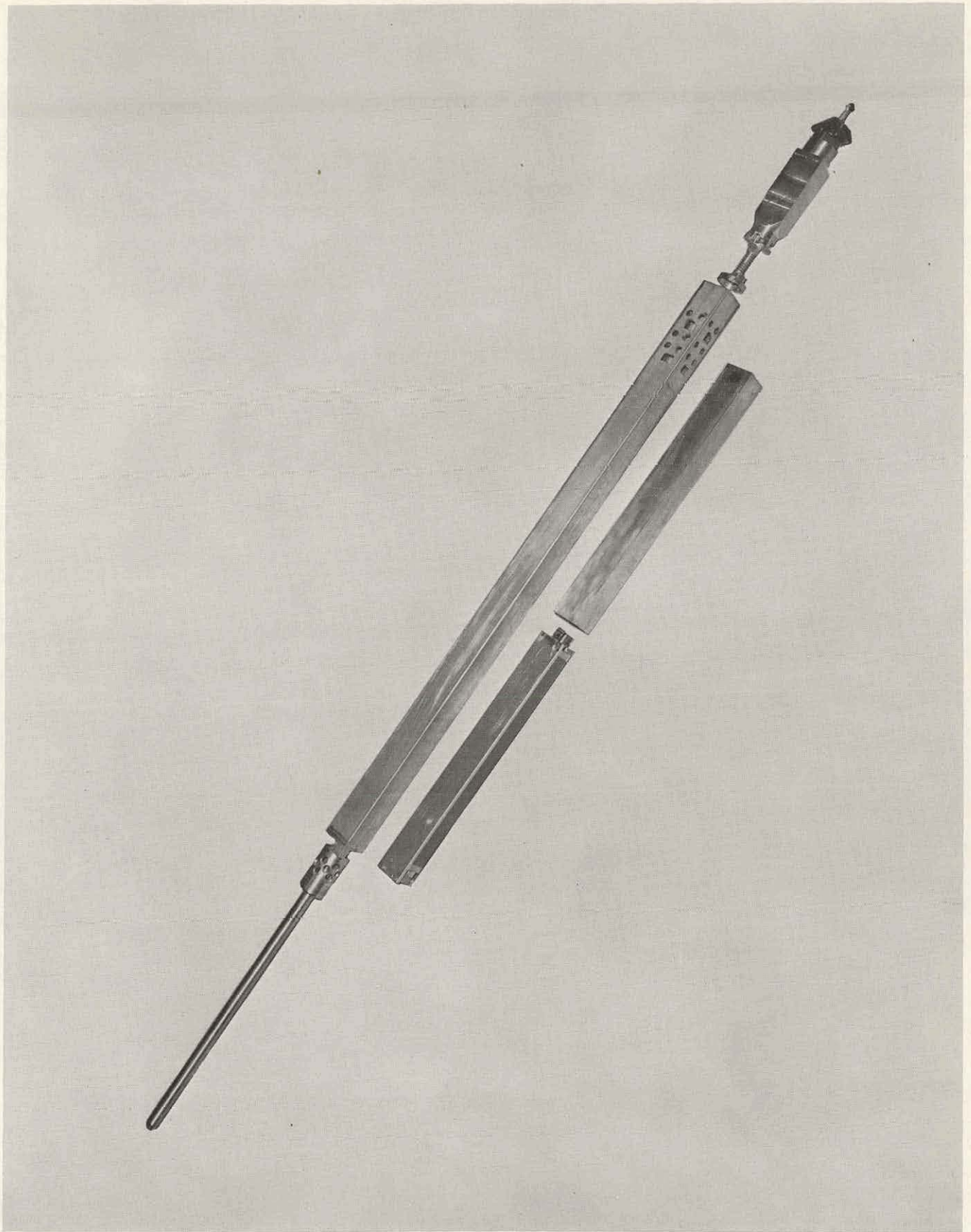


FIG. 1.3 - CONTROL ROD ASSEMBLY

THIS PAGE
WAS INTENTIONALLY
LEFT BLANK

1. 2. 3 Fuel Element Structure

Stationary fuel elements contain up to 18 stainless steel- UO_2 matrix fuel plates each loaded with 46.3 gm U^{235} . Control rod fuel elements contain up to 16 similar fuel plates each loaded with 42.2 gm U^{235} . The fuel plates are of the SM-1 type with increased thickness of the matrix from 0.020 in. to 0.030 in. to accommodate the higher UO_2 loading. The matrix is clad with 0.005 in. stainless steel and is framed by approximately 1/8 in. and 5/8 in. stainless steel on the edges and ends respectively.

Flexibility of number and distribution of fuel plates in both the stationary and control rod fuel elements is provided by extruded polystyrene grooves which hold the fuel plates erect and act as fuel plate spacers. The grooves are sufficiently wide to accommodate extra steel sheets to mock-up heavier fuel plate cladding. Figures 1.4 and 1.5 show stationary and control rod fuel elements in the partially assembled state. Fuel element side plate thicknesses were increased by the addition of steel sheet between the basic side plate and the polystyrene grooves.

1. 2. 4 Steel Reflector Assembly

The reflector assembly consists of a number of 1/2 in. stainless steel sheets along the reactor sides and triangular bars at the corners (Figure 1.1). Laminations of steel and water were obtained with the use of plexiglas edge spacers. Foil activations through the assembly are accommodated by access ports.

1. 3 Experimental Techniques

1. 3. 1 Method of Loading Uniform Burnable Poison

Nuclear poisons such as B_4C may be added to Mylar film in much the same manner as ferrous oxide is added in the production of magnetic tapes. Mylar is a tough, flexible polymer formed by the condensation reaction between ethylene glycol and terephthalic acid. When used with a high temperature silicone or rubber base adhesive, Mylar film loaded with boron dispersed in ferrous oxide provides an ideal method of adding known and controlled amounts of boron to fuel plate surfaces. Mylar tapes with various boron loadings were used in these experiments. Boron in the form of B_4C in particle sizes of one to three microns was added to 0.0005 in. Mylar film.

The Mylar tape was procured in widths approximating the matrix widths of both stationary and control fuel plates. Figure 1.6 shows the simple wringer type tape dispenser used for applying the Mylar. Ap-

THIS PAGE
WAS INTENTIONALLY
LEFT BLANK

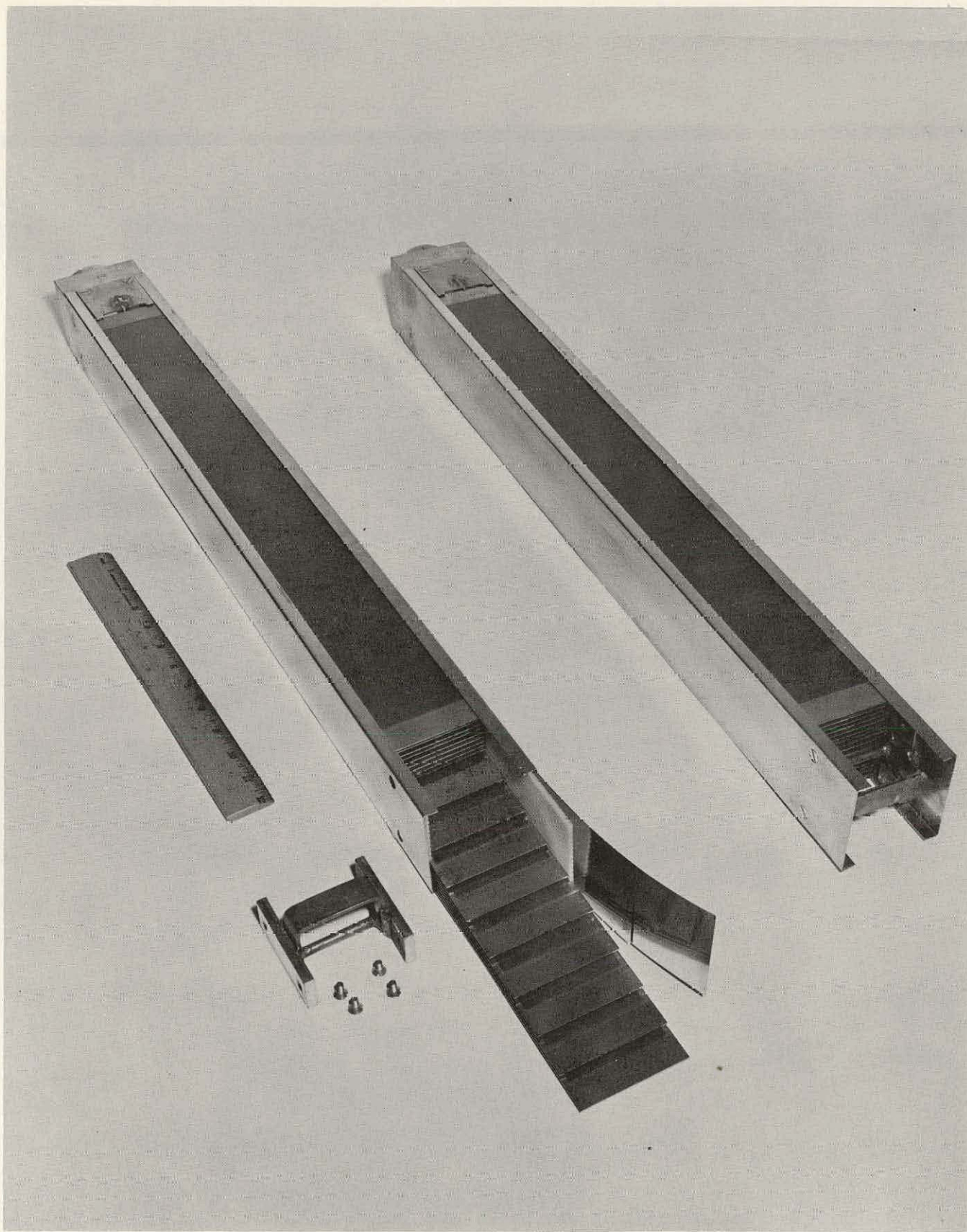


FIG. 1.4 - STATIONARY FUEL ELEMENT

THIS PAGE
WAS INTENTIONALLY
LEFT BLANK

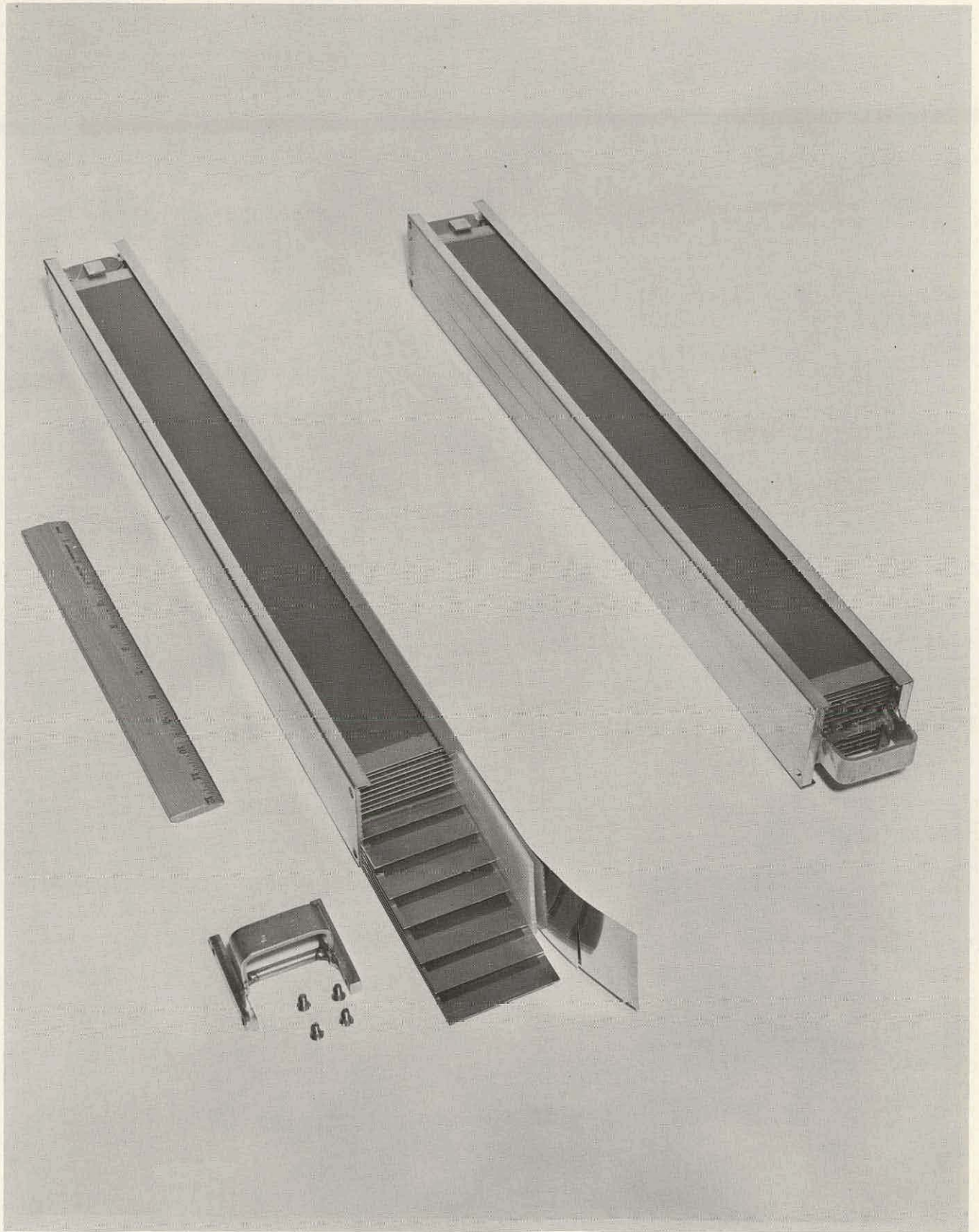


FIG. 1.5 - CONTROL ROD FUEL ELEMENT

THIS PAGE
WAS INTENTIONALLY
LEFT BLANK

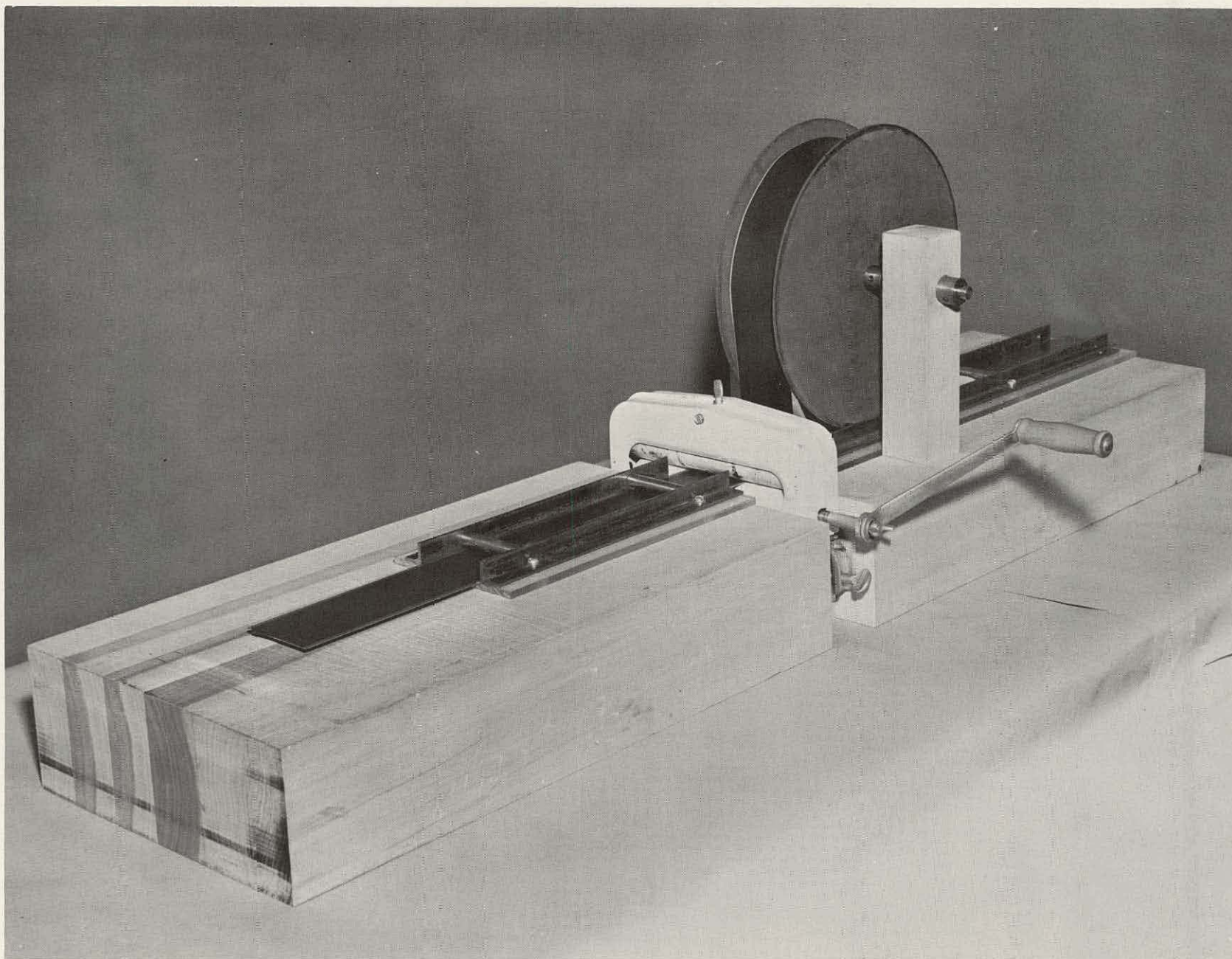


FIG. 1.6 - BORON TAPE APPLICATOR

THIS PAGE
WAS INTENTIONALLY
LEFT BLANK

proximately five man days were required using this device to load a complete SM-2 core with one layer of tape. Additional layers were applied as desired and the plate ends were trimmed at the matrix boundaries. Boron loadings were determined from areal loadings, chemical analyses, and boron standard determinations (see Chapter 3).

1.3.2 Reactivity Coefficients of Uranium

Reactivity coefficients of U^{235} were determined by substitution techniques utilizing fuel plates with U^{235} loadings both greater and less than the normal loading of 46.3 gm U^{235} per plate.

1.4 Nomenclature and Explanations

1.4.1 Active Core

That region defined by the upper and lower average limits of the U^{235} distributions in the stationary fuel elements and the cell boundaries of the outer row of stationary elements.

1.4.2 Cadmium Fraction

The ratio of bare foil activity minus cadmium covered foil activity to bare foil activity. The cadmium used was 0.020 in. thick for which the cadmium cut-off energy is 0.5 ev.

1.4.3 Control Rod Withdrawal

Refers to the withdrawal of the absorber section of the control rod from the active core and the consequent simultaneous insertion of fuel.

1.4.4 Control Rod Position

Control rod positions are reported as the distance withdrawn from the position of deepest insertion measured in inches. Deepest insertion represents the nominal alignment of the bottom of the active core with the top limit of U^{235} distribution in the control rod fuel element. Bank positions result from the average of positions of the individual rods comprising the bank. Individual rod positions usually differ from the bank position by less than ± 0.01 in. Unless otherwise stated, control rod positions are accurate to ± 0.063 in. and have a precision of ± 0.001 .

1.4.5 Core Array, 7 x 7

The arrangement of stationary fuel elements depicted in Figures A. 1 and A. 2 of Appendix A.

1. 4. 6 Data Point, Experimental

All experimental data points are plotted as a point (circled, squared, or other). Points derived from experimental data by cross plot or integration are represented by crosses.

1. 4. 7 Error, Experimental

All reported errors are probable errors (50% confidence interval) in precision unless otherwise noted.

1. 4. 8 Reactivity

Reactivity measurements were obtained by the usual period technique of calibrating control rods. The control rod calibration curves are therefore described as $\frac{d\rho}{dx}$, where $\rho = \frac{\Delta K}{K}$.

Excess K determined experimentally for a perturbation corresponding to a change in rod position from x_1 to x_2 is reported as $\Delta K_E = \int_{x_1}^{x_2} \frac{d\rho}{dx} dx$.

For ΔK_E less than \$1.00, the expression $\Delta K_E = \frac{\Delta K}{K}$ is satisfactory.

However, when ΔK_E is large, the expression $\rho = 1 - e^{-\Delta K_E}$ (3) should be used, where ρ is the hypothetical reactivity that would result if the total reactivity change were measured in one large step.

Reactivity ρ and ΔK_E are reported in dollars and cents using the in-hour equation to convert from reactor period. A complete description of the method used is reported in Appendix D.

1. 4. 9 Rod Array

The open and closed 7 rod arrays referred to in this report are described by Figures A. 1 and A. 2 of Appendix A.

1. 4. 10 Temperature

Unless otherwise noted all measurements were taken at 69°F.

1. 4. 11 Trend Digit

Where data is reported with the last digits underlined, these digits are to be interpreted as indicative rather than significant.

1.5 Criticality Safety Data

Experiments were performed to determine the multiplication of the open 7 array on scram for the most pessimistic case of maximum U^{235} loading and no boron. The minimum critical lattice of 18 plate stationary elements and a single 16 plate central control rod with no boron loading was also determined.

1.5.1 Minimum Critical Lattice

The minimum critical lattice for 18 plate stationary elements was determined to be an array of eight stationary elements and one control rod. (See reference loading (i) in Appendix A.) The system contained 7343 grams U^{235} and was critical with rod C withdrawn to 18.566 inches. Period measurements indicated the balance of rod C to be worth about 48 cents.

1.5.2 Criticality of Open 7 Array

The open 7 control rod array was simulated by stationary elements loaded as described by reference loading (ii) in Appendix A. Each of six stationary elements carried 18 plates with no boron and the array was controlled by a 16 plate control rod located in position 44. This system had an inverse multiplication of about 0.35.

THIS PAGE
WAS INTENTIONALLY
LEFT BLANK

CHAPTER 2. - PARAMETER STUDIES

2.1 Introduction

The flexible portion of the critical experiments for the SM-2 reactor consisted of a series of parameter studies performed as a basic step in the understanding of the potentialities and limitations of the 7 x 7 SM-2 core array. The SM-2 core configuration was approached by varying the number of fuel plates in a fuel element and also by varying the boron loading on the fuel plates. By the use of this technique it was possible to approximate the boron loadings at which the SM-2 core would be critical with the rods fully inserted or withdrawn.

2.2 Experimental Techniques

2.2.1 Procedure

The initial critical cores consisted of U^{235} loadings with no distributed boron. After determining the minimum number of plates per element for criticality, the U^{235} loading was gradually increased by adding fuel plates in a symmetrical fashion. After each loading the reactor was taken critical and the 7 rod bank calibrated by the period technique. This process allowed for 7 rod bank calibrations almost over the entire bank travel.

This procedure was repeated for several distributed boron loadings. Fuel plates were gradually added and the bank calibrated for each case.

2.2.2 Fuel Plate Arrangements

The side plates used in the parametric study were 2.848 in. and 2.621 in. wide for the stationary element and control rod elements, respectively. The fuel plates used contained 46.30 gm U^{235} and 42.24 gm U^{235} per stationary element fuel plate and control rod element fuel plate, respectively. Complete data on the side plates, fuel plates, and other core materials may be found in Appendix A.

In increasing the uranium loading a standard placement of fuel plates in the elements was used, so that as boron loadings were changed, the uranium fuel plate distributions could be repeated exactly. The positions used are as shown in Tables 2.1 and 2.2. The position notation is described in Figures A.3 and A.4 of Appendix A.

TABLE 2. 1
STATIONARY FUEL PLATE ARRANGEMENT IN PARAMETER STUDIES

| <u>Plates per Element</u> | <u>Positions Used</u> |
|---------------------------|--|
| 3 | d, j, o |
| 4 | c, g, l, p |
| 5 | c, g, j, m, q |
| 6 | b, e, h, k, n, q |
| 7 | b, d, g, j, l, o, q |
| 8 | a, c, f, h, k, m, p, r |
| 9 | a, c, e, g, j, l, n, p, r |
| 10 | a, c, e, h, i, k, l, o, p, r |
| 11 | b, c, e, f, h, i, k, l, n, o, q |
| 12 | a, c, d, f, g, i, j, l, m, o, p, r |
| 13 | a, b, d, e, g, h, j, k, l, n, o, q, r |
| 14 | a, b, d, e, f, h, i, j, k, m, n, o, q, r |
| 15 | a, b, c, d, f, g, h, j, k, l, m, o, p, q, r |
| 16 | a, b, c, d, f, g, h, i, j, k, l, m, o, p, q, r |
| 17 | a, b, c, d, e, f, g, h, j, k, l, m, n, o, p, q, r |
| 18 | a, b, c, d, e, f, g, h, i, j, k, l, m, n, o, p, q, r |

TABLE 2. 2
CONTROL ROD FUEL PLATE ARRANGEMENT IN PARAMETER STUDIES

| <u>Plates per Element</u> | <u>Positions Used</u> |
|---------------------------|--|
| 3 | c, h, n |
| 4 | b, f, j, n |
| 5 | b, e, h, l, o |
| 6 | a, d, g, j, m, p |
| 7 | a, d, f, i, k, n, p |
| 8 | a, c, e, g, i, k, m, o |
| 9 | a, c, e, g, h, j, l, n, p |
| 10 | a, c, d, f, h, i, k, m, n, p |
| 11 | a, b, d, e, g, h, j, k, m, n, p |
| 12 | a, b, c, e, f, g, i, j, k, m, n, o |
| 13 | a, b, d, e, f, g, i, j, k, l, m, o, p |
| 14 | a, b, c, d, e, g, h, i, j, l, m, n, o, p |
| 15 | a, b, c, d, e, f, g, i, j, k, l, m, n, o, p |
| 16 | a, b, c, d, e, f, g, h, i, j, k, l, m, n, o, p |

2. 2. 3 Metal to Water Ratio

The metal to water ratio was determined as a function of loaded mass of U^{235} in the core, Table 2. 3 and Figure 2. 1. Loaded core masses were defined as the masses present in the core with the control rods fully withdrawn. The active core masses were those masses within the active core at criticality, with control rods partially withdrawn and the contribution of the absorber sections neglected. By using loaded U^{235} mass it was possible to avoid the difficulty that the active core mass does not include the entire control rod fuel element.

TABLE 2. 3
VARIATION OF METAL TO WATER RATIO WITH LOADED U^{235} MASS

| <u>M/W</u> | <u>Mass U^{235} (gm)</u> |
|------------|---------------------------------------|
| 0. 070 | 6155. 24 |
| 0. 085 | 8220. 32 |
| 0. 100 | 10275. 40 |
| 0. 116 | 12330. 48 |
| 0. 133 | 14385. 56 |
| 0. 150 | 16440. 64 |
| 0. 167 | 18495. 72 |
| 0. 185 | 20550. 80 |
| 0. 203 | 22605. 88 |
| 0. 222 | 24660. 96 |
| 0. 242 | 26716. 04 |
| 0. 262 | 28771. 12 |
| 0. 283 | 30826. 20 |
| 0. 305 | 32881. 28 |
| 0. 324 | 34640. 68 |
| 0. 344 | 36400. 08 |

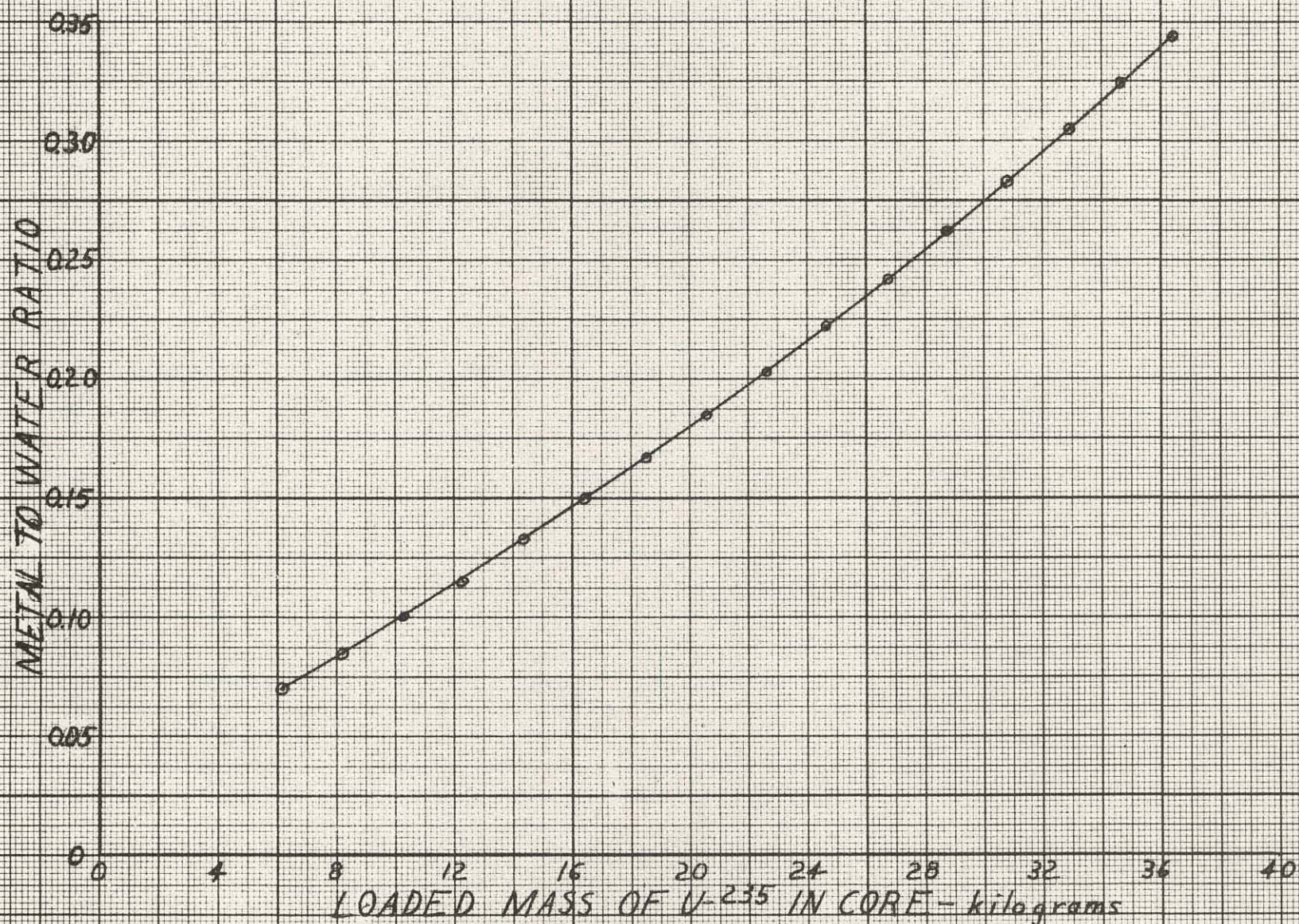
2. 2. 4 Boron Loadings

The boron loadings were varied by the use of boron impregnated Mylar tapes as discussed in Chapter 1. The tapes covered the approximate meat areas on the fuel plates, $348.4 \pm 7.0 \text{ cm}^2$ and $323.6 \pm 7.2 \text{ cm}^2$ for the stationary tape and control rod tape, respectively. The boron tape was always located on the north side of the fuel plate corresponding to the orientation used in Appendix A, Figures A. 1, A. 3, and A. 4. Table 2. 4 describes the content of each boron loading.

THIS PAGE
WAS INTENTIONALLY
LEFT BLANK

FIGURE 21

METAL TO WATER RATIO vs. LOADED U^{235} MASS



THIS PAGE
WAS INTENTIONALLY
LEFT BLANK

TABLE 2.4
BORON LOADINGS

| Boron Loading | Mass B ¹⁰ /stationary tape (gm) | Mass B ¹⁰ /control rod tape (gm) | gm B ¹⁰ /Kg U ²³⁵ in core |
|---------------|---|--|--|
| No Boron | 0 | 0 | 0 |
| 1 | 0.060 ± 0.001 | 0.056 ± 0.001 | 1.305 |
| 2 | 0.120 ± 0.002 | 0.112 ± 0.002 | 2.610 |
| 3 | 0.0211 ± 0.0005 | 0.0196 ± 0.0005 | 0.456 |

2.3 Seven Rod Bank vs. Mass of U²³⁵ and Worth

2.3.1 Seven Rod Bank vs. Mass of U²³⁵

The 7 rod bank critical positions and the masses of U²³⁵ in the active core are tabulated by reference loading number (Appendix A) for the various boron loadings, Table 2.5, and are plotted in Figure 2.2. The correspondence between boron loading and reference loading number is presented in Section 2.3.2.

The probable errors in points plotted in Figure 2.2 are within the symbols about each point.

TABLE 2.5
SEVEN ROD BANK CRITICAL POSITION VS. MASS OF U²³⁵ IN ACTIVE CORE

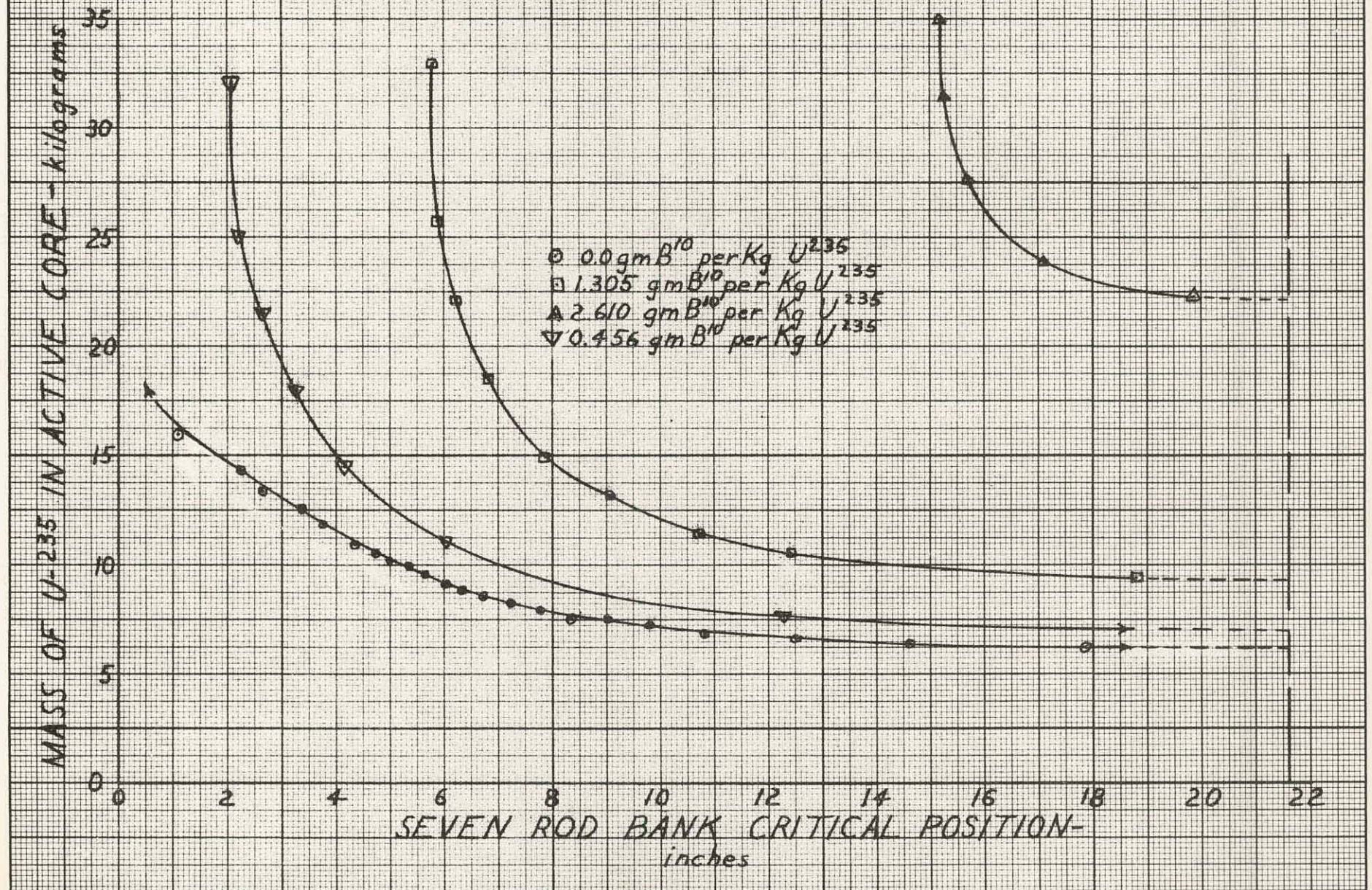
| Reference Loading No. | Total Mass of U ²³⁵ in Active Core (gm) | Seven Rod Bank Critical Position*(in.) |
|--------------------------|---|---|
| 2 | 6240 ± 10 | 17.884 |
| 3 | 6433.2 ± 8.6 | 14.595 |
| 4 | 6691.4 ± 7.5 | 12.508 |
| 5 | 6971.0 ± 6.7 | 10.818 |
| 6 | 7240.4 ± 6.3 | 9.800 |
| 7 | 7523.8 ± 5.9 | 9.043 |
| 8 | 7596.4 ± 7.0 | 8.316 |
| 9 | 7930.2 ± 6.7 | 7.771 |
| 10 | 8264.6 ± 6.5 | 7.235 |
| 11 | 8599.7 ± 6.2 | 6.710 |

| Reference Loading No. | Total Mass of U ²³⁵ in Active Core (gm) | Seven Rod Bank Critical Position (in.) |
|--------------------------|---|--|
| 12 | 8897.6 \pm 6.0 | 6.320 |
| 13 | 9201.4 \pm 5.9 | 6.018 |
| 14 | 9546.7 \pm 5.7 | 5.644 |
| 15 | 9895.3 \pm 5.5 | 5.320 |
| 16 | 10243.0 \pm 5.4 | 4.982 |
| 17 | 10549.5 \pm 5.3 | 4.720 |
| 18 | 10905.7 \pm 6.2 | 4.332 |
| 19 | 11971.6 \pm 5.9 | 3.770 |
| 20 | 12629.7 \pm 6.7 | 3.336 |
| 21 | 13674.6 \pm 6.4 | 2.632 |
| 22 | 14317.2 \pm 7.2 | 2.251 |
| 23 | 15951.7 \pm 6.9 | 1.089 |
| 24 | 11421 \pm 10 | 10.716 |
| 26 | 10538 \pm 11 | 12.407 |
| 27 | 9409 \pm 13 | 18.760 |
| 28 | 13168 \pm 10 | 9.054 |
| 29 | 14922 \pm 11 | 7.876 |
| 30 | 18511 \pm 12 | 6.822 |
| 31 | 22117 \pm 14 | 6.229 |
| 32 | 25740 \pm 16 | 5.889 |
| 33 | 32916 \pm 18 | 5.799 |
| 37 | 23871 \pm 29 | 17.103 |
| 38 | 27586 \pm 32 | 15.703 |
| 39 | 31436 \pm 36 | 15.280 |
| 40 | 34937 \pm 35 | 15.198 |
| 41 | 22292 \pm 31 | 19.883 |
| 42 | 7702.4 \pm 7.4 | 12.366 |
| 43 | 11041.1 \pm 7.0 | 6.010 |
| 44 | 14522.9 \pm 8.1 | 4.164 |
| 45 | 18033.8 \pm 9.5 | 3.272 |
| 46 | 21536 \pm 11 | 2.623 |
| 47 | 25048 \pm 13 | 2.215 |
| 48 | 32114 \pm 14 | 2.070 |

*Seven rod bank positions are in error \pm 0.063 in. (probable error in accuracy.)

FIGURE 22

SEVEN ROD BANK CRITICAL POSITION vs. MASS OF U^{235} IN ACTIVE CORE



THIS PAGE
WAS INTENTIONALLY
LEFT BLANK

2.3.2 Seven Rod Bank Calibration

The 7 rod bank calibrations, corresponding bank positions and reference loading numbers for all boron loadings are tabulated in Tables 2.6, 2.7, 2.8 and 2.9 and plotted in Figures 2.3, 2.4, 2.5, and 2.6. The no boron case is represented by reference loading numbers 2 thru 23; boron loading No. 1, reference loading nos. 23 thru 33; boron loading no. 2, reference loading nos. 37 thru 41, and boron loading no. 3, reference loading nos. 42 thru 48.

The probable errors in points plotted in Figures 2.3, 2.4, 2.5 and 2.6 are within the symbols indicating each point.

TABLE 2.6
SEVEN ROD BANK POSITION VS. SEVEN ROD BANK WORTH FOR
0.0 gm B¹⁰ per kg U²³⁵

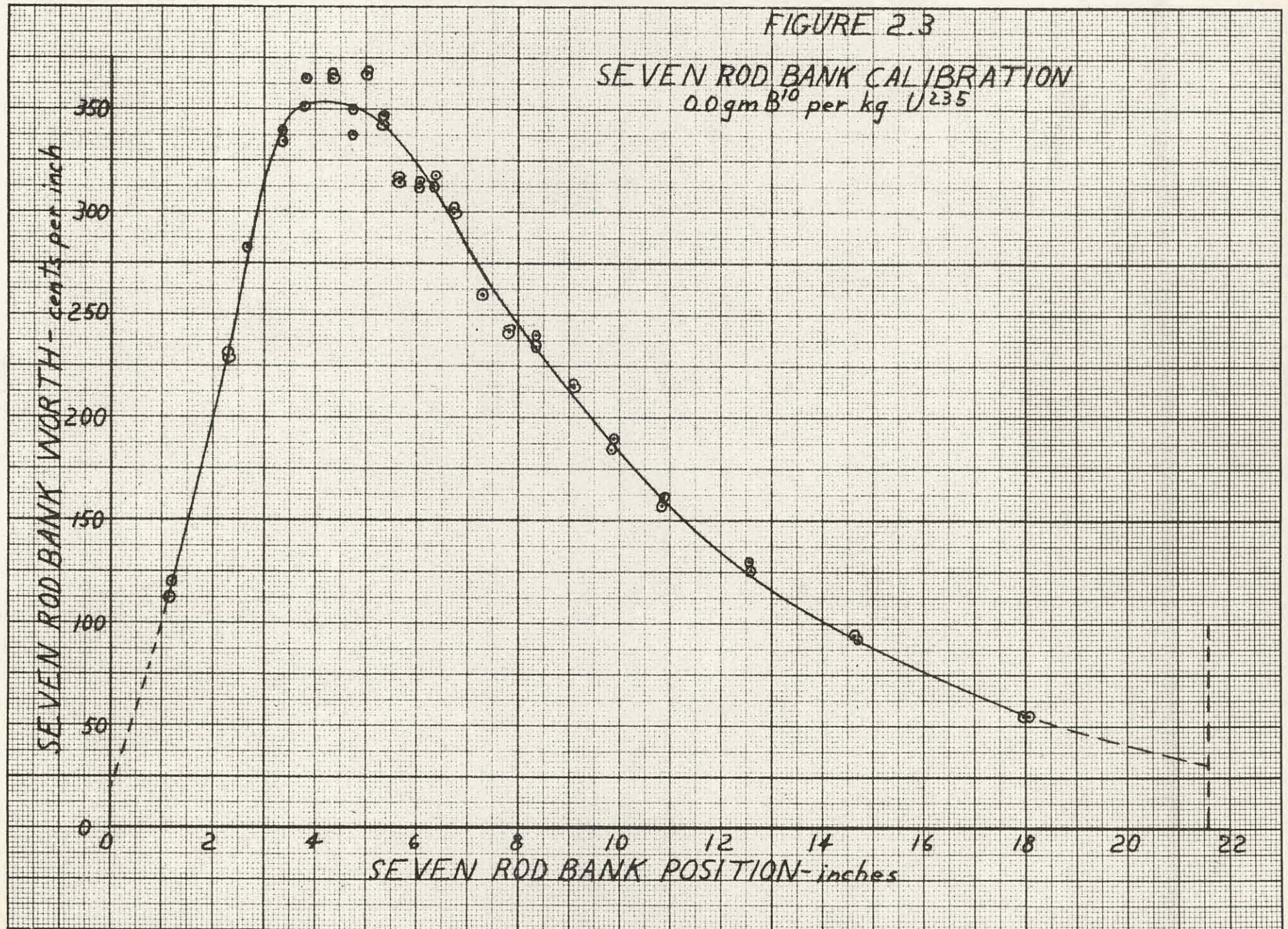
| <u>Reference Loading No.</u> | <u>Seven Rod Bank Position* (in.)</u> | <u>Seven Rod Bank Worth (cents/in.)</u> |
|----------------------------------|--|--|
| 2 | 18.060 | 55.1 ± 1.1 |
| 2 | 17.972 | 55.11 ± 0.57 |
| 3 | 14.703 | 92.59 ± 0.93 |
| 3 | 14.650 | 94.6 ± 1.8 |
| 4 | 12.585 | 125.8 ± 1.3 |
| 4 | 12.555 | 130.9 ± 2.1 |
| 5 | 10.889 | 162.0 ± 1.4 |
| 5 | 10.850 | 157.1 ± 3.2 |
| 6 | 9.868 | 189.7 ± 1.5 |
| 6 | 9.855 | 183.9 ± 1.8 |
| 7 | 9.095 | 214.0 ± 1.9 |
| 7 | 9.095 | 216.4 ± 1.9 |
| 8 | 8.351 | 241.4 ± 2.9 |
| 8 | 8.363 | 237.2 ± 2.1 |
| 9 | 7.816 | 242.7 ± 2.3 |
| 9 | 7.816 | 242.2 ± 2.2 |
| 10 | 7.294 | 259.8 ± 1.7 |
| 10 | 7.273 | 259.7 ± 2.7 |
| 11 | 6.756 | 302.2 ± 2.2 |
| 11 | 6.756 | 298.7 ± 2.2 |
| 12 | 6.345 | 313.2 ± 4.1 |
| 12 | 6.365 | 318.0 ± 2.3 |

| Reference Loading No. | Seven Rod Bank Position (in.) | Seven Rod Bank Worth (cents/in.) |
|--------------------------|-----------------------------------|--------------------------------------|
| 13 | 6. 044 | 311. 5 \pm 3. 9 |
| 13 | 6. 055 | 315. 1 \pm 2. 8 |
| 14 | 5. 687 | 317. 2 \pm 2. 4 |
| 14 | 5. 672 | 314. 3 \pm 3. 6 |
| 15 | 5. 350 | 346. 7 \pm 3. 4 |
| 15 | 5. 350 | 343. 3 \pm 3. 4 |
| 16 | 5. 012 | 367. 3 \pm 3. 4 |
| 16 | 5. 015 | 367. 7 \pm 3. 1 |
| 17 | 4. 751 | 348. 4 \pm 3. 2 |
| 17 | 4. 756 | 350. 0 \pm 2. 8 |
| 18 | 4. 360 | 364. 9 \pm 3. 6 |
| 18 | 4. 365 | 366. 6 \pm 3. 1 |
| 19 | 3. 785 | 351. 7 \pm 6. 8 |
| 19 | 3. 806 | 365. 3 \pm 2. 8 |
| 20 | 3. 373 | 333. 8 \pm 2. 7 |
| 20 | 3. 366 | 339. 0 \pm 3. 4 |
| 21 | 2. 665 | 283. 3 \pm 3. 1 |
| 21 | 2. 677 | 283. 2 \pm 2. 3 |
| 22 | 2. 306 | 230. 3 \pm 1. 9 |
| 22 | 2. 305 | 228. 7 \pm 1. 9 |
| 23 | 1. 150 | 112. 3 \pm 1. 6 |
| 23 | 1. 174 | 120. 0 \pm 1. 2 |

* Seven rod bank positions are in error ± 0.063 in. (probable error in accuracy)

FIGURE 2.3

SEVEN ROD BANK CALIBRATION
 0.0 gm B¹⁰ per kg U²³⁵



THIS PAGE
WAS INTENTIONALLY
LEFT BLANK

TABLE 2. 7
SEVEN ROD BANK POSITION VS. SEVEN ROD BANK WORTH FOR
1. 305 gm B¹⁰ per kg U²³⁵

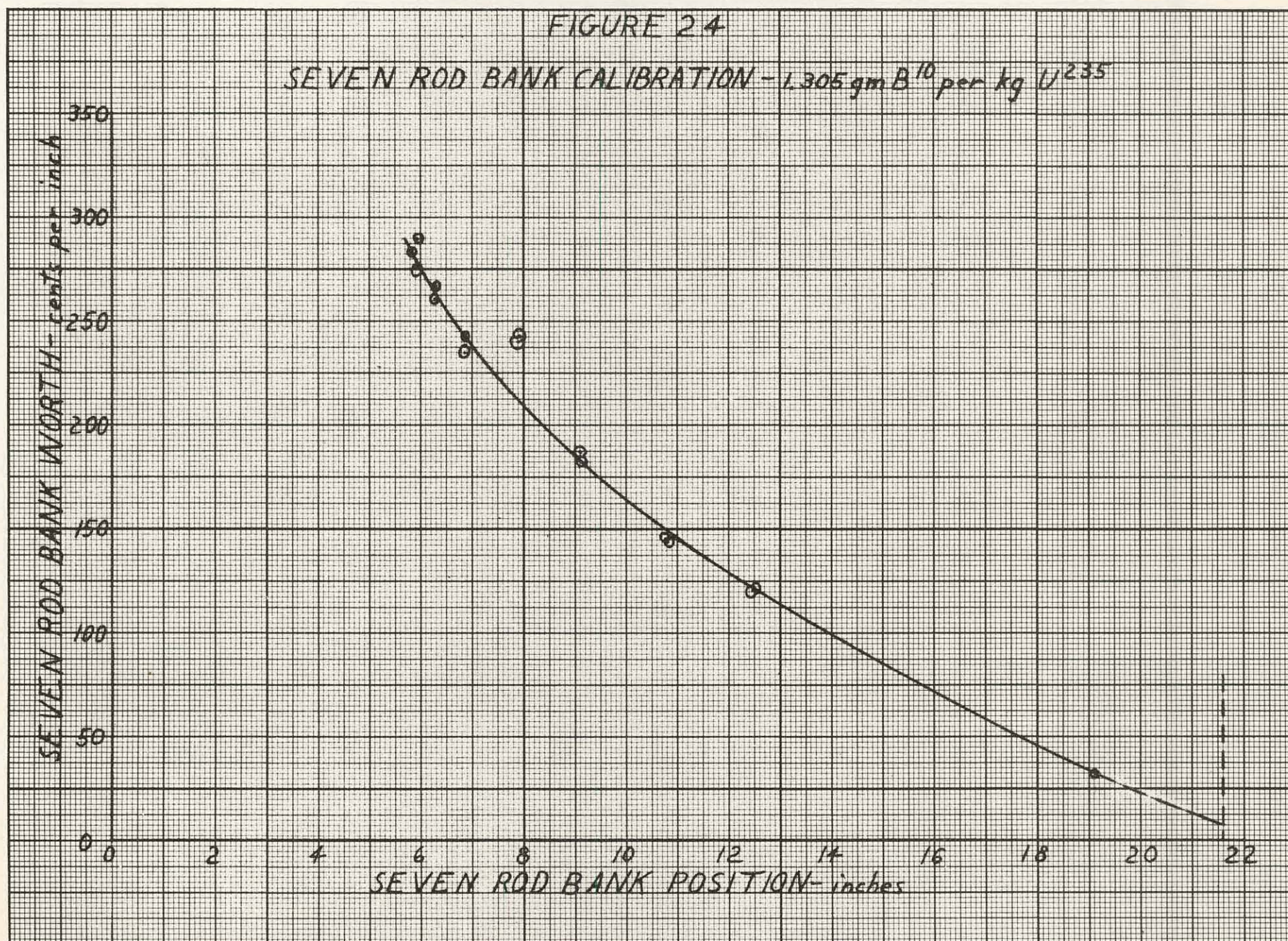
| Reference Loading No. | Seven Rod Bank Position* (in.) | Seven Rod Bank Worth (cents/inch) |
|--------------------------|------------------------------------|--------------------------------------|
| 24 | 10. 789 | 146. 2 \pm 1. 4 |
| 24 | 10. 798 | 149. 4 \pm 1. 2 |
| 26 | 12. 484 | 120. 8 \pm 1. 3 |
| 26 | 12. 495 | 121. 1 \pm 1. 1 |
| 27 | 19. 110 | 32. 62 \pm 2. 9 |
| 28 | 9. 092 | 181. 6 \pm 2. 6 |
| 28 | 9. 107 | 182. 9 \pm 1. 9 |
| 29 | 7. 914 | 239. 6 \pm 2. 6 |
| 29 | 7. 928 | 242. 9 \pm 1. 9 |
| 30 | 6. 853 | 235. 3 \pm 3. 3 |
| 30 | 6. 864 | 242. 8 \pm 2. 4 |
| 31 | 6. 275 | 260. 9 \pm 2. 2 |
| 31 | 6. 279 | 266. 7 \pm 2. 0 |
| 32 | 5. 925 | 275. 7 \pm 2. 8 |
| 32 | 5. 934 | 290. 1 \pm 2. 2 |
| 33 | 5. 839 | 283. 8 \pm 2. 5 |

* Seven rod bank positions are in error $\pm 0. 063$ in. (probable error in accuracy)

THIS PAGE
WAS INTENTIONALLY
LEFT BLANK

FIGURE 2.4

SEVEN ROD BANK CALIBRATION - 1.305 gm B¹⁰ per kg U²³⁵



THIS PAGE
WAS INTENTIONALLY
LEFT BLANK

TABLE 2.8
SEVEN ROD BANK POSITION VS. SEVEN ROD BANK WORTH FOR

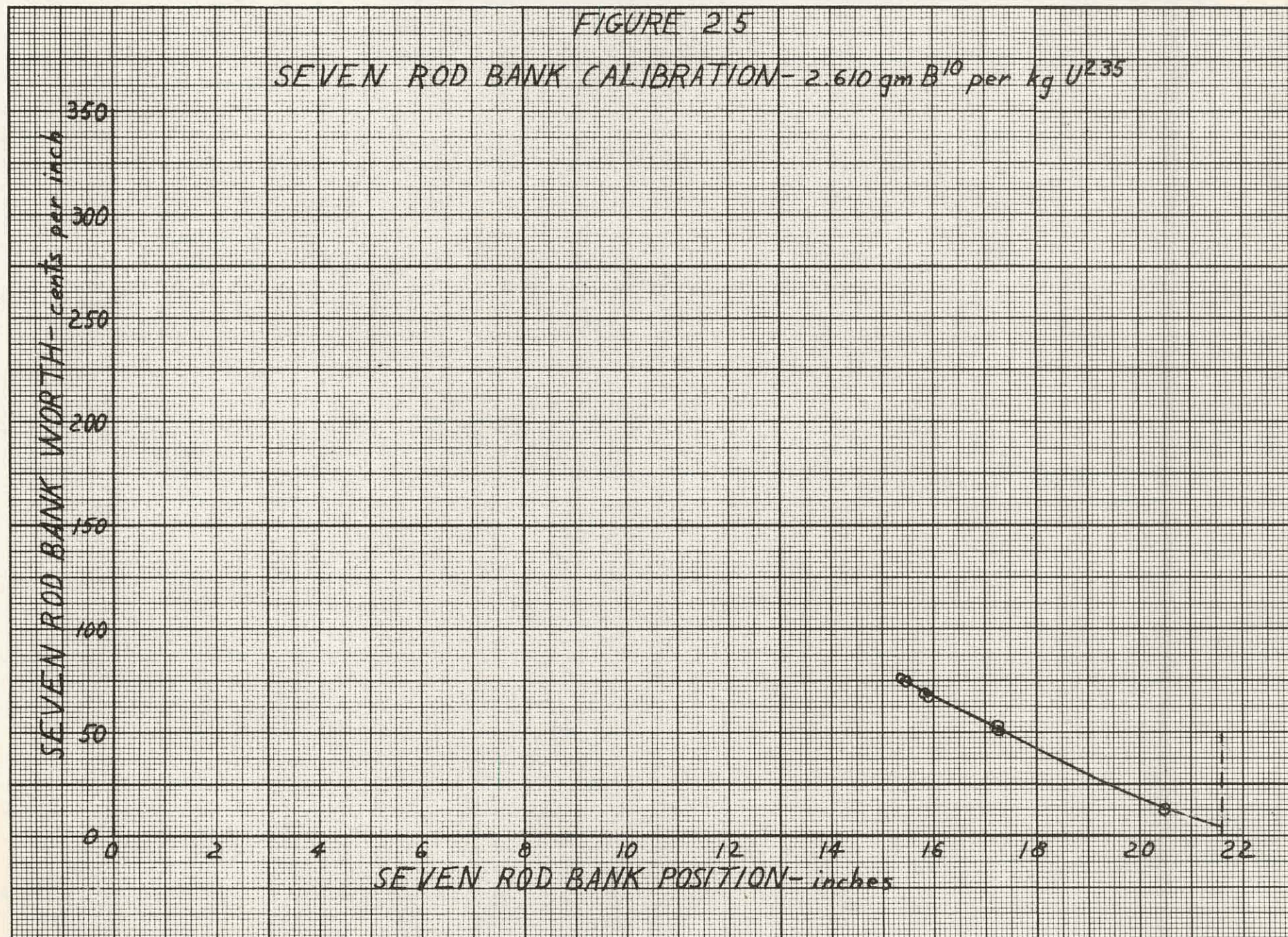
| <u>Reference Loading No.</u> | <u>Seven Rod Bank Position* (in.)</u> | <u>Seven Rod Bank Worth (cents/inch)</u> |
|----------------------------------|--|--|
| 37 | 17.25 <u>2</u> | 51.6 <u>8</u> \pm 0.6 <u>7</u> |
| 37 | 17.26 <u>0</u> | 52.4 <u>0</u> \pm 0.6 <u>4</u> |
| 38 | 15.83 <u>4</u> | 68.7 <u>0</u> \pm 0.7 <u>6</u> |
| 38 | 15.86 <u>9</u> | 67.9 <u>8</u> \pm 0.6 <u>0</u> |
| 39 | 15.38 <u>0</u> | 76.0 \pm 1.0 |
| 39 | 15.41 <u>0</u> | 75.0 <u>0</u> \pm 0.7 <u>7</u> |
| 41 | 20.49 <u>2</u> | 12.8 <u>9</u> \pm 0.1 <u>6</u> |

* Seven rod bank position are in error \pm 0.063 in. (probable error in accuracy)

THIS PAGE
WAS INTENTIONALLY
LEFT BLANK

FIGURE 2.5

SEVEN ROD BANK CALIBRATION - 2.610 gm B^{10} per kg U^{235}



THIS PAGE
WAS INTENTIONALLY
LEFT BLANK

TABLE 2.9
SEVEN ROD BANK POSITION VS. SEVEN ROD BANK WORTH FOR
0.456 gm B¹⁰ per kg. U²³⁵

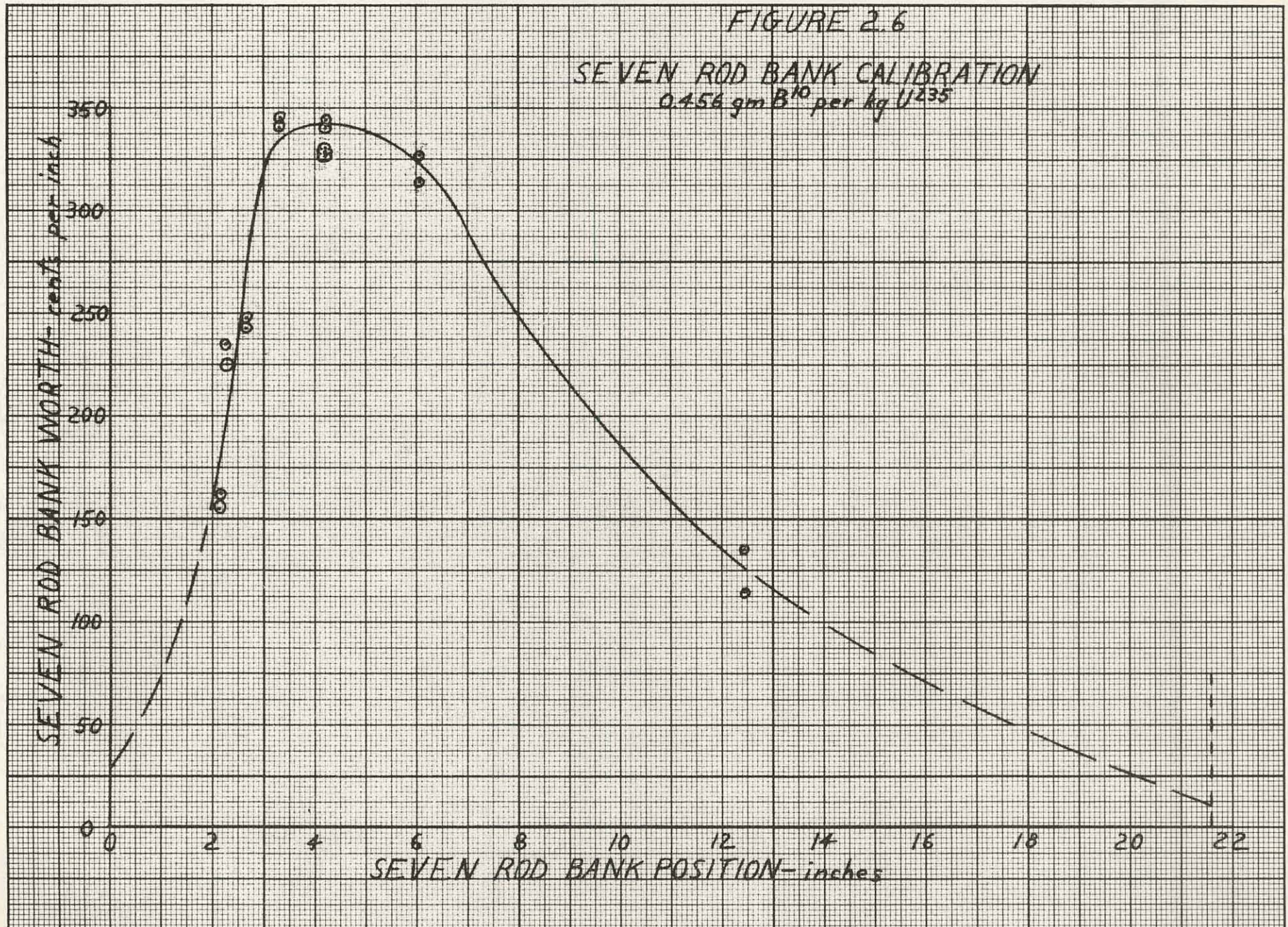
| <u>Reference Loading No.</u> | <u>Seven Rod Bank Position* (in.)</u> | <u>Seven Rod Bank Worth (cents/inch)</u> |
|----------------------------------|--|--|
| 42 | 12.43 <u>4</u> | 136.0 \pm 1.4 |
| 42 | 12.34 <u>5</u> | 115.3 \pm 1.2 |
| 43 | 6.05 <u>1</u> | 313.6 \pm 2.5 |
| 43 | 6.04 <u>5</u> | 326.8 \pm 2.9 |
| 44 | 4.19 <u>4</u> | 339.8 \pm 3.4 |
| 44 | 4.19 <u>7</u> | 343.9 \pm 3.1 |
| 44 | 4.20 <u>5</u> | 328.3 \pm 3.8 |
| 44 | 4.21 <u>4</u> | 331.0 \pm 2.9 |
| 44 | 4.21 <u>0</u> | 327.4 \pm 3.3 |
| 45 | 3.30 <u>6</u> | 345.6 \pm 3.0 |
| 45 | 3.30 <u>1</u> | 341.4 \pm 3.5 |
| 46 | 2.66 <u>1</u> | 242.9 \pm 2.6 |
| 46 | 2.67 <u>2</u> | 248.0 \pm 2.1 |
| 47 | 2.26 <u>5</u> | 224.8 \pm 2.0 |
| 47 | 2.25 <u>9</u> | 234.7 \pm 2.3 |
| 48 | 2.13 <u>5</u> | 162.3 \pm 1.5 |
| 48 | 2.12 <u>5</u> | 154.6 \pm 1.8 |

* Seven rod bank positions are in error ± 0.063 in. (probable error in accuracy)

THIS PAGE
WAS INTENTIONALLY
LEFT BLANK

FIGURE 2.6

SEVEN ROD BANK CALIBRATION
0.456 gm B^{10} per kg U^{235}



THIS PAGE
WAS INTENTIONALLY
LEFT BLANK

2.4 Excess K (ΔK_E)

2.4.1 Integration of Calibration Curves

The "excess K" is defined as:

$$\Delta K_E = \int_{x_1}^{x_2} \frac{d\rho}{dx} dx, \text{ where}$$

$\frac{d\rho}{dx}$ is described by the calibration curves for the various boron loadings (Figures 2.3, 2.4, 2.5, and 2.6.) The limits of integration are established as x_1 = the critical seven rod bank position and x_2 = the position of the fully withdrawn seven rod bank (21.6 in.).

Integrating the calibration curves directly, yields ΔK_E as a function of bank position for the various boron loadings. From Figure 2.2 the mass of U^{235} in the active core, for these bank positions, is obtained.

2.4.2 ΔK_E Vs. Mass of U^{235} in Active Core

Figure 2.7 represents ΔK_E as a function of the mass U^{235} in the active core for the various boron loadings. Experiments with boron loading numbers 1, 2, and 3 were all terminated at the SM-2 U^{235} loading, while it was impossible to achieve this loading in the no boron case. The dashed curve in Figure 2.7 connects all the SM-2 points.

2.4.3 ΔK_E Vs. Mass of B^{10} for SM-2 Configuration

From Figure 2.7 there are three SM-2 points that have known boron loadings and ΔK_E 's. Obtaining the masses of B^{10} in the active core for these points from Appendix A, ΔK_E is plotted vs. mass of B^{10} in the active core for the SM-2 configuration. (Figure 2.8, crosses 1, 2 and 3 corresponding to crosses 1, 2 and 3 of Figure 2.7).

2.5 Data Evaluation

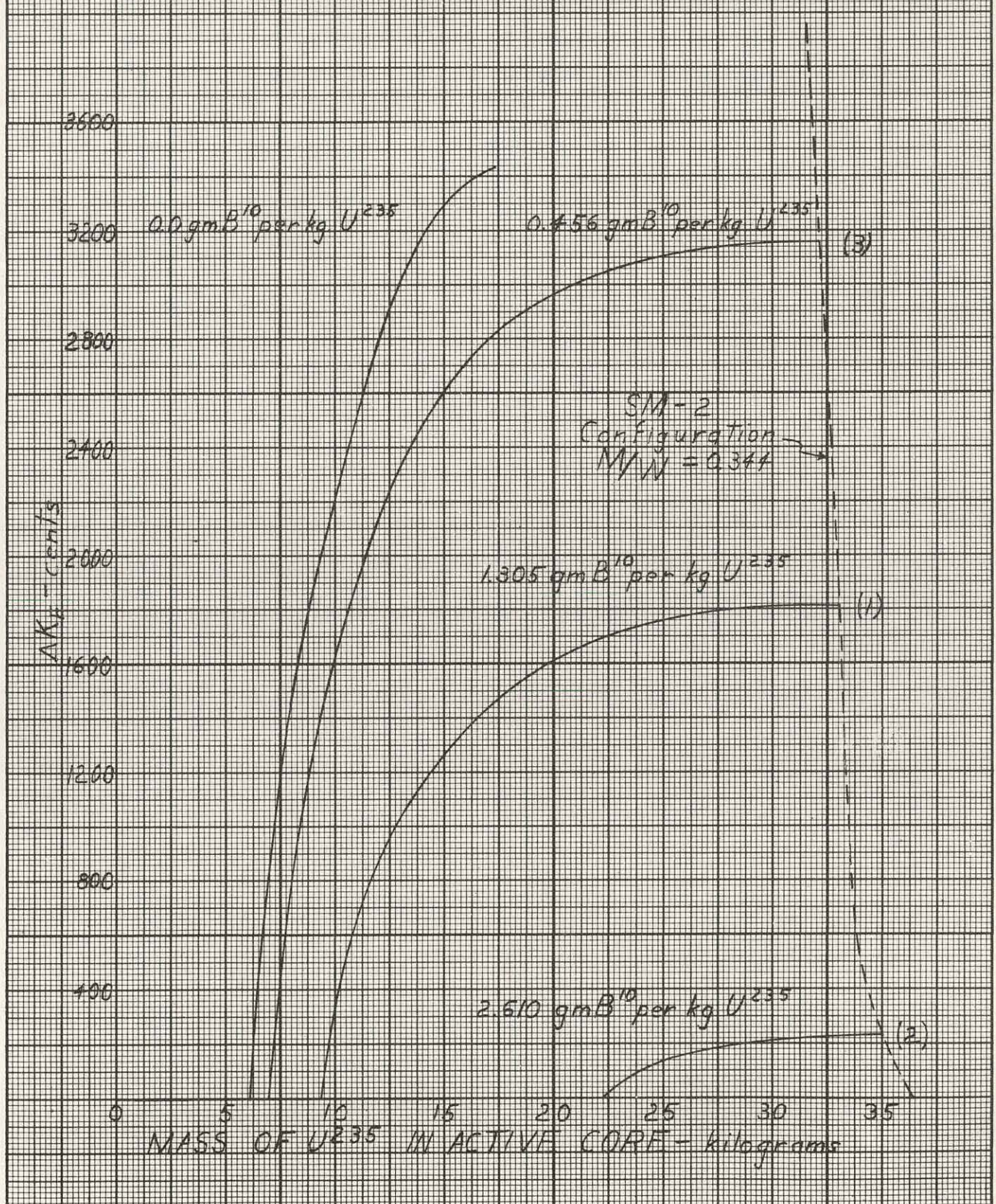
2.5.1 ΔK_E Mass B^{10} in the Active Core for the SM-2 Configuration

Since the integrals of Figure 2.7 and 2.8 were obtained assuming invariance of the calibration curves with metal to water ratio some deviation of the final SM-2 mockup K_E (reference loading 53 with data reported in

THIS PAGE
WAS INTENTIONALLY
LEFT BLANK

FIGURE 2.7

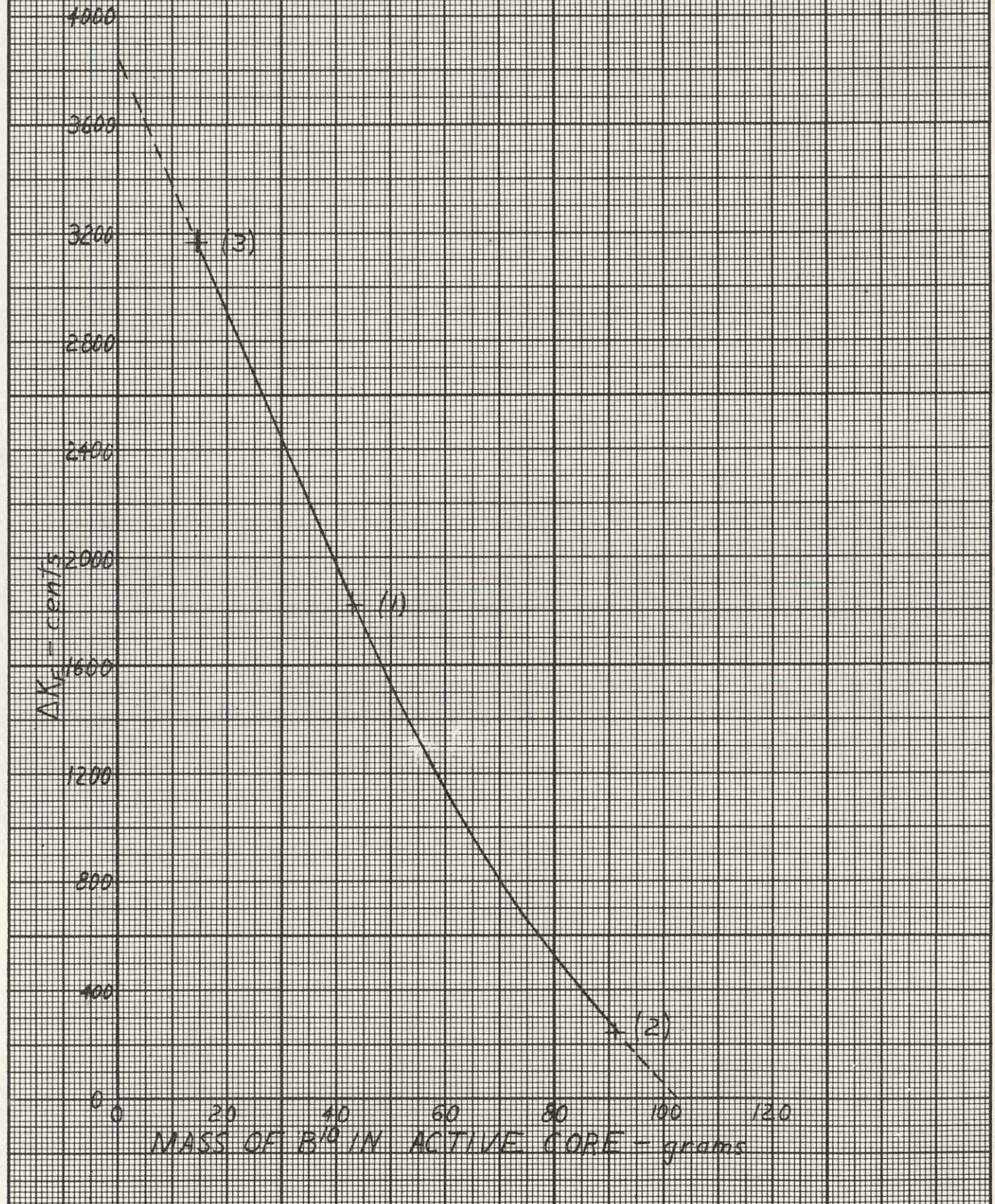
ΔK_E vs MASS OF U^{235} IN ACTIVE CORE



THIS PAGE
WAS INTENTIONALLY
LEFT BLANK

FIGURE 2.8

ΔK_E vs MASS OF B^{10} IN ACTIVE CORE FOR
SM-2 CONFIGURATION



THIS PAGE
WAS INTENTIONALLY
LEFT BLANK

Chapter 4) from these curves should be noted. Referring to Figure 4. 5 of Chapter 4, which is based on integration of a composite calibration curve, one notes, in fact, a variation of from 3% to 5% for each of the points corresponding to points 1, 2 and 3 of Figure 2. 8. Since interpolation of Figures 2. 7 and 2. 8 is extremely sensitive to curve shape, a reliable K_E for the SM-2 final mockup is best determined from the composite integral, Figure 4. 4 of Chapter 4.

2. 5. 2 Final SM-2 Mockup

The preliminary SM-2 loadings of B¹⁰ and U²³⁵ predicted analytically prior to the performance of these experiments appear to be satisfactory.

THIS PAGE
WAS INTENTIONALLY
LEFT BLANK

CHAPTER 3 - SM-1 MOCKUP EXPERIMENTS

3.1 Introduction

The SM-1 mockup experiments were performed using the SM-2 flexible critical experiment rig in order to determine the limitations of the system flexibility. In the course of the experiment, heterogeneity factors for different mockups were obtained which serve as a measure of the ability of the system to mockup 18 plate fuel elements with fewer plates. Also during the experiment, a standard method for determining the amount of boron on the Mylar tape, and hence in the flexible reactor, was developed using a physical technique. As a consequence of this work an experimental estimate of the SM-1 boron loading was determined.

In the past, two other assemblies of SM-1 core components were made at the Alco Critical Facility: the ZPE-1⁽⁴⁾ and the ZPE-2⁽⁵⁾. The SM-1 mockups assembled during the experimental program were actually mockups of the ZPE-2 configuration. However, the fuel elements in the ZPE-2 were experimentally proven to be identical with the fuel elements in the SM-1, and the only structural differences between the SM-1 and ZPE-2 which affected the reactivity were the presence of a steel skirt in the SM-1 and slight fabrication differences in the absorber section structure. The ZPE-1, which used the same fuel elements as the ZPE-2, mocked-up the SM-1 reactivity exactly since it used the actual SM-1 core support. A summary of these assemblies is presented in Table 3.1.

TABLE 3.1
SUMMARY OF SM-1 EXPERIMENTS AT ALCO

| | SM-1 | ZPE-1 | ZPE-2 | Preliminary Mockup | Final SM-1 Mockup |
|-------------------|--------|--------|--------|--------------------|-------------------|
| Boron Absorbers | ZPE-1 | ZPE-1 | ZPE-2 | ZPE-2* | ZPE-2* |
| Steel Skirt | Yes | Yes | No | No | No |
| Fuel Elements | SM-1 | ZPE-1 | ZPE-1 | Pre. Mockup | Final Mockup |
| U-235 gm/element | | | | | |
| Stationary | 514.62 | 514.62 | 514.62 | 509.3 | 509.3 |
| Control | 417.76 | 417.76 | 417.76 | 422.4 | 422.4 |
| B10 gm/element | | | | | |
| Stationary | ? | ? | ? | 0.231 | 0.347 |
| Control | ? | ? | ? | 0.196 | 0.284 |
| Critical Position | | | | | |
| 5 Rod Bank | 3.7 | 3.7 | 3.12 | 1.699 | 3.258 |

* New boron absorbers shown experimentally to be identical with those used during ZPE-2.

The core compositions of the two SM-1 mockups made during this experiment are defined by reference loading numbers 50 and 51 (Appendix A).

3.2 Preliminary SM-1 Mockup

Since the amount of boron in the SM-1 was somewhat uncertain it was necessary to make two mockups of the SM-1 in order to obtain a mockup which would accurately describe the SM-1. The critical position of the preliminary mockup was 1.699 inches on the 5 rod bank with rods F and G full out, compared with 3.120 inches for the ZPE-2.

Calibration points for the 5 rod bank were obtained at various bank positions. They are plotted in Figure 3.1 along with points obtained during the ZPE-1 experiment and the final mockup.

Substitution measurements were made using a standard SM-1 element. The mockup element was replaced by the SM-1 element and the change in reactivity noted. The total change for all 38 stationary elements was minus 177 cents.

An initial determination of the amount of boron in the SM-1 was made after the preliminary mockup using a boron worth of 68 cents/gm (ZPE-1 Data ⁽⁴⁾) and the total reactivity defect due to the SM-1 element substitutions.

3.3 Final SM-1 Mockup

The final SM-1 mockup configuration was determined using the results of the preliminary mockup. Sufficient measurements were made so that any differences between it and the SM-1 could be accounted for.

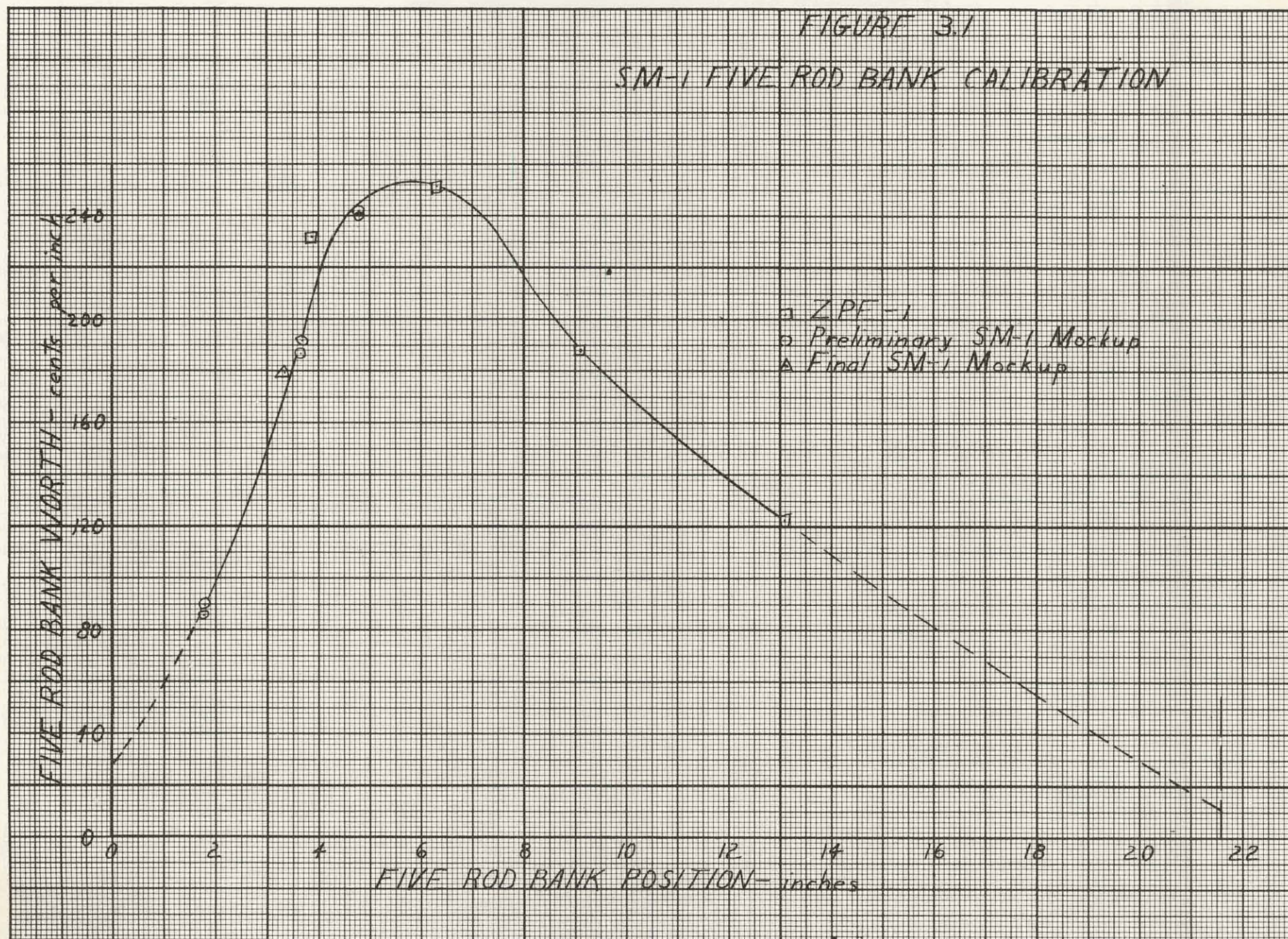
3.3.1 Reactivity Evaluation

The final mockup had a 5 rod bank critical position of 3.258 inches compared to 3.120 inches for the ZPE-2. The small difference in bank position indicated that the mockup was quite good. The 5 rod bank calibration point taken at the critical position agreed well with the ZPE-1 and preliminary mockup points, as can be seen in Figure 3.1. An integral of this worth curve is presented in Figure 3.2. The total ΔK_E determined in the original ZPE-1 and during this experiment differ slightly due to incorrect extrapolation of the ZPE-1 worth curve.

3.3.2 Uranium Worth Measurements

The worth of U ²³⁵ in the core was measured by using fuel plates with slightly higher U ²³⁵ content than the basic plates in a single element. This

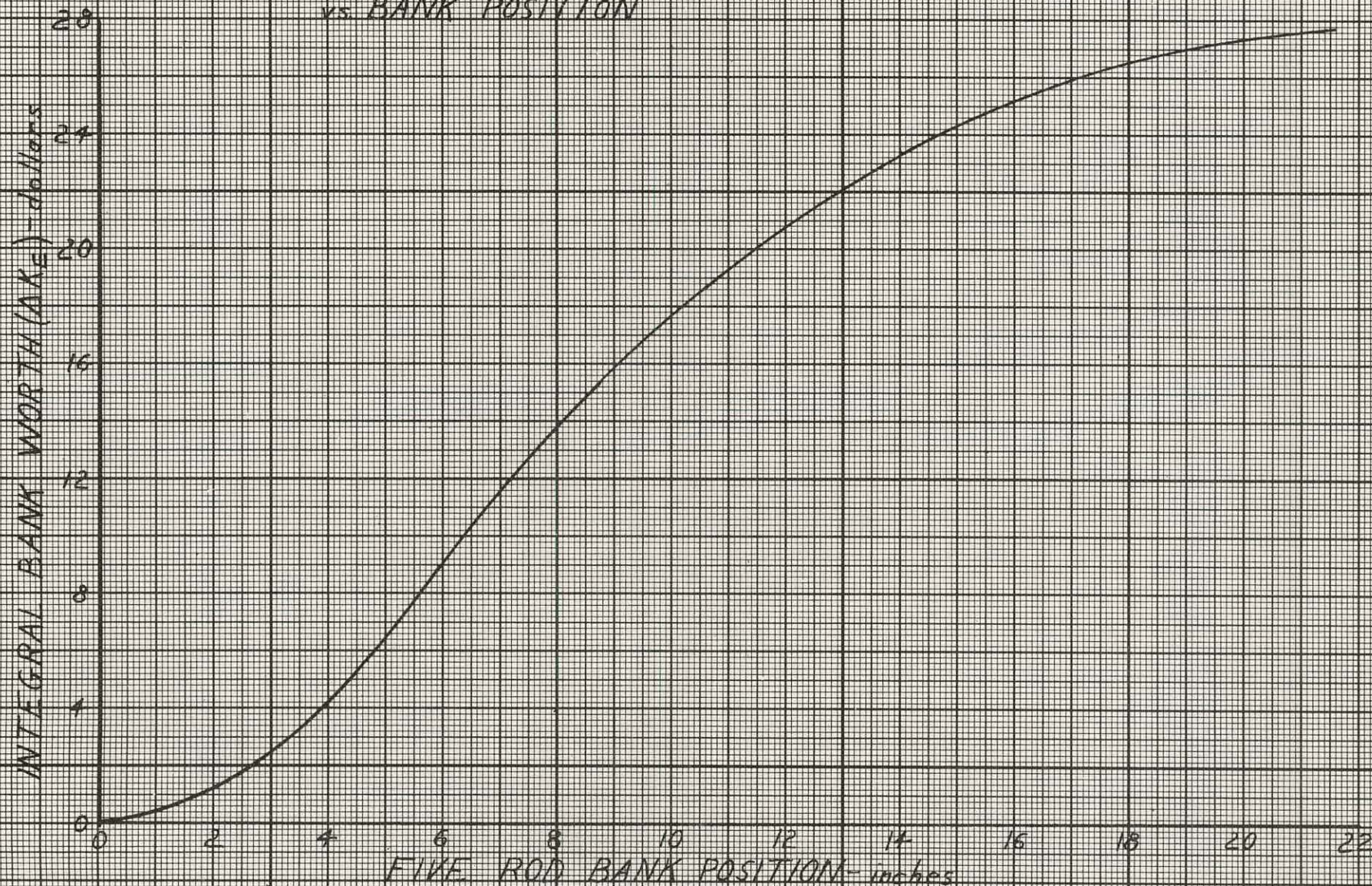
FIGURE 3.1
SM-1 FIVE ROD BANK CALIBRATION



THIS PAGE
WAS INTENTIONALLY
LEFT BLANK

FIGURE 3.2

INTEGRAL SM-1 FIVE ROD BANK NORTH
vs. BANK POSITION



THIS PAGE
WAS INTENTIONALLY
LEFT BLANK

element was then substituted for several element positions. An average U^{235} worth in the stationary elements was determined by integrating over the core volume using symmetry conditions for the element positions not measured. Table 3.2 presents the data.

TABLE 3.2
 U^{235} WORTH FOR VARIOUS ELEMENT POSITIONS

| Element No. | Reactivity Change in Cents | Cents/gm U^{235} |
|-------------|-------------------------------|--------------------|
| 12 | 2.072 | 0.0819 |
| 13 | 2.294 | 0.0907 |
| 14 | 4.554 | 0.180 |
| 22 | 4.883 | 0.193 |
| 23 | 3.340 | 0.132 |
| 34 | 7.059 | 0.279 |
| 52 | 5.743 | 0.227 |
| 53 | 5.313 | 0.210 |

Average U^{235} worth in stationary elements = 0.154 cents/gm U^{235}

The average U^{235} worth of 0.154 cents/gm U^{235} compares fairly well with the reported value of 0.187 cents/gm U^{235} for the ZPE-2⁽⁵⁾. The difference between these two values can be partially attributed to the differences in experimental techniques. In the ZPE-2 experiments the uranium was added in the form of uranium-aluminum alloy strips (11.0 x 0.5 x 0.005 inches). These strips were inserted into the water hole region between fuel plates. The method used in the final mockup experiment was more realistic since the additional U^{235} was uniformly distributed throughout the fuel plate matrix.

3.3.3 Boron Worth Measurements

The worth of B^{10} in the core was measured by removing the boron from all the plates of a single element and substituting this element in several positions. An average B^{10} worth in the stationary elements was obtained by using symmetry relationships. Table 3.3 presents the data.

TABLE 3.3
B¹⁰ WORTH FOR VARIOUS ELEMENT POSITIONS

| <u>Element No.</u> | <u>Reactivity Change in Cents</u> | <u>Cents/gm U²³⁵</u> |
|--------------------|---------------------------------------|---------------------------------|
| 12 | 11.73 | 40.7 |
| 13 | 12.80 | 44.4 |
| 14 | 7.81 | 27.1 |
| 22 | 23.03 | 79.9 |
| 23 | 23.23 | 80.6 |
| 34 | 24.78 | 86.0 |
| 52 | 21.35 | 74.1 |
| 53 | 31.41 | 109 |

Average B¹⁰ worth in stationary elements = 60.3 cents/gm B¹⁰.

In the ZPE-1 experiment the B¹⁰ worth was not obtained directly⁽⁴⁾ since boron-stainless steel containing 1.01% boron was used in the experiment. However, the B¹⁰ worth value of 68 cents/gm obtained during ZPE-1 compares favorably with the final mockup result, considering that in the ZPE-1 experiment the boron was inserted in a different flux region and the effect of the stainless steel was not taken into account.

3.3.4 Substitution Measurements

A standard SM-1 element was substituted for the mockup elements one by one in order to measure the exact difference between a mockup element and an SM-1 element. The total reactivity change for all 38 of the stationary elements was 16.95 cents positive. The average value was 0.446 cents per stationary element.

3.4 Experimental Techniques Evaluation

3.4.1 Heterogeneity Measurements

A fuel grouping technique was used for the heterogeneity measurements. The plastic separators on the side plates were modified so that the fuel plates and stainless clad in the mockup elements could be assembled in discrete bundles. The eleven fuel plates per element which mocked-up fuel loading of the SM-1 were first assembled into one discrete bundle along with the stainless steel clad in the mockup in the center of the element. They were then assembled into two discrete bundles, three discrete bundles, etc., until the maximum of eleven bundles was reached.

Figure 3.3 shows the curve of reactivity change versus number of fuel bundles obtained from these measurements. Since the curve is essentially flat between 9 and 11 bundles, it seemed reasonable to linearly extrapolate it to 18 bundles, the actual SM-1 fuel element configuration. The heterogeneity worth thus obtained was 0.75 cents for element 22 in which the measurements were made. The average heterogeneity worth was 0.60 cents/stationary element, obtained by dividing the value determined for element number 22 by the local to average uranium worth ratio.

3.4.2 Boron Standard

Previous parametric studies indicated inconsistencies in the chemical analysis of the boron impregnated Mylar tape. Therefore, it was decided that a physical method should be used to determine the amount of loaded boron. Numerous samples were made with the same dimensions as the Mylar tape. These samples contained a physically determined amount of B_4C . The B_4C used in their preparation was of the same batch as that used in the manufacture of the Mylar tape. (Appendix B). The reactivity correlation of the samples was considered excellent and standards were established. On the basis of these standards, the following Mylar tape loadings were determined and are compared with the chemical analysis in Table 3.4.

TABLE 3.4
MYLAR TAPE LOADINGS

| Batch | Exper. Mg. B^{10}/cm^2 | Average L. Pitkin Chem. Anal. mg. B^{10}/cm^2 | Average BMI Chem. Anal. mg B^{10}/cm^2 |
|-------|-----------------------------|--|---|
| 1-1 | 0.173 | 0.1840 | 0.210 |
| 1-2 | 0.148 | 0.1468 | 0.156 |
| 2-1 | 0.0605 | 0.0755 | 0.0668 |
| 2-2 | 0.0585 | 0.0646 | 0.0636 |

Figure 3.4 is a curve of B^{10} per cm^2 versus reactivity in cents obtained using this standard sample technique. The amount of B^{10} in all cores was determined using this curve. The amount of boron determined to be in the final SM-1 mockup using this method was 13.17 grams in the stationary elements and 1.99 grams in the control elements.

3.5 Experimental Evaluation of Boron in SM-1 Core 1

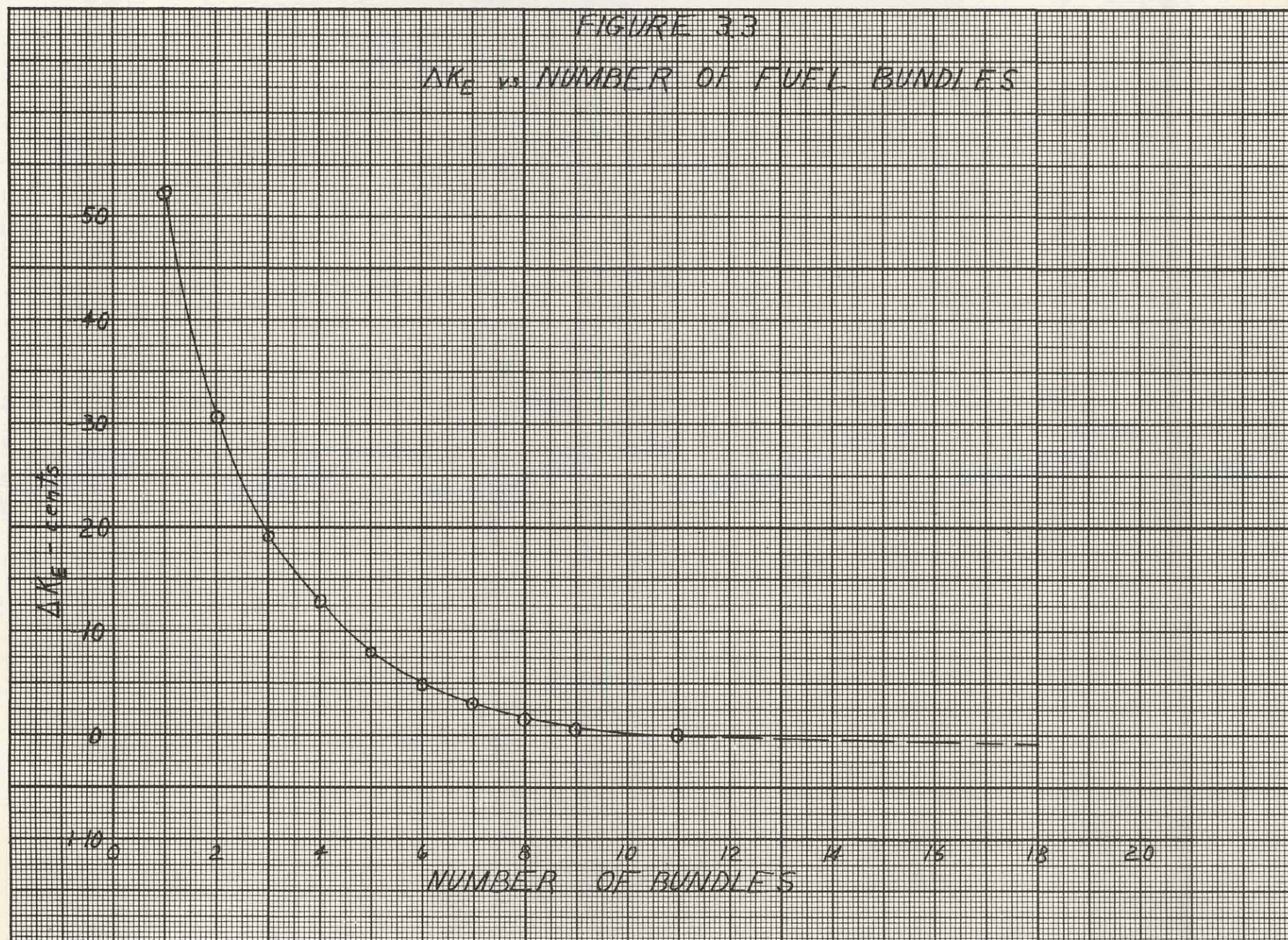
3.5.1 Procedure

The amount of B^{10} in the SM-1 was determined by taking the amount of B^{10} in the final mockup and adjusting it by use of the reactivity coefficients measured.

THIS PAGE
WAS INTENTIONALLY
LEFT BLANK

FIGURE 3.3

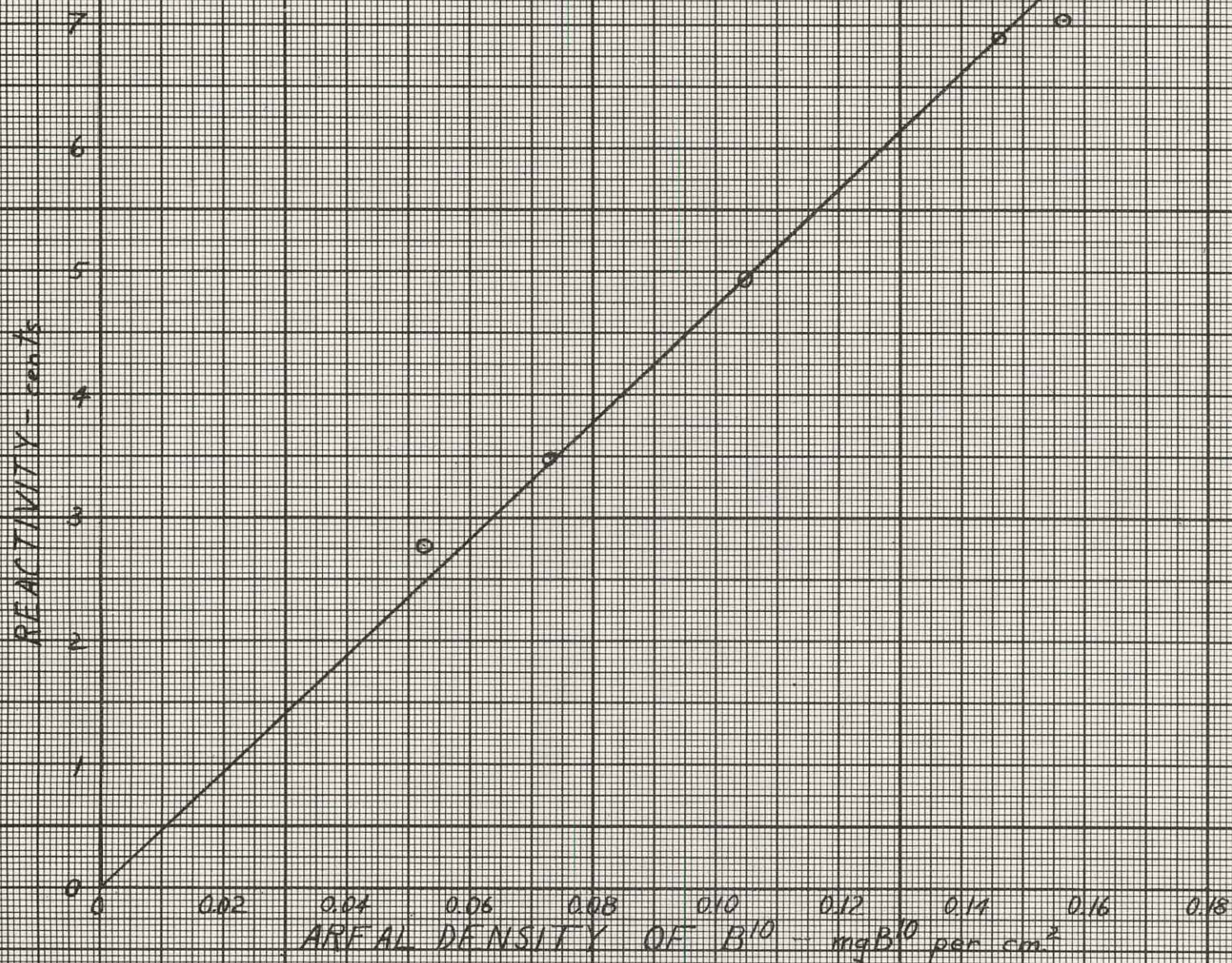
ΔK_E vs. NUMBER OF FUEL BUNDLES



THIS PAGE
WAS INTENTIONALLY
LEFT BLANK

FIGURE 3.4

AREAL DENSITY OF B^{10} vs. REACTIVITY



THIS PAGE
WAS INTENTIONALLY
LEFT BLANK

Since only two of the control rods were full out and the other five were almost fully inserted, the boron adjusting was done for the 38 stationary elements. The substitution measurements using a standard SM-1 element gave an exact determination of how the reactivity of an average stationary element should be changed to give a 5 rod bank position of 3.120 inches. The ratio of boron per stationary element to boron per control element was the same in the final mockup and the SM-1 (6). Therefore, in order to determine the total loading in the SM-1, the amount of boron in the final mockup control elements was adjusted proportionally to this ratio.

The substitution measurements using a standard SM-1 element gave a positive reactivity, i. e., these measurements indicated that the mockup core had too much boron. However, since the mockup had 5.32 grams of U^{235} too little in each stationary element, and the heterogeneity factor was negative, the resultant reactivity change indicated that the mockup core had less boron than the SM-1. This amount was calculated using the measured boron-10 material coefficient.

3.5.2 Data Compilation

Table 3.5 is a tabulation of the different factors in the boron determination for the SM-1. The probable errors indicated for the various quantities were calculated using the methods outlined in Appendix C.

TABLE 3.5
FACTORS IN BORON DETERMINATION

| | |
|--|--------------------------|
| Reactivity difference by substitution measurements | $+ 17.0 \pm 3.1$ cents |
| Reactivity difference due to uranium difference | $- 31.15 \pm 0.61$ cents |
| Reactivity difference due to heterogeneity factor | $- 22.7 \pm 8.0$ cents |
| Net reactivity difference | $- 36.9 \pm 8.6$ cents |
| Compensating Amount of B^{10} to be added to stationary elements | 0.61 ± 0.14 grams |
| Amount of B^{10} in mockup stationary elements | 13.17 ± 0.28 grams |
| Determined amount of B^{10} in SM-1 stationary elements | 13.78 ± 0.33 grams |
| Determined amount of B^{10} in SM-1 core | 15.84 ± 0.38 grams |

3.5.3 Comparison of Results with Chemical Analysis

Using the determined value of 15.84 grams of B^{10} in the SM-1 core, the percent loss of B^{10} based on a specified (6) amount of 20.29 grams is $22.0\% \pm$

1.9%. This agrees well with the results of chemical analysis by Martin Nuclear and ORNL⁽⁷⁾ which showed a 22.4% loss for fuel plates fabricated by ORNL.

The above analysis does not take into account any reactivity effect due to having the boron on the fuel plate surface instead of in the matrix. This reactivity effect was not taken into account since no experimental data was available.

CHAPTER 4 - SM-2 MOCKUP REACTIVITY EXPERIMENTS

4.1 Introduction

During the course of the program, various reactivity measurements were made on the cold clean SM-2 core mockup. Two different mockups were used during these experiments. The measurements made on the preliminary mockup included comparison of control rod arrays, rod bank calibrations, critical control rod configurations, and reflector effects. The core material coefficients, temperature coefficients, reflector effects, effect of rotating elements, and effect of substituting stationary elements for control rods were measured on the final mockup.

4.1.1 Preliminary Mockup

The core composition of the preliminary mockup is described in Appendix A, reference loading number 33. It contained 47.5 grams of B¹⁰. With a water reflector on all sides the 7 rod bank critical position was 5.738 inches withdrawn, and the average 7 rod bank worth was 283 cents per inch at 5.839 inches. The experiments discussed in sections 4.5.1, 4.6 and 4.7 were performed on this mockup with a water reflector.

4.1.2 Final Mockup

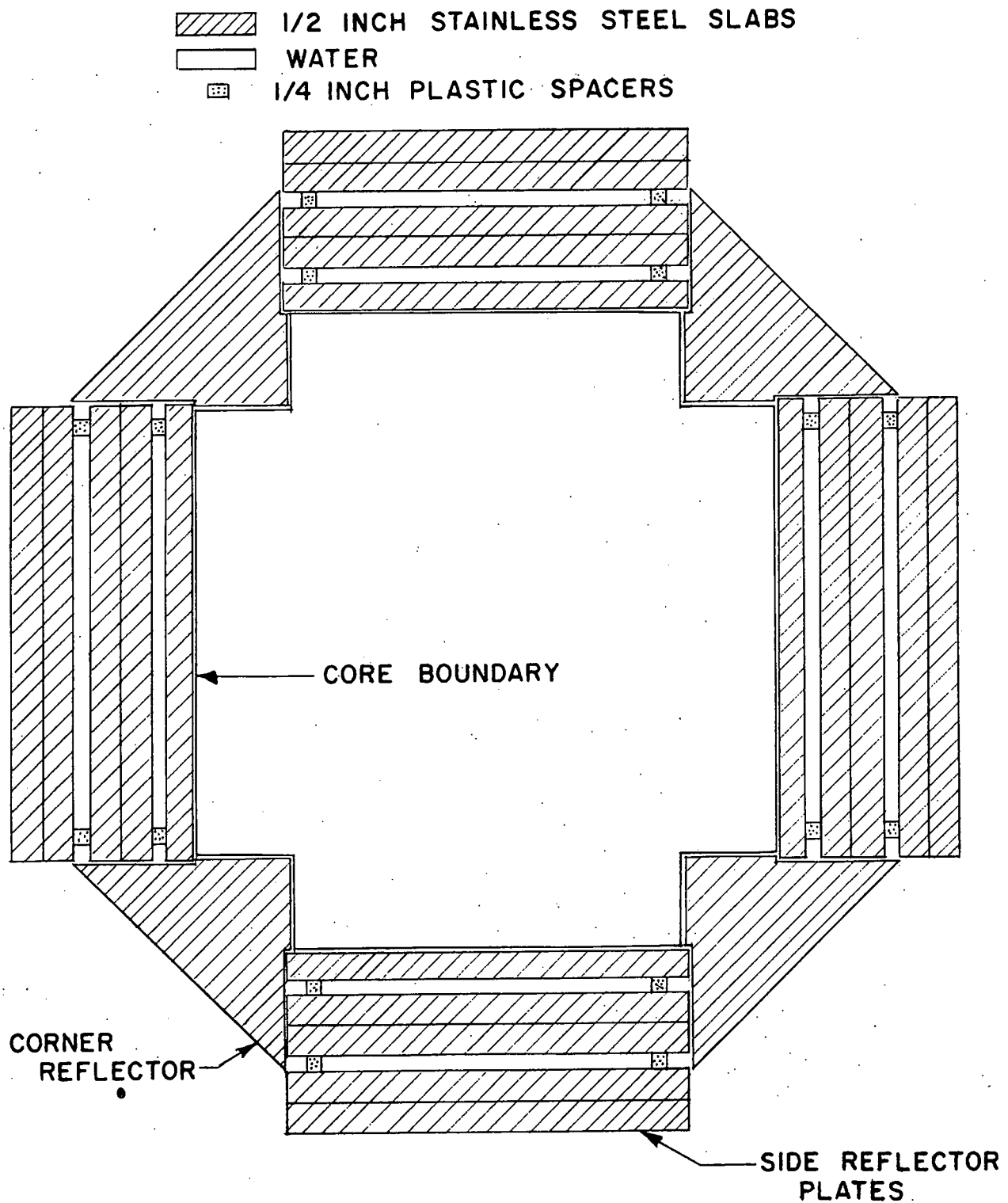
The core composition for this mockup is described in Appendix A, reference loading number 53. It contained 60.98 grams of B¹⁰. Unless otherwise noted, the reactor configuration for this mockup included the 2-1/2 inch laminated reflector on all four sides with four solid corners as described in Figure 4.1. The 7 rod bank critical position for this configurations was 6.974 inches withdrawn, and the average 7 rod bank worth was 263 cents per inch at 7.008 inches.

With a water reflector, the 7 rod bank critical position was 7.142 inches withdrawn and the average 7 rod bank worth was 283 cents per inch at 7.177 inches.

The reactivity measurements made on the two mockups are not listed separately, since the differences in the mockups are not large enough to cause an appreciable neutron spectrum shift, and hence do not appreciably affect the reactivity coefficients. Data obtained on mockups other than the final mockup with reflector as described in Figure 4.1, are so noted.

THIS PAGE
WAS INTENTIONALLY
LEFT BLANK

FIGURE 4.1
FULL REFLECTOR OF SM-2 MOCKUP
REFERENCE APPENDIX A
(Not Drawn To Scale)



THIS PAGE
WAS INTENTIONALLY
LEFT BLANK

4.2 Seven Rod Bank Evaluation

4.2.1 Bank Calibration

The bank calibration for the SM-2 core is derived from the numerous calibrations measured in the parametric study described in Chapter 2. Figure 4.2 is a composite of all the calibrations made during the critical experiment program, and assumes that the worth of the open 7 bank array in the 7 x 7 core is invariant to changes in metal-to-water ratio, uranium loading, boron loading, side plate thickness or reflector configuration within an experimental error expressed for a confidence interval of 95%.

However, when one compares the calibration curve at 68°F with one measured at higher simulated temperatures, Figure 4.3, a pronounced shift in calibration is noted as water is displaced by aluminum. The latter data were measured during the temperature coefficient experiments discussed in Section 4.3. Due to the large amount of aluminum added to the core for the temperature measurement and the consequent severe increase in metal-to-water ratio, it is likely that this shift was due to a hardening of the neutron spectrum.

4.2.2 Integral Worth

The integral of the calibration curve is shown in Figure 4.4. The total worth (ΔK_E) of the bank fully withdrawn is 33.18 ± 0.43 . Since the probable error of the integral is a function of the bank calibration and rod position, the reported error should be considered an end point value only.

4.2.3 Data Evaluation

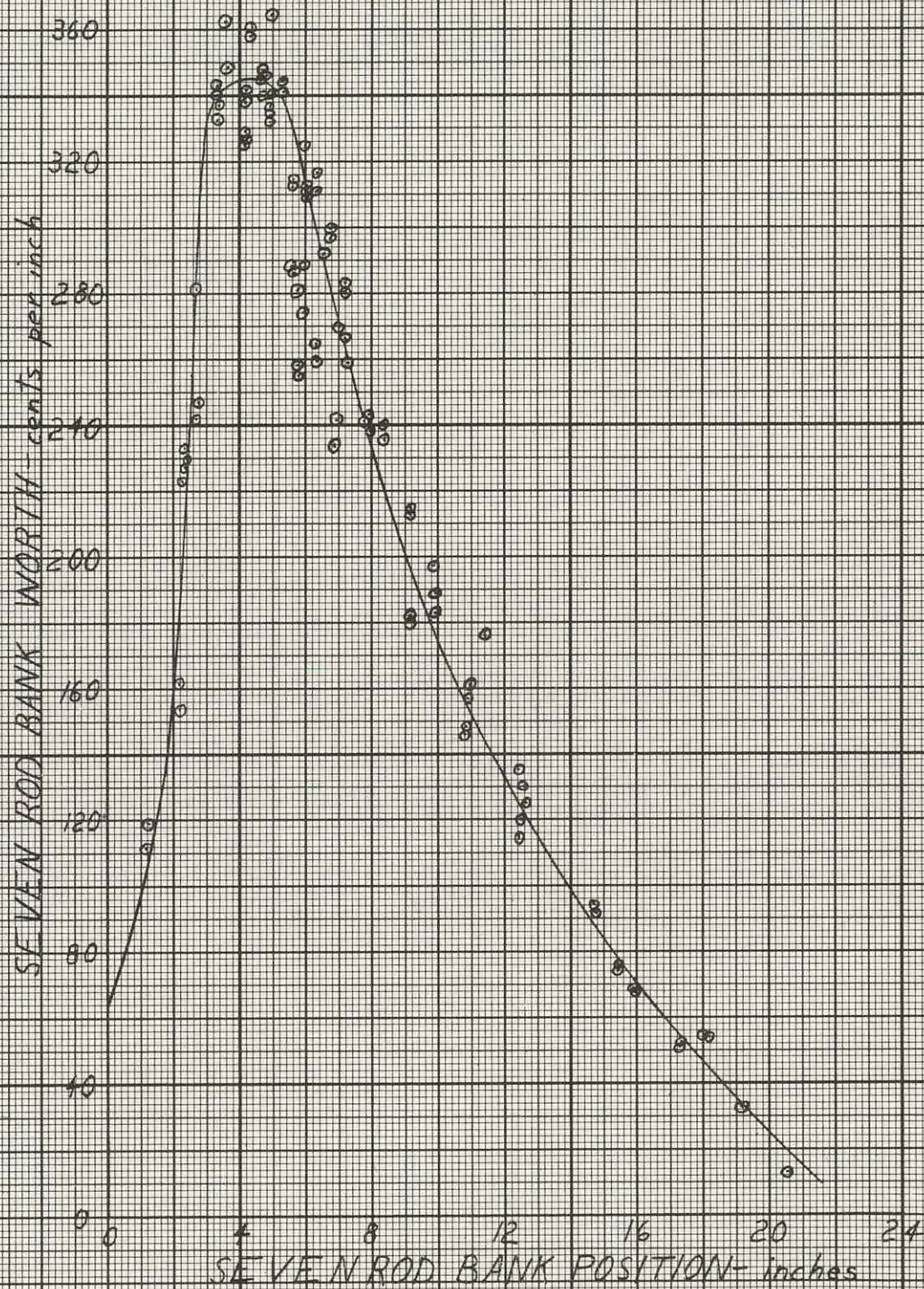
In Chapter 2, Figure 2.8, a curve of ΔK_E versus mass of B^{10} in the active core for the SM-2 configuration cases was presented. The ΔK_E values plotted on this curve were obtained by integrating the calibration curves, a function of metal-to-water ratio, for the various boron loadings. In order to evaluate the validity of the composite calibration curve, as drawn, Figure 4.5 was prepared with the excess reactivities determined by integration of the composite 7 rod bank worth curve.

The differences observed by a point by point comparison of the three SM-2 cases plotted in Figures 2.8 and 4.5 imply a reasonable agreement between, though not complete independence of, the alternate paths of integration. It would therefore seem that the assumptions made in drawing the composite curve are reasonable.

THIS PAGE
WAS INTENTIONALLY
LEFT BLANK

FIGURE 4.2

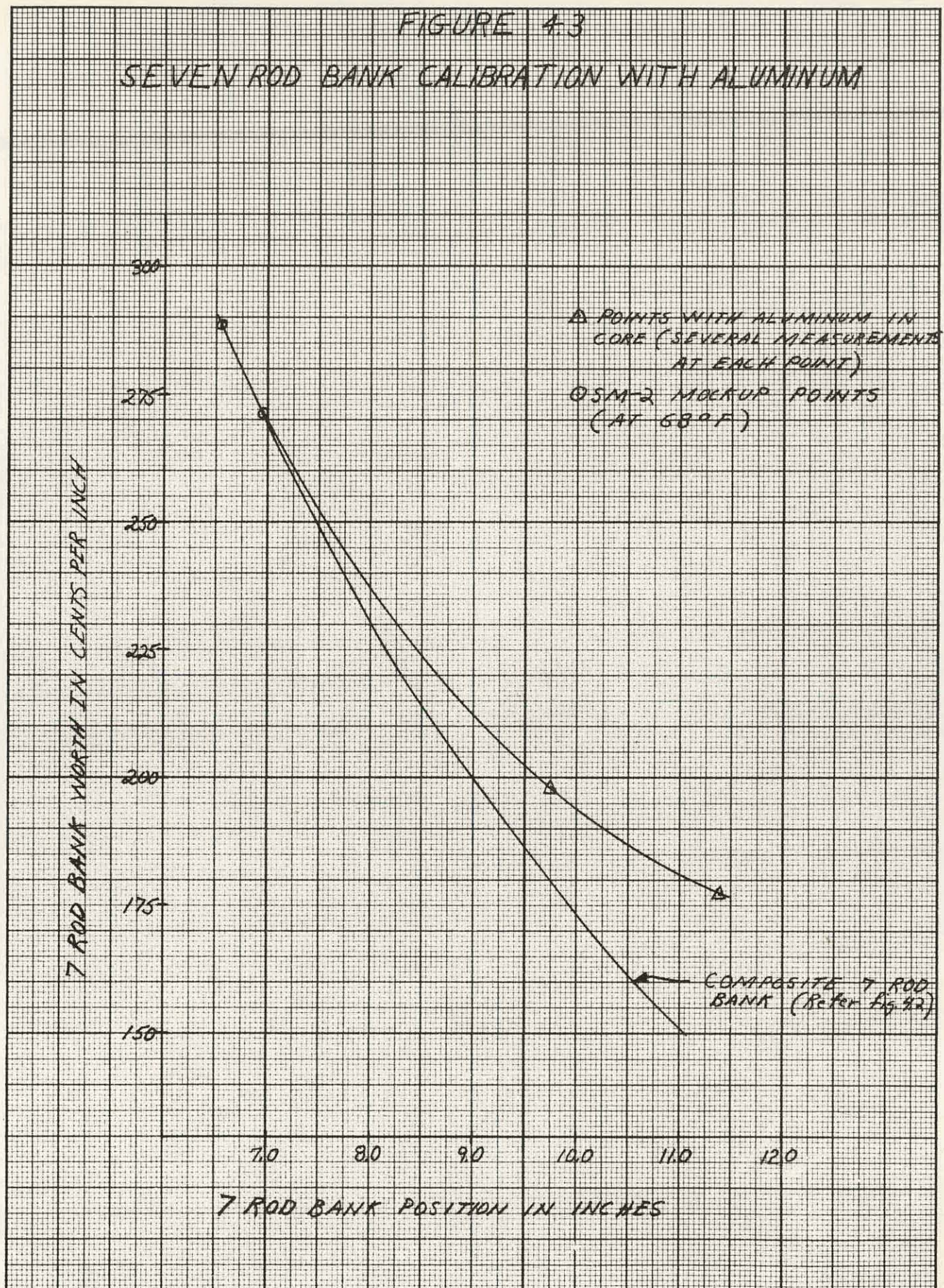
COMPOSITE SEVEN ROD BANK CALIBRATION



THIS PAGE
WAS INTENTIONALLY
LEFT BLANK

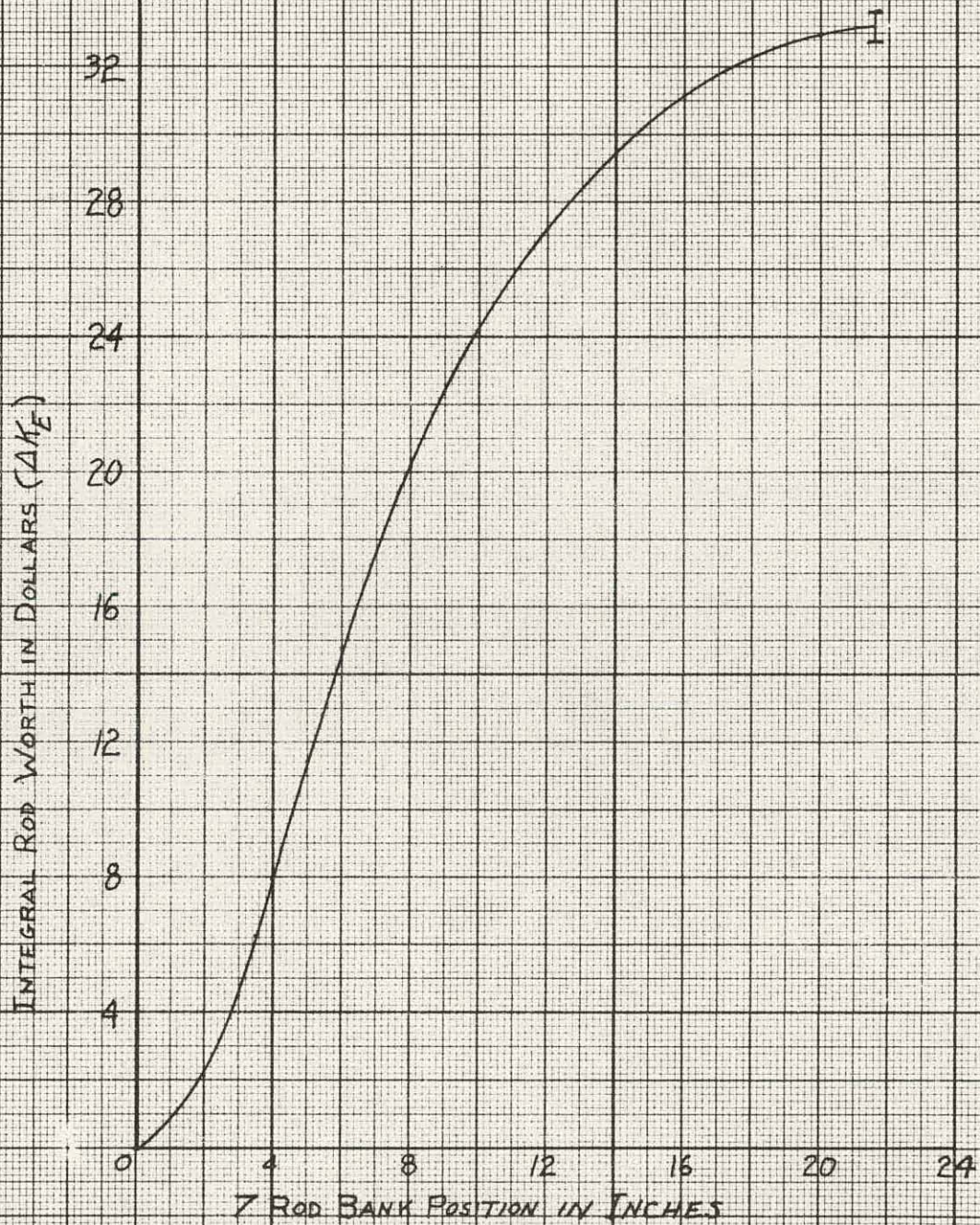
FIGURE 4.3

SEVEN ROD BANK CALIBRATION WITH ALUMINUM



THIS PAGE
WAS INTENTIONALLY
LEFT BLANK

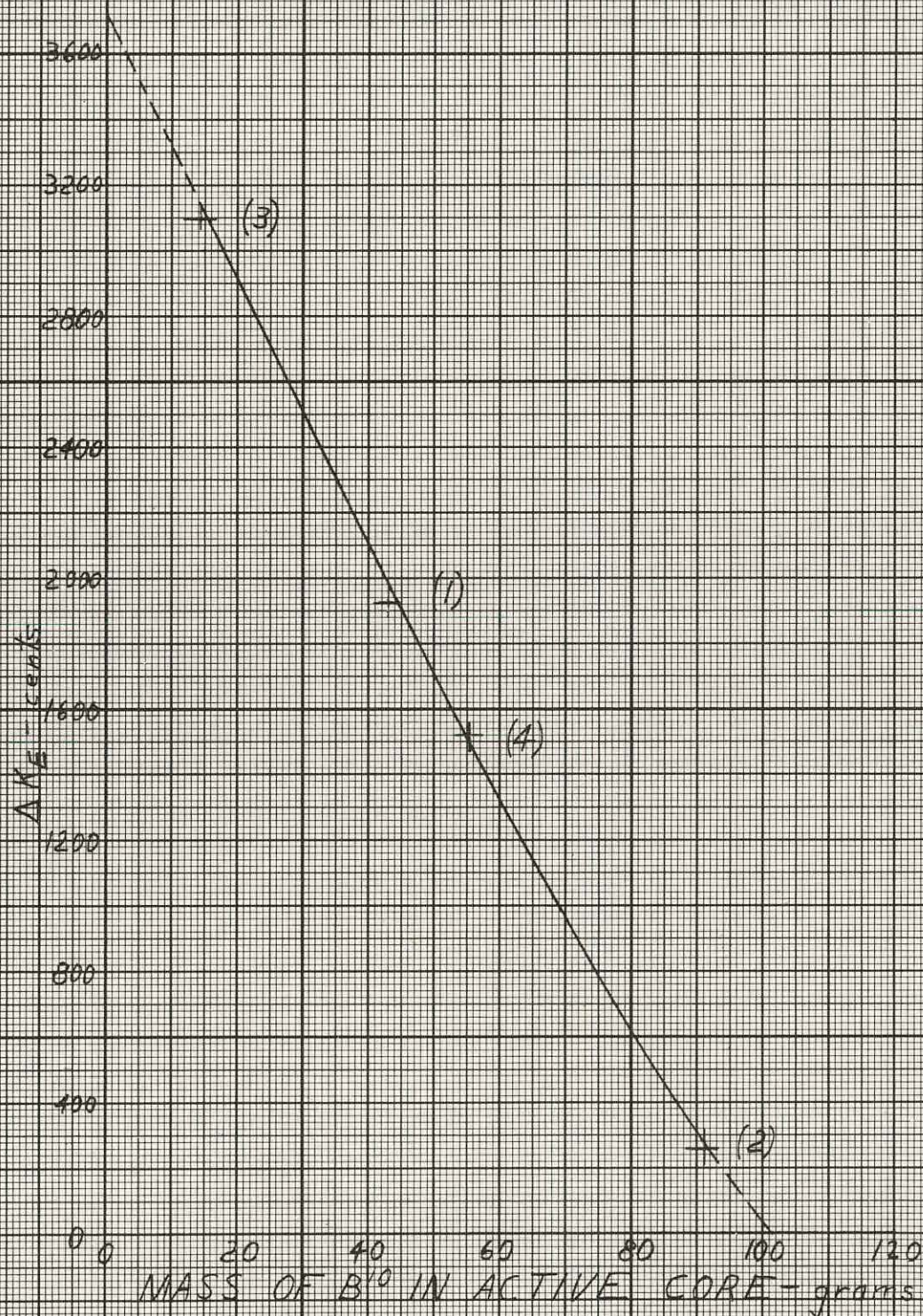
FIGURE 4.4
INTEGRAL SEVEN ROD BANK WORTH



THIS PAGE
WAS INTENTIONALLY
LEFT BLANK

FIGURE 4.5

ΔK_E vs. MASS OF B^{10} IN ACTIVE CORE



THIS PAGE
WAS INTENTIONALLY
LEFT BLANK

On this basis, the SM-2 final mockup ΔK_E was determined from Figure 4. 4 to be 15.20 ± 0.30 .

The error reported is a probable error in precision and assumes a truly statistical distribution of the points in Figure 4. 2. Some variances with metal-to-water ratio has already been admitted.

4. 3 Temperature Coefficients

It was not feasible to directly measure the temperature coefficients of the SM-2 over the temperature range desired (room temp. to 510°F). Therefore, two separate experimental methods were used, the results of which, together, describe the temperature coefficient of the SM-2 over the required range. For a temperature range from 68 to 155°F, the temperature coefficient, at normal atmospheric pressure, was directly determined by heating the water in the reactor tank. In order to determine the temperature coefficient above 155°F, aluminum strips were used to displace the water and thus simulate moderator temperatures up to 510°F. The measurements were made for the SM-2 (reference loading 53, Appendix A) with stainless steel reflector as described in Figure 4. 1.

4. 3. 1 Experimental Technique

The water in the reactor tank was heated by two 15 KVA immersion heaters. An agitator was employed to stir the water and insure a uniform temperature throughout the core. The water temperature was measured by four iron-constantan thermocouples located in the core. The thermocouples were connected directly to a Brown recorder. The print-out on the Brown recorder could be read within $\pm 0.1^\circ\text{F}$; however, the absolute temperature determination was only within $\pm 2.0^\circ\text{F}$.

The reactor was heated continuously, and the temperature plotted as a function of time. As the reactor temperature increased, the reactor period became negative. The reactor was then put on a long positive period and the 7 rod bank position recorded to ± 0.001 inches. The increasing temperature decreased the reactivity, returning the reactor to criticality. The exact time of criticality was noted to ± 0.5 minutes.

Aluminum strips 2.266 x 0.0154 x 23.0 inches were inserted between the fuel plates of the stationary and control rod fuel elements to displace water and thus simulate water temperatures up to 510°F. In the first three measurements aluminum strips were inserted in the stationary elements only, but in subsequent measurements the aluminum strips were added to both the stationary and control rod fuel elements.

The equivalent water temperatures were determined for both normal atmospheric pressure and 2000 psi. The density of water at 70°F at normal atmospheric pressure is the same as the density of water at 103.5°F and 2000 psi.

A measurement was made with aluminum strips in the center of the absorber sections equivalent to 510.2°F to determine the effect of reduced water density in that region.

The effect of decreasing the hydrogen density in the water gaps of the stainless steel reflector was measured by inserting styrene plastic sheets in the water gaps. The equivalent water temperature in the reflector for this measurement was 477°F, with the elements and absorber sections at 510°F.

4.3.2 Experimental Data

Table 4.1 presents the results of the heating measurements.

TABLE 4.1
HEATING MEASUREMENT

| Temp. °F | Run 1 | |
|----------|-----------------------------|--|
| | 7 Rod Bank Position, In. | Integrated ΔK_E from 69°F, Cents Negative |
| 69.0 | 6.978 | 0 |
| 91.9 | 6.996 | 4.89 |
| 96.5 | 7.002 | 6.5 |
| 99.9 | 7.009 | 8.4 |
| 103.1 | 7.015 | 10.0 |
| 107.2 | 7.021 | 11.6 |
| 111.5 | 7.030 | 14.0 |
| 114.2 | 7.037 | 16.0 |
| 117.6 | 7.045 | 18.2 |
| 120.8 | 7.056 | 21.1 |
| 123.8 | 7.063 | 23.0 |
| 126.4 | 7.072 | 25.5 |
| 128.3 | 7.080 | 27.6 |

TABLE 4. 1 (Cont' d)

| Temp. °F | Run 2 | |
|----------|-----------------------------|---|
| | 7 Rod Bank Position, In. | Integrated ΔK_E from 69° F, Cents Negative |
| 129. 6 | 7. 087 | 29. 5 |
| 133. 2 | 7. 101 | 33. 0 |
| 135. 5 | 7. 113 | 36. 2 |
| 137. 9 | 7. 124 | 39. 3 |
| 141. 2 | 7. 140 | 43. 5 |
| 144. 3 | 7. 152 | 46. 1 |
| Run 3 | | |
| 137. 8 | 7. 120 | 37. 5 |
| 140. 7 | 7. 130 | 40. 2 |
| 143. 9 | 7. 141 | 43. 2 |
| 147. 6 | 7. 152 | 46. 0 |
| 151. 5 | 7. 169 | 50. 6 |
| 154. 5 | 7. 181 | 54. 0 |
| 155. 7 | 7. 184 | 54. 5 |

Table 4. 2 presents the results of the aluminum measurements. Unless otherwise noted the measurements were made with aluminum in the stationary and control rod fuel elements.

TABLE 4. 2
ALUMINUM MEASUREMENTS

| Equivalent Temp. °F. at 2000 psi | 7 Rod Bank Position, In. | Integrated ΔK_E , Cents Negative |
|----------------------------------|-----------------------------|---|
| 103. 5* | 6. 978 | 0 |
| 128. 0** | 7. 041 | 17. 0 |
| 147. 4** | 7. 111 | 35. 6 |
| 165. 0** | 7. 178 | 53. 2 |
| 165. 0 | 7. 210 | 61. 8 |
| 180. 3 | 7. 277 | 79. 3 |
| 209. 3 | 7. 451 | 124. 0 |
| 292. 5 | 8. 068 | 274. 9 |
| 301. 0 | 8. 149 | 239. 9 |

* No aluminum in reactor, equivalent temperature for 2000 psi.

** Aluminum strips in stationary elements only. Equivalent temperature for stationary elements.

TABLE 4. 2 (Cont'd)

| Equivalent Temp. °F at 2000 psi | 7 Rod Bank Position, In. | Integrated ΔK_E , Cents Negative |
|------------------------------------|-----------------------------|---|
| 372. 9 | 8. 895 | 460. 9 |
| 435. 5 | 9. 722 | 631. 7 |
| 510. 2 | 11. 291 | 927. 9 |
| 510. 2*** | 11. 172 | 906. 5 |
| 510. 2**** | 11. 079 | 889. 7 |

*** Aluminum strips in absorber sections also. Equivalent temperature in center of absorber sections is same as for elements.

**** Aluminum strips in elements and absorbers. Hydrogen density in reflector decreased 18. 75% by use of styrene plastic. Equivalent reflector temperature at 2000 psi equals 477° F.

Table 4. 3 gives the 7 rod bank worth determined by period measurements with aluminum in the core.

TABLE 4. 3
SEVEN ROD BANK CALIBRATION

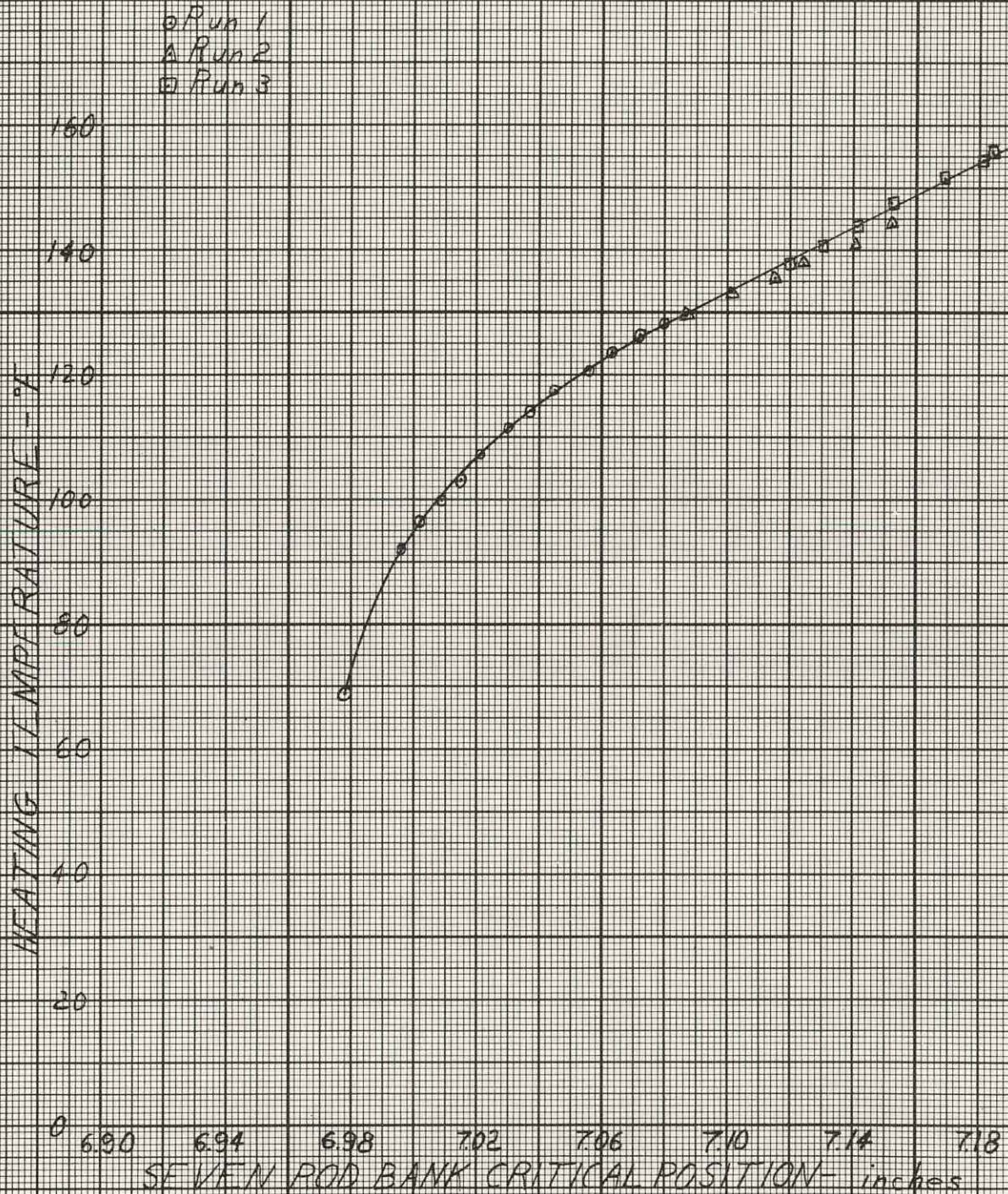
| Equiv. Temp., °F at 2000 psi | Bank Worth cents/ In. | Ave. Bank Position, In. |
|---------------------------------|--------------------------|----------------------------|
| 436. 0 | 197. 2 | 9. 748 |
| 510. 2 | 177. 3 | 11. 271 |

4. 3. 3 Discussion of Results

An inspection of Figure 4. 8 shows that above a temperature of 130° F the negative ΔK_E versus temperature curves obtained by heating the reactor water and inserting aluminum in the stationary and control elements are almost parallel. Therefore it was decided that the temperature coefficients reported here should be determined by the slope of the ΔK_E versus temperature curve obtained using aluminum for temperatures above 130° F. This method of normalization does not take into account the absorption of neutrons in the aluminum or the imperfect distribution of aluminum in the core.

FIGURE 4.6

SEVEN ROD BANK CRITICAL POSITION - vs
HEATING TEMPERATURE



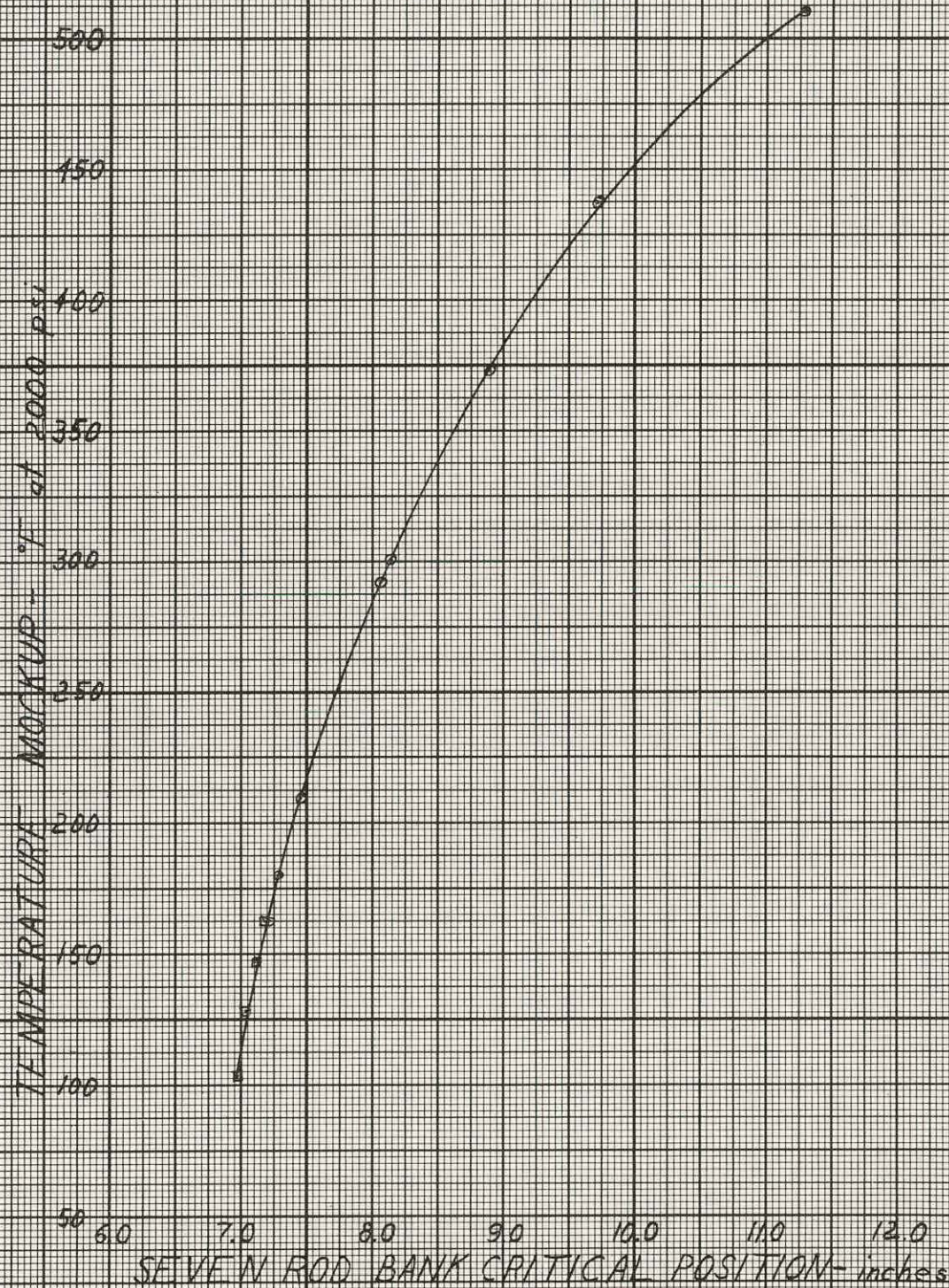
THIS PAGE
WAS INTENTIONALLY
LEFT BLANK

FIGURE 4.7

SEVEN ROD BANK CRITICAL POSITION

^{v.s.}
ALUMINUM EQUIVALENT TEMPERATURE AT
2000 PSI

- Stationary Elements Only
- Total Core



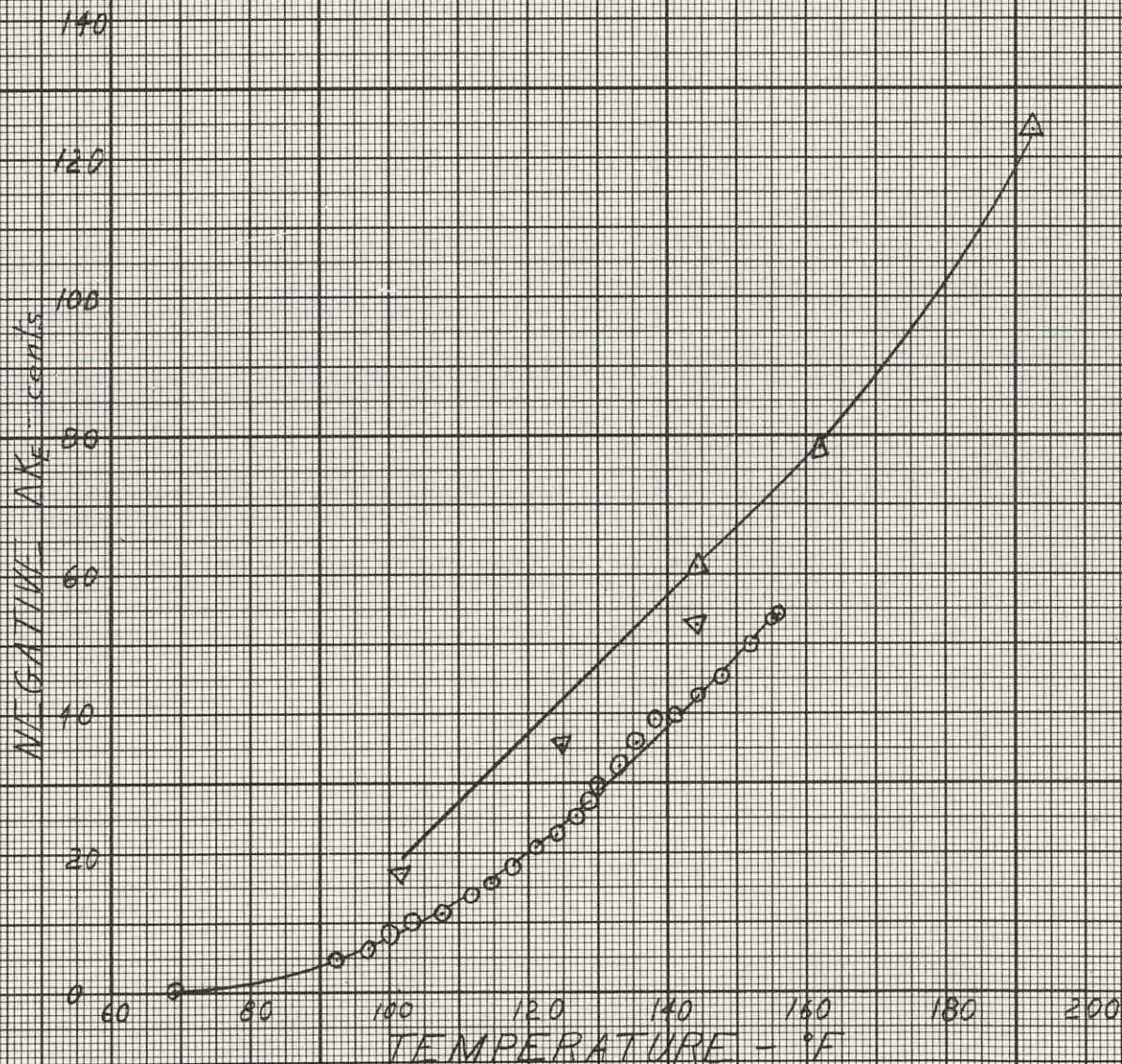
THIS PAGE
WAS INTENTIONALLY
LEFT BLANK

FIGURE 48

ΔK_F vs TEMPERATURE

Note: Aluminum points plotted at equivalent temperature for NAP

- Heating Points
- △ Aluminum Points
- ▽ Aluminum Points (stationary elements only)



THIS PAGE
WAS INTENTIONALLY
LEFT BLANK

However, the absorption cross section of aluminum is known to be small, and Figure 4.10, obtained using aluminum, is nearly linear as should be expected. Table 4.4 lists several temperature coefficients determined using this method. The slopes were taken from Figure 4.9.

TABLE 4.4
TEMPERATURE COEFFICIENTS

| Temp. °F. at 2000 psi | 7 Rod Bank Position/In. | Temp. Coefficients Cent/°F |
|--------------------------|-------------------------|-------------------------------|
| 150 | 7.150 | -1.15 |
| 370 | 8.850 | -2.50 |
| 510 | 11.291 | -5.20 |

It should be noted that the aluminum points plotted in Figure 4.8, 4.9 and 4.10 have aluminum in the stationary, or stationary and control elements only. The aluminum points with aluminum in the absorber sections and styrene in the reflector were not plotted since they were obtained at 510°F equivalent temperature only.

From Table 4.2 it is seen that displacing water from the absorber section centers results in a positive ΔK_E of 21.4 cents. Also, the effect of decreasing the water density in the reflector gaps to an equivalent 477°F is 16.8 cents positive. The determined negative ΔK_E due to increasing the core temperature, at 2000 psi, from 103.5°F to 510.2°F, and the reflector temperature from 103.5°F to 477°F, measured by displacing water with aluminum, is 889.7 cents.

The ΔK_E integrals were computed using the 7 rod bank calibration curve obtained with aluminum in the core. (Figure 4.3).

4.4 Core Material Coefficients

4.4.1 Experimental Technique

Individual periods were used throughout in determining rod worths and reactivity differences. All material coefficients were determined at room temperature and pressure, in reference loading 53.

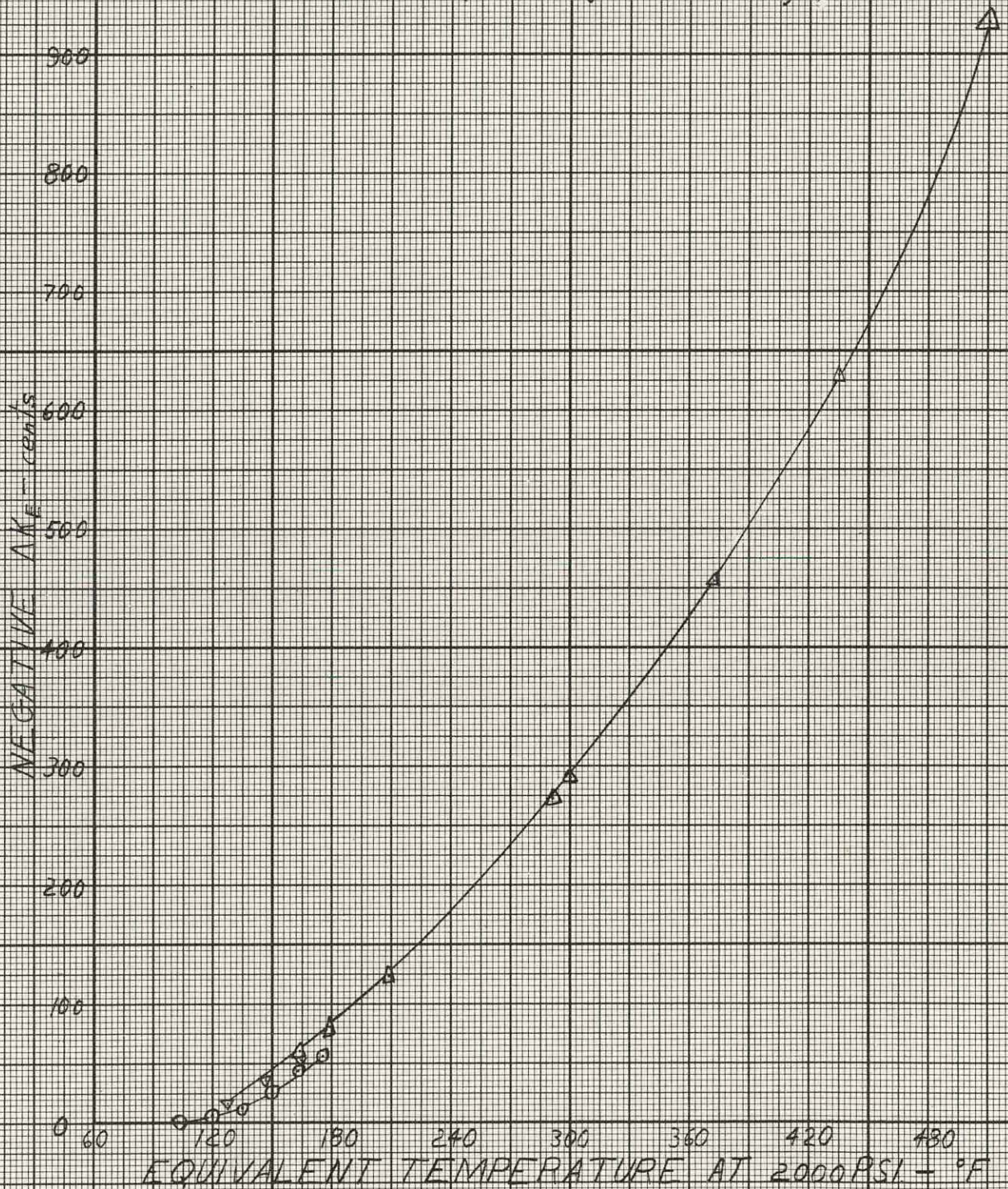
In determining the boron and uranium coefficients, a standard SM-1 element was substituted in the core for element #72 and a critical bank position obtained. Using this as a reference point, element #72 was then

THIS PAGE
WAS INTENTIONALLY
LEFT BLANK

FIGURE 4.9

ΔK_E vs. EQUIVALENT TEMPERATURE AT 2000 PSI.

- Heating Points
- △ Aluminum Points
- ▽ Aluminum Points (stationary elements only)



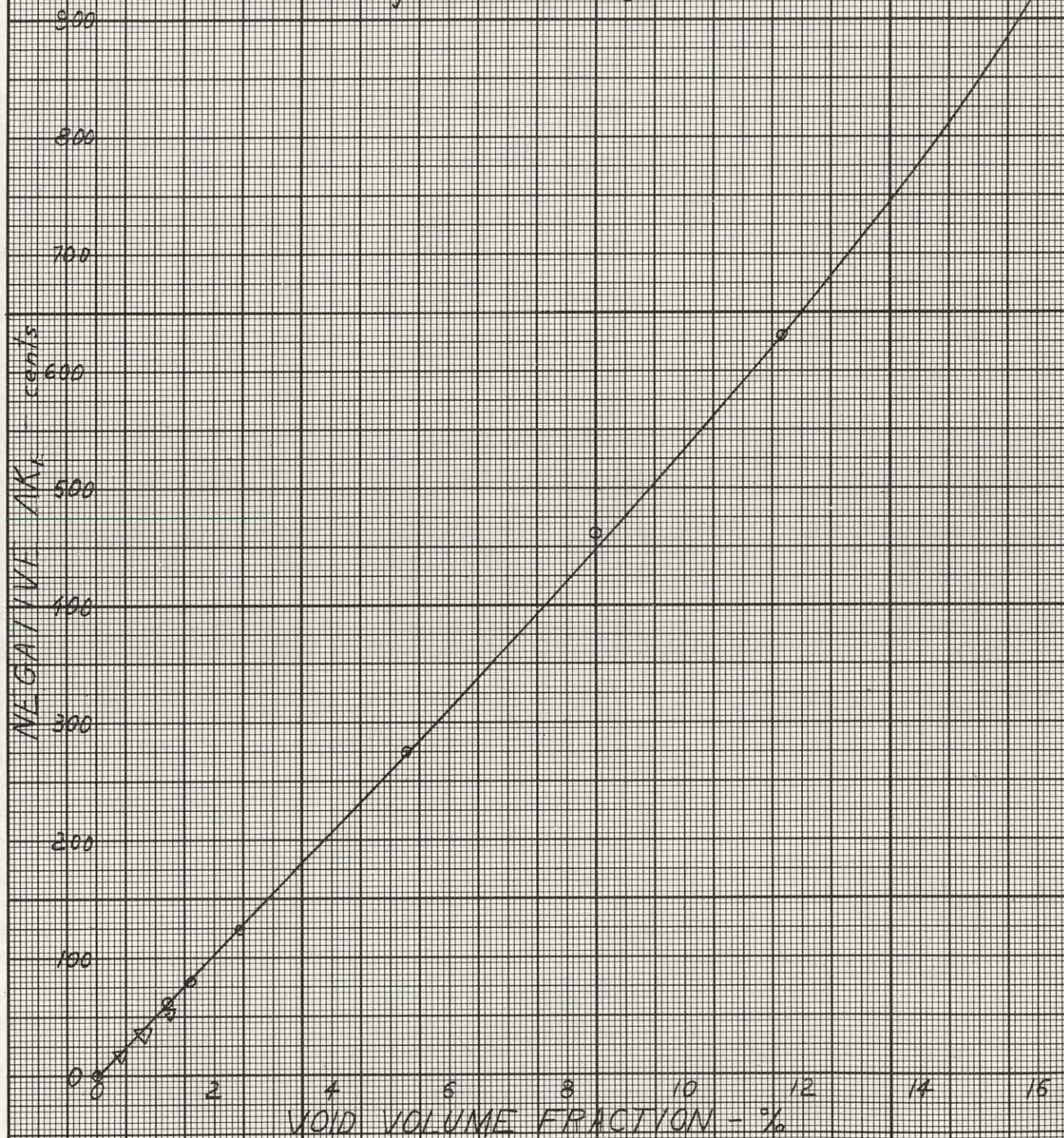
THIS PAGE
WAS INTENTIONALLY
LEFT BLANK

FIGURE 410

ΔK_F vs VOID VOLUME FRACTION IN CORE

Note: Void Mocked-Up with Aluminum

○ Stationary and Control Elements
 ▽ Stationary Elements Only



THIS PAGE
WAS INTENTIONALLY
LEFT BLANK

employed as a standard substitution element. Measurements were made in the fourth quadrant of the core, and core symmetry was used to calculate average coefficients for the whole core.

4.4.2 Boron Reactivity Coefficients

To measure the reactivity coefficient of boron, element #72 was stripped clean of boron and substituted for elements in other core positions. The uranium loading was held constant. These measurements indicated that B^{10} in the core was worth an average of 42.54 cents per gram.

TABLE 4.5
REACTIVITY COEFFICIENTS OF BORON -10

| <u>Element Position</u> | <u>B^{10} Worth in Cents/grams</u> |
|-------------------------|---|
| 45 | 87.5 |
| 46 | 58.9 |
| 47 | 25.5 |
| 54 | 87.7 |
| 55 | 79.5 |
| 57 | 22.6 |
| 65 | 57.0 |
| 66 | 38.6 |
| 67 | 14.6 |
| 74 | 28.0 |
| 75 | 25.6 |
| 76 | 17.0 |

4.4.3 Uranium Reactivity Coefficients

For the uranium measurements, element #72 was loaded with ten regular SM-2 fuel plates and eight depleted fuel plates. The total uranium loading was then 463.9 grams in element #72.

Boron -10 was also added in the proper amount to maintain the B^{10} loading constant during these measurements. In this manner a known amount of 369.5 grams U^{235} was removed in each element substitution and reactivity changes measured. Table 4.6 presents the results of these measurements. The average uranium worth for the core is 0.157 cents per gram.

TABLE 4. 6
REACTIVITY COEFFICIENTS OF URANIUM U²³⁵

| <u>Element Position</u> | <u>U²³⁵ Worth in Cents/gram</u> |
|-------------------------|--|
| 45 | 0. 312 |
| 46 | 0. 220 |
| 47 | 0. 098 |
| 54 | 0. 321 |
| 55 | 0. 295 |
| 57 | 0. 084 |
| 65 | 0. 211 |
| 66 | 0. 146 |
| 67 | 0. 057 |
| 74 | 0. 110 |
| 75 | 0. 098 |
| 76 | 0. 067 |

4. 4. 4 Polystyrene Measurements

The effect of the plastic side plate grooves on core reactivity was determined by adding extra polystyrene to the core in the form of sheets placed between the side plates of adjacent elements. The worth of 195. 67 in.³ of polystyrene was 0. 57 cents negative. This indicates that the total volume of side plate grooves (267. 78 in.³) is worth less than 1 cent in reactivity.

4. 4. 5 Conclusions

Inspection of the data in Tables 4. 5 and 4. 6 indicates an almost linear relationship between the two material worths as a function of position in the core. The consistency of this data with the APAE 21⁽⁵⁾ and ORNL-2128⁽⁸⁾ data for U²³⁵ and B¹⁰ is noteworthy.

The polystyrene data verifies the minimal reactivity effect assumed for the side plate grooves. For all practical purposes, these grooves can be considered the same as water in the core.

4. 5 Reflector Measurements

4. 5. 1 Preliminary Mockup - Open 7 and Closed 7 Array

Using the water reflected preliminary mockup as a reference, various steel reflector thicknesses were studied. With an open 7 control rod array,

the worths of 1/8 and 1/4 inch reflectors were measured by placing 1/8 and 1/4 inch thick sheets of carbon steel on one side and one corner of the active core. The worths of these reflectors on four sides and four corners were determined by factoring the results for the one side, one corner measurements by four. The worth of a two inch reflector was also measured. The reflector configuration was the same as shown in Figure 4. 1 except the sides had 1 inch of SS, 1/4 inch of water, and 1 inch of SS lamination instead of that shown.

With a closed 7 control rod array the two inch reflector worth was measured using a 5 and a 7 rod bank. The reflector was identical to the two inch reflector described in Section 4. 5. 1. The reflector worth data for both the open and the closed 7 rod array are tabulated in Table 4. 7.

TABLE 4. 7
REFLECTOR EFFECTS VERSUS CONTROL ROD ARRAY

| <u>Control Rod Array</u> | <u>Reflector Worth Cents</u> | | |
|--------------------------|------------------------------|----------------------|--------------------|
| | <u>1/8 in. steel</u> | <u>1/4 in. steel</u> | <u>2 in. steel</u> |
| Open 7 | | | |
| 7 Rod Bank | -50. 2 | -62. 1 | +39. 7 |
| Closed 7 | | | |
| 7 Rod Bank | --- | --- | +50. 4 |
| 5 Rod Bank* | --- | --- | +45. 3 |

* Rods F and G fully withdrawn

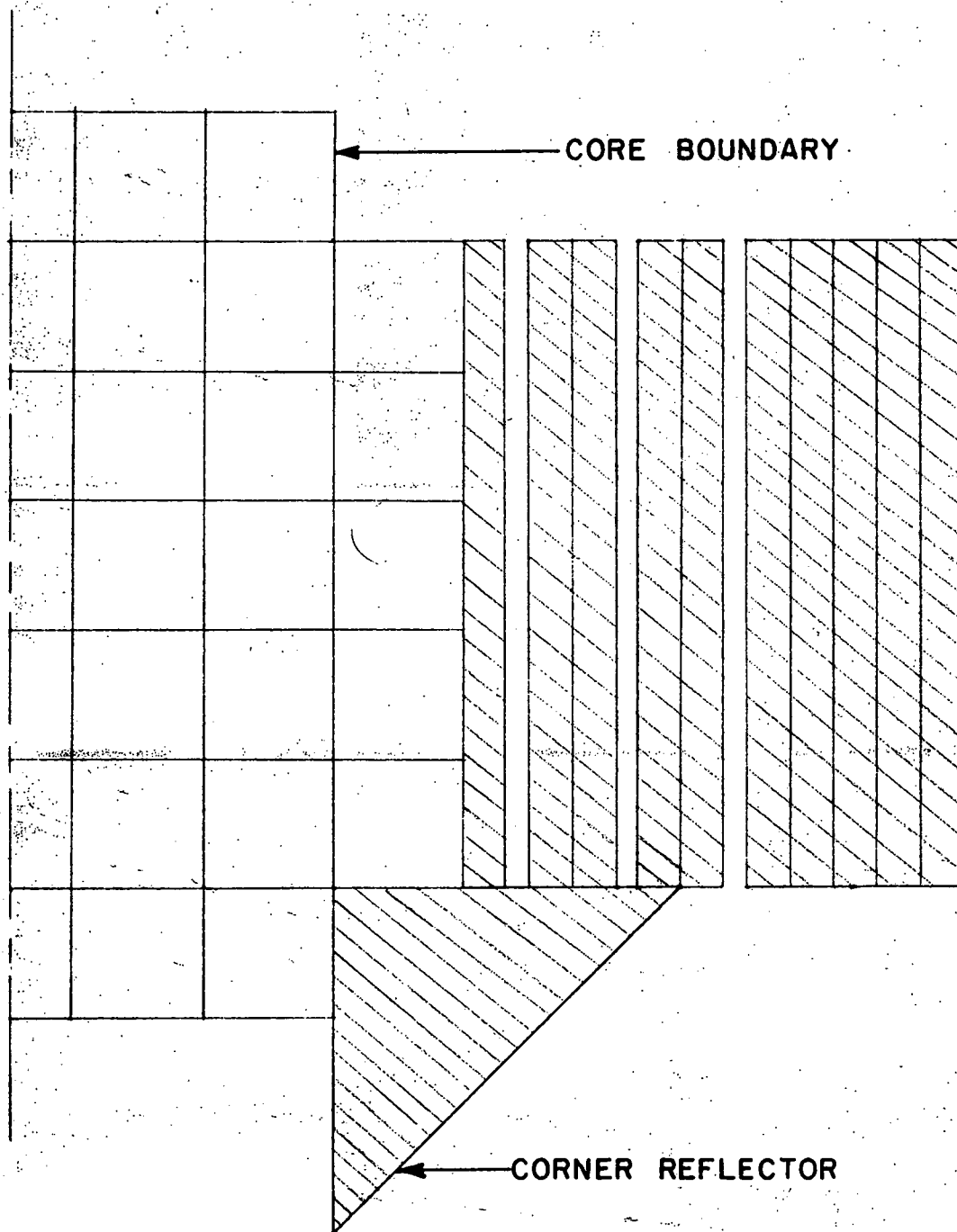
4. 5. 2 Final Mockup - Open 7 Array

During the final mockup experiments, more complete reflector measurements were made. Figure 4. 11 shows how the side reflector was assembled for steel thicknesses up to 5 inches.

Since the maximum steel available allows for only 2-1/2 inches of steel on all 4 sides, data were obtained for both four sides, four cornered reflection, and two adjacent sides-two corner reflection. Figure 4. 12 describes the reactivity effects of the design lamination of steel and water side reflectors and solid steel corner reflectors. The preliminary mockup reflector points are also plotted in Figure 4. 12. It should be noted that all the final mockup reflectors had the same corner reflectors, i. e. , even though the side reflectors

THIS PAGE
WAS INTENTIONALLY
LEFT BLANK

FIGURE 4.II

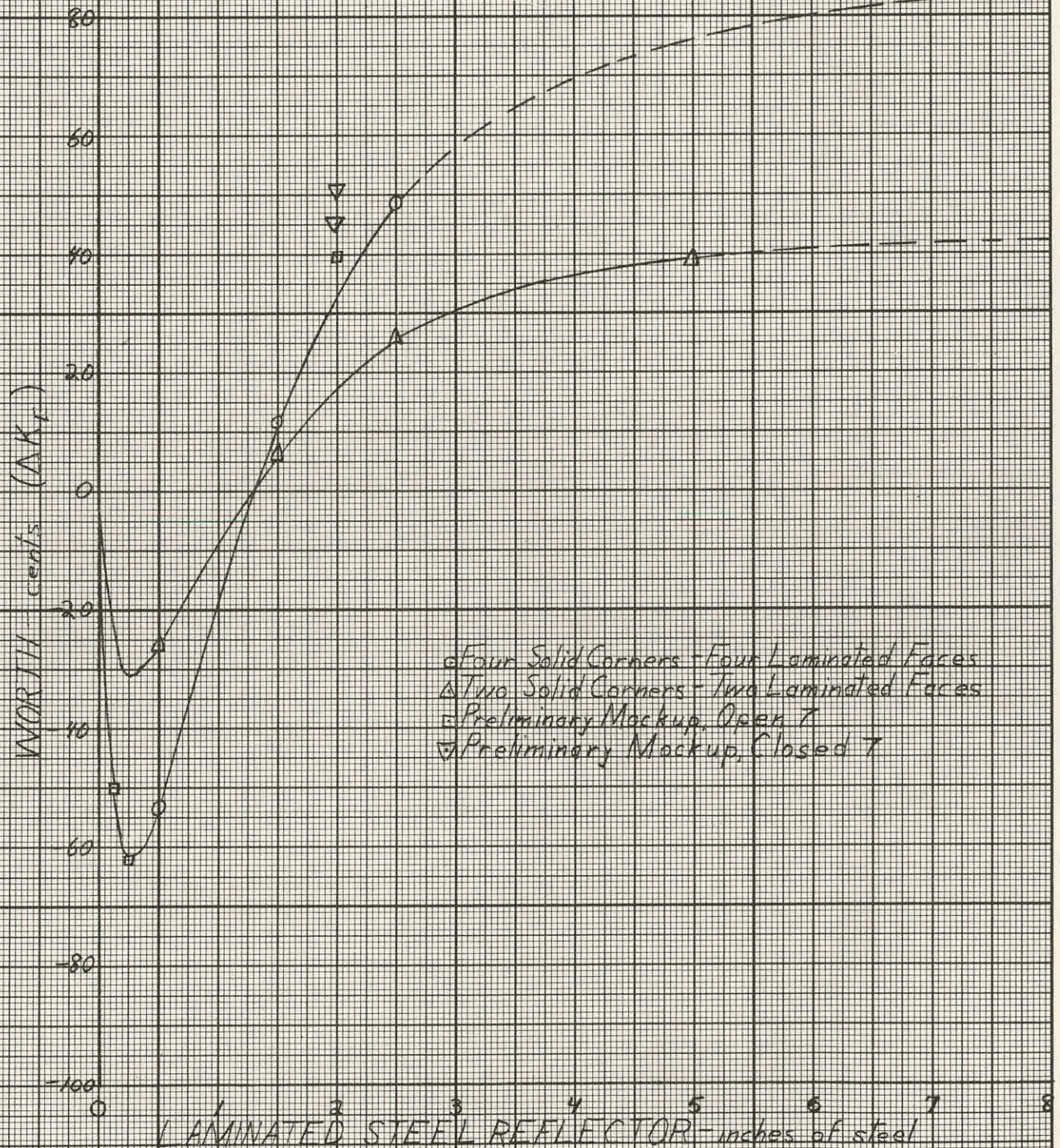


LAMINATED STEEL REFLECTOR
ASSEMBLY

THIS PAGE
WAS INTENTIONALLY
LEFT BLANK

FIGURE 4.12

ΔK_F vs. LAMINATED STEEL REFLECTOR THICKNESS
COLD CLEAN SM-2 MOCKUP



THIS PAGE
WAS INTENTIONALLY
LEFT BLANK

varied in thickness, the thickness of the corners remained constant. If the reflector corners had been varied in thickness the shape of the curve in Figure 4.12 would change slightly. Table 4.8 presents the data.

TABLE 4.8
EFFECT OF VARYING REFLECTOR THICKNESS FOR THE
OPEN 7 CONTROL ROD ARRAY

| Laminated Reflector Thickness Inches of Steel | ΔK_E - Cents | |
|--|----------------------|--------------------|
| | 4 Sides, 4 Corners | 2 Sides, 2 Corners |
| 0.5 | -53.5 | -26.2 |
| 1.5 | +11.6 | +6.3 |
| 2.5 | +48.5 | +25.9 |
| 5.0 | | +38.9 |

The data overlap shown in Table 4.8 indicates a ratio of almost a factor of two for the reactivity effect of 4 sided-4 cornered reflectors to 2 sided-2 cornered reflectors. This factor applied in the thick reflector region resulted in a four side-four cornered laminated reflector worth not exceeding +85.0 cents in the SM-2 final cold clean mockup. The nature of the curves presented is such that this treatment should be viewed with reasonable confidence.

4.6 Control Rod Array Evaluation

The control rod array evaluation measurements were made on the preliminary mockup. For comparison, the critical positions for the open 7 and closed 7 bank arrays are tabulated in Table 4.9.

TABLE 4.9
CRITICAL BANK POSITION VERSUS CONTROL ROD ARRAY

| Control Rod Array | Critical Bank Position, Inches | |
|-------------------|--------------------------------|---------------------|
| | Water Reflector | 2 inch SS Reflector |
| Open 7 | | |
| 7 Rod Bank | 5.738 | 5.598 |
| Closed 7 | | |
| 7 Rod Bank | 5.681 | 5.500 |
| 5 Rod Bank* | 4.180 | 3.910 |

* Rods F and G fully withdrawn

An inspection of Table 4.9 shows that the open 7 rod array has a higher initial critical bank position. However, with the bank calibration data obtained for the closed 7 array it is not possible to determine which control rod array controls the greater excess reactivity. Rather, one should compare the integral rod bank worth of the closed 7 rod array with the integral rod bank worth of the open seven array, by generating a calibration curve similar to Figure 4.2 for the closed 7 array. However, the critical rod configurations described in Section 4.7 imply that the open 7 array is slightly more reactive than the closed 7 array.

4.7 Critical Control Rod Configurations

Tables 4.10 and 4.11 present the critical control rod configurations and rod worths for various cases of both open and closed 7 arrays. All cases had an infinite water reflector on all sides of the core. Rods omitted in the tables were fully inserted.

TABLE 4.10
CRITICAL ROD CONFIGURATIONS - OPEN 7 ARRAY

| Case | Rods Withdrawn 21.56" | Critical Rod | Critical- Position-inches | Worth - Cents/in. |
|------|--------------------------|--------------|------------------------------|-----------------------|
| 1 | C | D | 11.700 | 50.4 @ 11.982 inches |
| 2 | C | E | 14.420 | 29.6 @ 14.855 inches |
| 3 | E | C | 14.580 | 29.75 @ 15.029 inches |
| 4 | E | F | 13.883 | 46.0 @ 14.153 inches |
| 5 | A, E | F | 4.271 | 34.2 @ 4.710 inches |
| 6 | B, E | D | 9.405 | 45.4 @ 9.733 inches |
| 7 | *D | E | 12.353 | 37.5 @ 12.758 inches |
| 8 | A, *D | C | 3.850 | 30.0 @ 4.295 inches |
| 9 | A, *D | E | 5.800 | 24.5 @ 6.298 inches |
| 10 | E, G | D | 6.733 | 52.4 @ 7.051 inches |

* Rod D maximum withdrawal 20.435 in.

TABLE 4.11
CRITICAL ROD CONFIGURATIONS - CLOSED 7 ARRAY

| | | | | |
|---|------|---|--------|-----------------------|
| 3 | F | A | 13.335 | 49.95 @ 13.647 inches |
| 4 | A | F | 11.316 | 36.6 @ 11.751 inches |
| 5 | A | B | 13.093 | 27.0 @ 13.609 inches |
| 6 | B | A | 13.495 | 29.6 @ 13.937 inches |
| 1 | F, G | D | 12.001 | 38.7 @ 12.452 inches |

The following pairs of rods fully withdrawn were subcritical:

C and D, A and E, F and C, F and D, and D and A.

It should be noted that the critical control rod configurations were obtained using the preliminary mockup; however, this data is conservative from a reactivity standpoint since the critical position of the final mockup had the rods further withdrawn.

4.8 Miscellaneous Reactivity Measurements

4.8.1 Effect of Rotating Elements

Elements 12, 13, 14, 15, 16, 72, 73, 74, 75, and 76 were rotated 90° to the normal element orientation with the boron tape facing the West side of the core (ref. Appendix A). This change was worth 8.91 cents negative.

4.8.2 Effect of Substituting Stationary Elements for Control Rods

Using the standard SM-1 element in position #72, critical six rod bank positions were taken and calibrations made with rods A, B, and C fully withdrawn in turn. Element #72, with its normal uranium and boron loading, was then substituted for rods A, B, and C respectively, and new critical positions and calibrations determined.

The substitution element differed from the control rods, having 157.6 grams more U^{235} and 0.34 grams more B^{10} . Table 4.12 shows the results of these measurements.

TABLE 4.12
EFFECT OF SUBSTITUTING STATIONARY FUEL ELEMENTS

| | 6 Rod Bank Critical Position | 6 Rod Bank Worth- cents/in. | Worth- cents |
|---------------------------------------|---------------------------------|--------------------------------|-----------------|
| Rod A withdrawn | 5.914" | 209 @ 5.945 " | +37.6 |
| #72 substitution in Rod A position | 5.733" | 206 @ 5.767" | |
| Rod B withdrawn | 6.175" | 239 @ 6.207" | +36.0 |
| #72 substitution in Rod B position | 6.022" | 231 @ 6.061" | |
| Rod C withdrawn | 5.720" | 217.5 @ 5.775" | +43.6 |
| #72 substitution in Rod C position | 5.520" | 219.0 @ 5.560" | |

Inspection of Table 4.12 reveals essentially no change in the bank calibration due to the substitutions made. The core is, as expected, more reactive due to the extra fuel in the substitution element.

CHAPTER 5. - SM-2 MOCKUP NEUTRON FLUX MEASUREMENTS

5.1 Introduction

Bare gold, bare uranium, and cadmium covered uranium foils 0.25 inches in diameter were activated in the SM-2 cold clean mock-up. Gross neutron axial flux measurements and fine structure studies were made with both an infinite water reflector and with the laminated steel reflector described in Figure 4.1. The seven rod bank position for the former case was 7.14 inches; for the latter case 6.97 inches.

The cadmium covered uranium activations were taken to investigate spectral variations. The cadmium covers were 0.020 inches thick.

All gold activations were taken with the foils taped to plexiglass stringers and inserted in the water gap between plates "i" and "j" of each element. (See Appendix A for plate locations.) The uranium and cadmium covered uranium activations were made by taping the foils directly to the fuel plates (plate "i" in each element unless otherwise stated). Figure 5.1 shows a fuel plate instrumented in this manner. These foils were placed on the south side of the plates in accordance with the core orientation of Figure A-1 in Appendix A. The centers of the foils were positioned with an accuracy of ± 0.020 inches.

The following nomenclature is used in this chapter to accurately define foil locations.

5.1.1 Position - location of foil measured from the bottom of the active core in inches.

5.1.2 Axial plane - plane perpendicular to the core axis and measured from the bottom of the active core in inches.

5.1.3 Radial plane - plane parallel to the north - south plane of the core, measured from the central radial plane.

5.1.4 Central radial plane - that plane parallel to the north-south plane of the core and passing through the core center line.

Figure 5.2 shows the locations of various radial planes in the west side of the core, these planes being perpendicular to the plane of the figure. In the following tables, W.R.P. stands for west radial plane; E.R.P. stands for east radial plane.

All activities unless otherwise noted are normalized to the core average = 1.00.

THIS PAGE
WAS INTENTIONALLY
LEFT BLANK

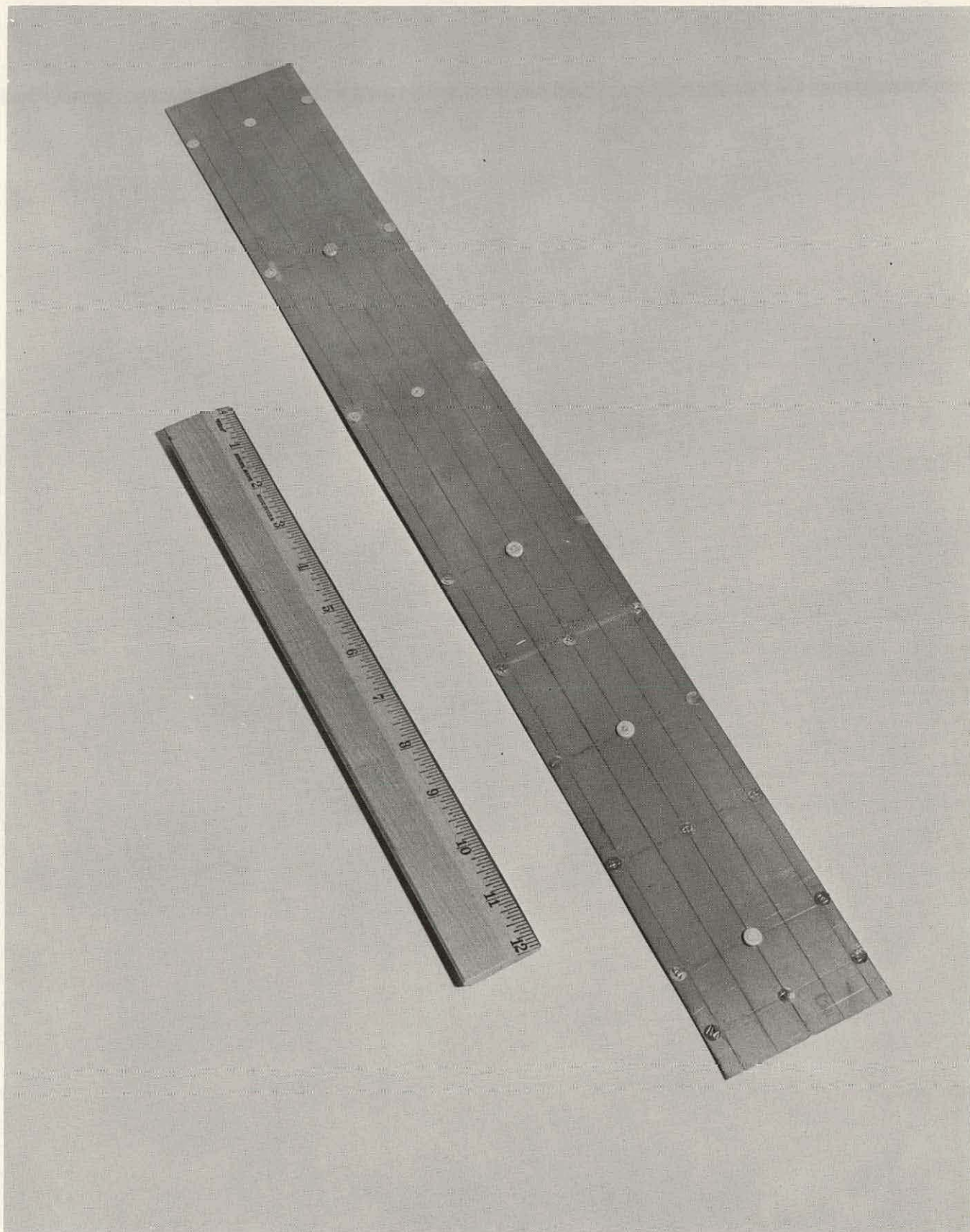


FIG. 5.1 - INSTRUMENTED FUEL PLATE

THIS PAGE
WAS INTENTIONALLY
LEFT BLANK

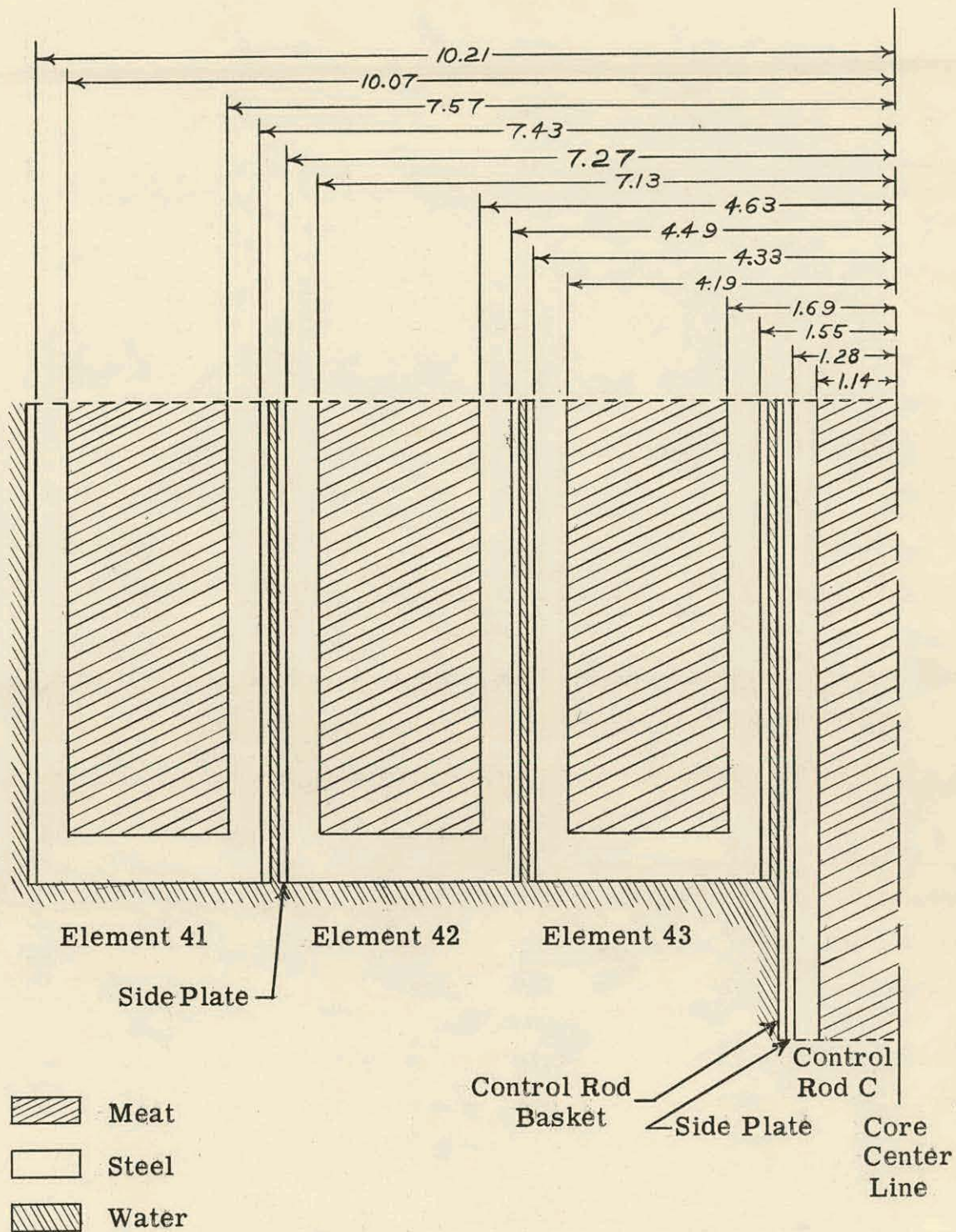


FIGURE 5.2
LOCATION OF RADIAL PLANES
Section of Core Through Center of Elements 41, 42, 43, and 44

THIS PAGE
WAS INTENTIONALLY
LEFT BLANK

5.2 Axial Traverse

5.2.1 Water Reflected

Tables 5.1 through 5.8 list all the foil measurements made for the water reflected case. Figures 5.3 and 5.4 show only the axial traverses made in elements 31, 33, 34, 41, 42, and 43 with gold foils.

5.2.2 Steel Reflected

Tables 5.9 through 5.14 list all the foil measurements made for the laminated steel reflected case. Figures 5.5 and 5.6 show only the axial traverses made in elements 31, 33, 34, 41, 42 and 43. As indicated on the figures, these measurements consist of normalized uranium and gold activations. Figure 5.7 shows the axial distribution of cadmium covered uranium foils in elements 41, 42, and 43.

5.3 Core Average

Because of the spectral shift at the bottom of the active core axial traverses were made with bare uranium foils in the zero to three inch axial positions, and with bare gold foils in the remaining axial positions. Sufficient overlap of data existed for proper normalization remote from regions of rapid spectral changes. These axial centerline traverses were plotted and integrated over the active core.

Fine structure measurements were obtained across the face of the center plate of elements 41, 42, and 43 at several axial positions. These measurements were combined to obtain an overall average-to-centerline ratio in each fuel cell. In the water reflected core, cell average-to-centerline ratios of 1.08, 1.17 and 1.44 were obtained for core rings B, C, and D, respectively. In the laminated steel reflected core, cell average-to-centerline ratios of 1.06, 1.16 and 1.16 were obtained for core rings B, C, and D, respectively. These ratios were applied to the centerline measurement to obtain the relative fuel cell power production which in turn were combined to render an overall core average which was normalized to unity.

This method approximates a core average which could be obtained if the fuel elements had been mapped at many axial positions in a manner similar to that illustrated in Figure 5.8.

All data reported in this chapter has a probable error of $\pm 10\%$.

TABLE 5.1
AXIAL FLUX TRAVERSES WITH WATER REFLECTOR-BARE GOLD ACTIVITY

| <u>Position</u> | <u>Element 12 in 5.88 W.R.P.</u> | <u>Element 13 in 2.94 W.R.P.</u> | <u>Element 14 in Central R. P.</u> |
|-----------------|--------------------------------------|--------------------------------------|--|
| -1/2 | 1.05 | 1.40 | 1.52 |
| 0 | .745 | 1.03 | .94 |
| 1 | .546 | .773 | .836 |
| 3 | .749 | 1.05 | 1.11 |
| 5 | .829 | 1.11 | 1.23 |
| 7 | .814 | 1.05 | 1.12 |
| 9 | .705 | .90 | .90 |
| 13 | .452 | .553 | .499 |
| 17 | .213 | .293 | .284 |
| 21 | .094 | .108 | .112 |

TABLE 5.2
AXIAL FLUX TRAVERSES WITH WATER REFLECTOR-BARE GOLD ACTIVITY

| <u>Position</u> | <u>Element 21 in 8.82 W.R.P.</u> | <u>Element 22 in 5.88 W.R.P.</u> | <u>Element 23 in 2.94 W.R.P.</u> |
|-----------------|--------------------------------------|--------------------------------------|--------------------------------------|
| -1/2 | 1.02 | 1.85 | 2.28 |
| 0 | .664 | 1.24 | 1.52 |
| 1 | .555 | .99 | 1.25 |
| 3 | .740 | 1.27 | 1.64 |
| 5 | .817 | 1.40 | 1.76 |
| 7 | .783 | 1.28 | 1.59 |
| 9 | .656 | 1.08 | 1.28 |
| 13 | .400 | .602 | .711 |
| 17 | .208 | .302 | .362 |
| 21 | .085 | .114 | .148 |

TABLE 5.3
AXIAL FLUX TRAVERSES WITH WATER REFLECTOR-BARE GOLD ACTIVITIES

| Position | Element 31 in 8.82 W. R. P. | Element 33 in 2.94 W. R. P. | Element 34 in Central R. P. | Element 41 in 8.82 W. R. P. |
|----------|--------------------------------|--------------------------------|--------------------------------|--------------------------------|
| -1/2 | 1.36 | 2.98 | 3.16 | 1.64 |
| 0 | .92 | 2.13 | 2.50 | 1.02 |
| 1 | .78 | 1.49 | 1.70 | .79 |
| 3 | .99 | 1.98 | 2.14 | 1.00 |
| 5 | 1.03 | 2.16 | 2.35 | 1.16 |
| 7 | .94 | 1.95 | 2.07 | 1.02 |
| 9 | .757 | 1.48 | 1.55 | .83 |
| 13 | .409 | .77 | .75 | .443 |
| 17 | .217 | .365 | .392 | .235 |
| 21 | .085 | .138 | .143 | .094 |

TABLE 5.4
AXIAL FLUX TRAVERSES WITH WATER REFLECTOR
ELEMENT 42

| Position | Bare Gold in 5.88 W. R. P. | Bare Uranium in 5.88 W. R. P. | Bare Uranium in 5.25 W. R. P. | Bare Uranium in 4.73 W. R. P. |
|----------|-------------------------------|----------------------------------|----------------------------------|----------------------------------|
| -1/2 | 2.47 | 5.70 | | |
| 0 | 1.69 | 2.85 | | 3.79 |
| 1 | 1.23 | 1.311 | | 2.15 |
| 3 | 1.71 | 1.69 | | 3.04 |
| 5 | 1.83 | 1.79 | 1.98 | 3.01 |
| 7 | 1.55 | | | |
| 7.15 | | 1.577 | 1.751 | 2.43 |
| 9 | 1.20 | 1.170 | 1.320 | 1.94 |
| 13 | .598 | .598 | | .966 |
| 17 | .312 | .282 | .331 | .463 |
| 21 | .112 | .129 | | .220 |

TABLE 5.5
AXIAL FLUX TRAVERSES WITH WATER REFLECTOR
ELEMENT 43

| Position | Bare Gold in 2.94 W.R.P. |
|----------|-----------------------------|
| -1/2 | 3.09 |
| 0 | 2.21 |
| 1 | 1.61 |
| 3 | 2.17 |
| 5 | 2.29 |
| 7 | 2.08 |
| 7.15 | |
| 9 | 1.56 |
| 13 | .78 |
| 17 | .385 |
| 21 | .141 |

TABLE 5.6

AXIAL FLUX TRAVERSES WITH WATER REFLECTOR
BARE URANIUM IN ELEMENT 43

| Position | Activity in 4.09 W.R.P. | Activity in 3.57 W.R.P. | Activity in 2.94 W.R.P. | Activity in 2.31 W.R.P. | Activity in 1.79 W.R.P. |
|----------|----------------------------|----------------------------|----------------------------|----------------------------|----------------------------|
| -1/2 | | | 6.96 | | |
| 0 | 4.14 | | 3.95 | | 4.30 |
| 1 | 2.164 | | 1.654 | | 2.49 |
| 3 | 2.678 | | 2.117 | | 3.17 |
| 5 | 3.090 | 2.286 | 2.271 | 2.392 | 3.33 |
| 7.15 | 2.65 | 2.02 | 2.02 | 2.16 | 3.32 |
| 9 | 1.932 | 1.546 | 1.537 | 1.537 | 1.734 |
| 13 | 1.020 | | .765 | | .761 |
| 17 | .516 | .384 | .371 | .356 | .373 |
| 21 | .228 | | .169 | | .172 |

TABLE 5.7
AXIAL FLUX TRAVERSES WITH WATER REFLECTOR
BARE URANIUM FOILS IN CONTROL ROD C.

| <u>Position</u> | <u>Activity in 1.04 W. R. P.</u> | <u>Activity in .57 W. R. P.</u> | <u>Activity in Central R. P.</u> | <u>Activity in .87 W. R. P.</u> |
|-----------------|--------------------------------------|-------------------------------------|--------------------------------------|-------------------------------------|
| -2-1/2 | | | | .682 |
| -2 | 1.470 | .832 | .812 | |
| -1-1/2 | | | | .977 |
| -1 | 2.08 | | | |
| -1/2 | 2.26 | | | |
| 0 | 2.23 | 1.486 | 1.411 | |
| 1 | 2.44 | 1.85 | 1.76 | |
| 3 | 3.31 | 2.32 | 2.30 | |
| 5 | 3.27 | 2.41 | 2.40 | |
| 7.15 | 6.24 | 6.82 | 6.80 | |
| 7.40 | 7.65 | | 10.63 | |

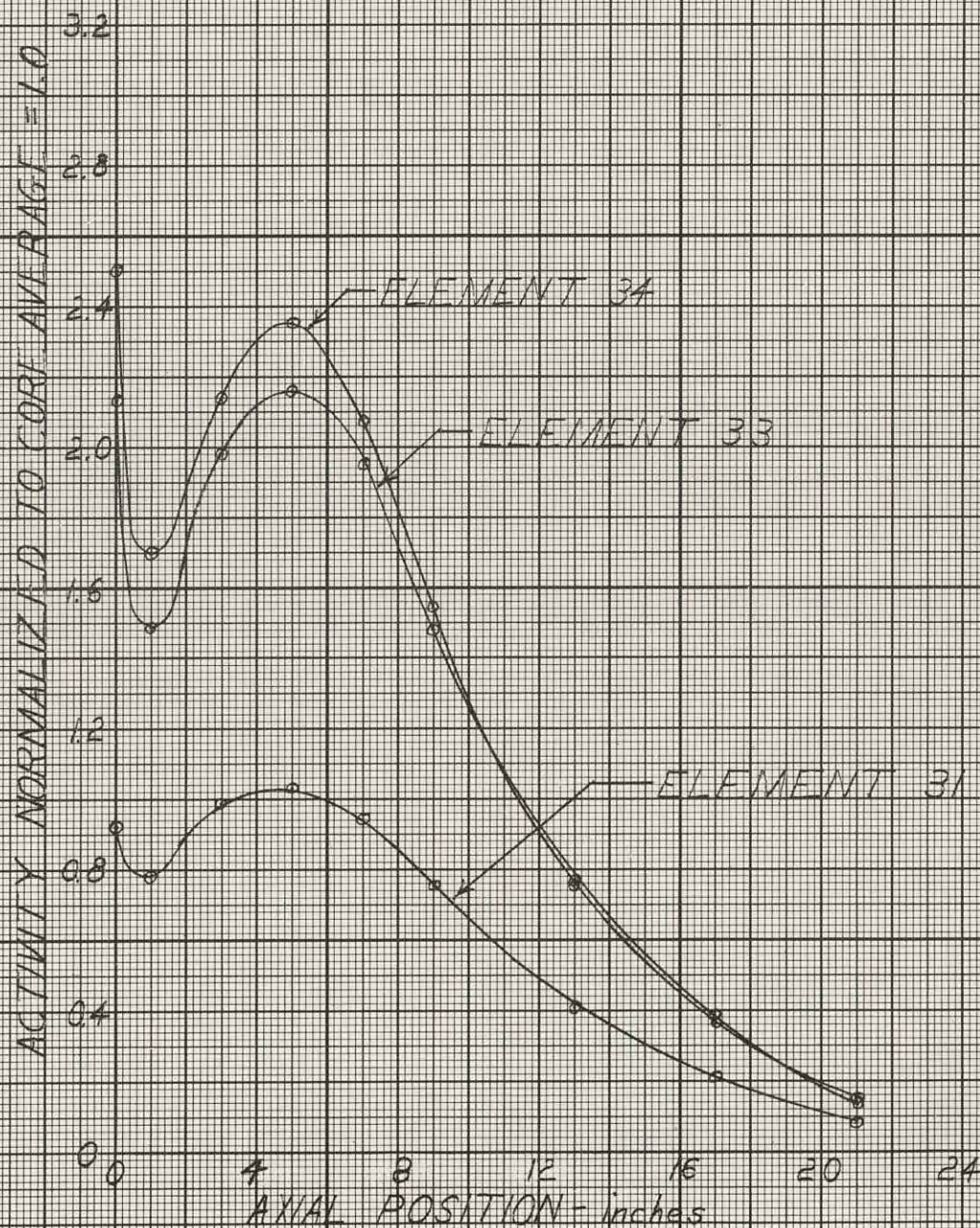
TABLE 5.8
NEUTRON FLUX MEASUREMENTS WITH WATER REFLECTOR -
BARE URANIUM FOILS IN 5 INCH AXIAL PLANE

| <u>Element 45</u> | <u>Activity</u> |
|------------------------|-----------------|
| in 1.69 ERP | 4.39 |
| in 4.19 ERP | 3.47 |
| <u>Element 46</u> | |
| in 4.63 ERP | 3.02 |
| in 5.88 ERP | 1.79 |
| in 7.13 ERP | 2.53 |
| <u>Element 47</u> | |
| in 7.57 ERP | 2.28 |
| in 8.82 ERP | 1.08 |
| in 10.07 ERP | 2.75 |
| in 10.07 ERP (Plate a) | 2.53 |
| <u>Element 57</u> | |
| in 10.07 ERP | 2.37 |
| in 10.07 ERP (Plate a) | 2.53 |
| <u>Element 67</u> | |
| in 10.07 ERP | 2.23 |
| in 7.57 ERP (Plate a) | 2.67 |
| in 8.82 ERP (Plate a) | 2.11 |
| in 10.07 ERP (Plate a) | 3.06 |
| <u>Element 76</u> | |
| in 7.13 ERP | 2.70 |
| in 7.13 ERP (Plate a) | 3.24 |
| in 7.13 ERP (Plate r) | 2.35 |

FIGURE 5.3

AXIAL BARE GOLD TRAVERSE WITH
INFINITE WATER REFLECTOR

ELEMENTS 31, 33 & 34

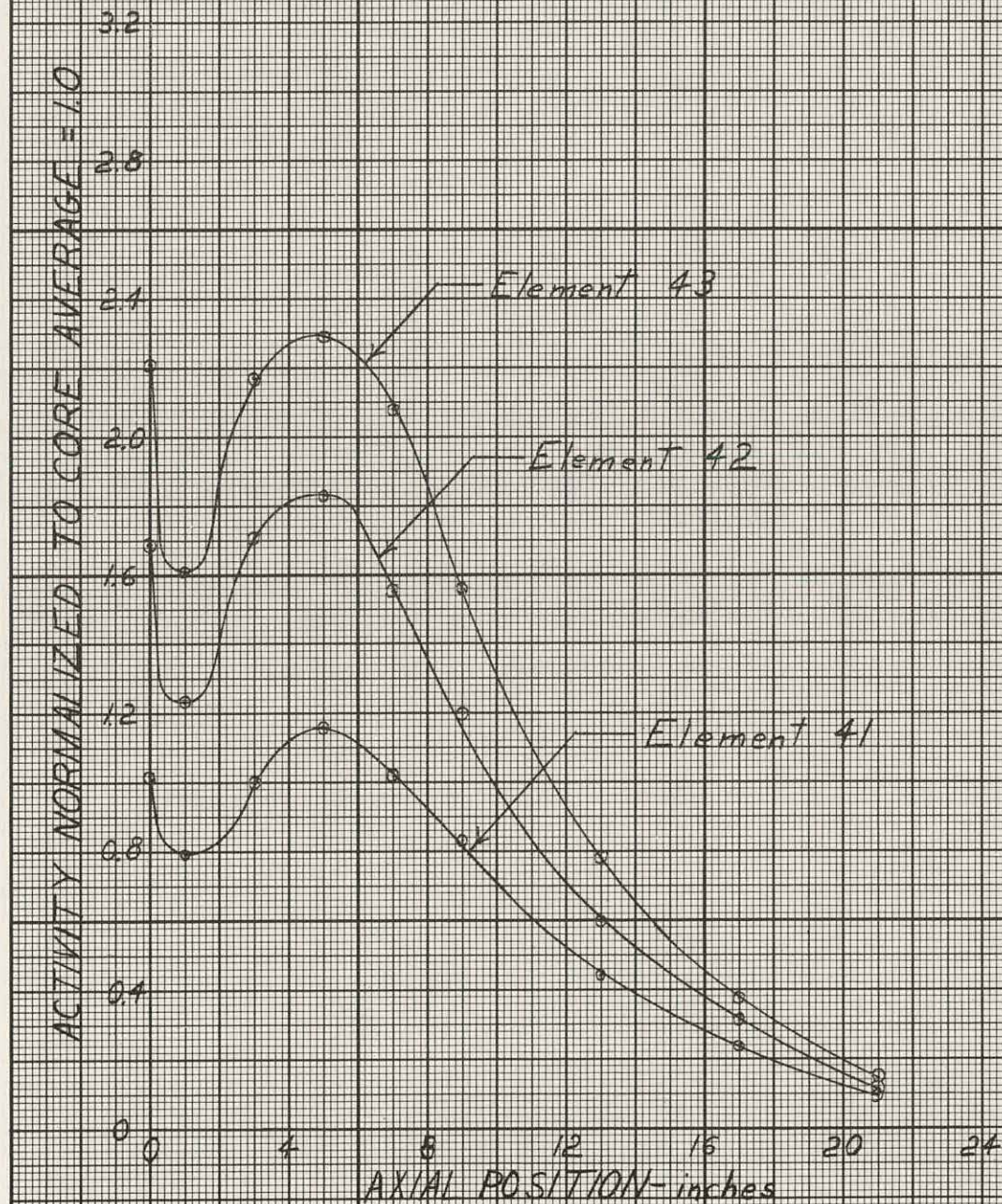


THIS PAGE
WAS INTENTIONALLY
LEFT BLANK

FIGURE 5.4

AXIAL BARE GOLD TRAVERSE WITH
INFINITE WATER REFLECTOR

ELEMENTS 41, 42 & 43



THIS PAGE
WAS INTENTIONALLY
LEFT BLANK

TABLE 5.9
AXIAL FLUX TRAVERSES WITH LAMINATED STEEL REFLECTOR

| Position | Element 12 in 5.88 W. R. P. | | Element 13 in 2.94 W. R. P. | | Element 14 in Central R. P. | |
|----------|-----------------------------|-----------|-----------------------------|-----------|-----------------------------|-----------|
| | Bare Uranium | Bare Gold | Bare Uranium | Bare Gold | Bare Uranium | Bare Gold |
| 0 | 1.57 | | 1.866 | | 1.640 | |
| 1 | .691 | | .869 | | .959 | |
| 3 | .899 | .92 | 1.147 | 1.17 | 1.257 | 1.30 |
| 5 | | 1.02 | | 1.30 | | 1.36 |
| 7 | | .99 | | 1.23 | | 1.24 |
| 9 | | .82 | | 1.03 | | 1.01 |
| 13 | | .55 | | .68 | | .61 |
| 17 | | .31 | | .36 | | .34 |
| 21 | | .136 | | .150 | | .136 |

BARE URANIUM IN ELEMENT 14 IN CENTRAL R. P.

| Position | Plate a | Plate i | Plate r |
|----------|---------|---------|---------|
| 0 | | | .908 |
| 1 | | | .733 |
| 3 | | | .940 |
| 5 | | | 1.029 |
| 7.15 | 2.74 | 1.164 | .980 |
| 9 | | | .852 |
| 13 | | | .477 |
| 21 | | | .107 |

TABLE 5.10
AXIAL FLUX TRAVERSE WITH LAMINATED STEEL REFLECTOR

| Position | Element 21 in 8.82 W.R. P. | | Element 22 in 5.88 W.R. P. | | Element 23 in 2.94 W.R. P. | |
|----------|----------------------------|-----------|----------------------------|-----------|-----------------------------|-----------|
| | Bare Uranium | Bare Gold | Bare Uranium | Bare Gold | Bare Uranium | Bare Gold |
| 0 | 1.486 | | 2.30 | | 3.03 | |
| 1 | .698 | | 1.089 | | 1.33 | |
| 3 | .917 | .88 | 1.43 | 1.40 | 1.63 | 1.89 |
| 5 | | .947 | | 1.59 | | 1.93 |
| 7 | | .94 | | 1.49 | | 1.78 |
| 9 | | .74 | | 1.14 | | 1.39 |
| 13 | | .47 | | .70 | | .779 |
| 17 | | .262 | | .35 | | .39 |
| 21 | | .108 | | .157 | | .150 |
| Position | Element 31 in 8.82 W.R. P. | | Element 33 in 2.94 W.R. P. | | Element 34 in Central R. P. | |
| | Bare Uranium | Bare Gold | Bare Uranium | Bare Gold | Bare Uranium | Bare Gold |
| 0 | 1.87 | | 4.12 | | 4.36 | |
| 1 | .875 | | 1.57 | | 1.81 | |
| 3 | 1.106 | 1.13 | 2.02 | 2.22 | 2.31 | 2.32 |
| 5 | | 1.17 | | 2.35 | | 2.44 |
| 7 | | 1.13 | | 2.05 | | 2.12 |
| 9 | | .84 | | 1.58 | | 1.71 |
| 13 | | .47 | | .80 | | .84 |
| 17 | | .26 | | .42 | | .41 |
| 21 | | .103 | | .154 | | .145 |

TABLE 5.11
AXIAL FLUX TRAVERSES WITH LAMINATED STEEL REFLECTOR
ELEMENT 41

| Position | Bare Gold in 8. 82 W. R. P. | Bare Uranium in 9. 97 W. R. P. | Bare Uranium in 8. 82 W. R. P. | Bare Uranium in 7. 67 W. R. P. | Cd. Covered Uranium in 8. 82 W. R. P. | Cd. Fraction in 8. 82 W. R. P. |
|----------|--------------------------------|-----------------------------------|-----------------------------------|-----------------------------------|---|--------------------------------------|
| 0 | | 1. 28 | 1. 71 | | . 224 | . 867 |
| 1 | | . 860 | . 87 | | . 265 | . 698 |
| 3 | 1. 23 | 1. 097 | 1. 13 | | . 340 | . 702 |
| 5 | 1. 30 | 1. 219 | 1. 28 | | . 364 | . 716 |
| 7 | 1. 19 | | | | | |
| 7. 15 | | 1. 129 | 1. 064 | 2. 02 | . 328 | . 692 |
| 9 | . 92 | . 977 | | | . 269 | |
| 13 | . 54 | . 551 | | | . 153 | |
| 17 | . 28 | | | | . 083 | |
| 21 | . 120 | . 124 | | | . 034 | |

THIS PAGE
WAS INTENTIONALLY
LEFT BLANK

TABLE 5.12
AXIAL FLUX TRAVERSES WITH LAMINATED STEEL REFLECTOR - ELEMENT 42

| Position | Bare Gold in 5.88 W. R. P. | Bare Uranium in 7.13 W. R. P. | Bare Uranium in 5.88 W. R. P. | Bare Uranium in 5.25 W. R. P. | Bare Uranium in 4.73 W. R. P. | Bare Uranium in 4.63 W. R. P. | Cd. Covered Uranium in 5.88 W. R. P. | Cd. Fraction in 5.88 W. R. P. |
|----------|-------------------------------------|--|--|--|--|--|---|-------------------------------------|
| 0 | | 3.42 | 3.23 | | 4.18 | 4.55 | .337 | .896 |
| 1 | | | | | | | .397 | |
| 3 | 1.96 | 2.51 | 1.74 | | 2.86 | 3.23 | .537 | .693 |
| 5 | 1.96 | 2.73 | 1.86 | | 2.94 | 3.63 | .566 | .698 |
| 6.98 | | 2.38 | 1.648 | 1.790 | 2.67 | 3.24 | | |
| 7 | 1.75 | | | | | | | |
| 7.15 | | | 1.616 | | | | .487 | .697 |
| 9 | 1.30 | 1.880 | 1.215 | 1.369 | 2.009 | 2.37 | .385 | .683 |
| 13 | .69 | | | | | | .202 | |
| 17 | .34 | .48 | .313 | .343 | .527 | .625 | .099 | .684 |
| 21 | .143 | | | | | | .037 | |

THIS PAGE
WAS INTENTIONALLY
LEFT BLANK

TABLE 5. 13
AXIAL FLUX TRAVERSES WITH LAMINATED STEEL REFLECTOR - ELEMENT 43

| Position | Bare Uranium in 4. 19 W. R. P. | Bare Uranium in 4. 09 W. R. P. | Bare Uranium in 3. 57 W. R. P. | Bare Uranium in 2. 94 W. R. P. | Bare Uranium in 2. 31 W. R. P. |
|----------|---|--------------------------------------|---|-----------------------------------|-----------------------------------|
| 0 | 4. 79 | 4. 31 | | 4. 06 | |
| 3 | 3. 36 | 2. 59 | | 2. 17 | |
| 5 | 3. 56 | 2. 85 | 2. 31 | 2. 29 | 2. 51 |
| 6. 98 | 3. 26 | 2. 53 | 2. 08 | 2. 02 | 2. 14 |
| 9 | 2. 33 | 2. 00 | | 1. 54 | |
| 17 | . 622 | . 487 | | . 391 | |
| Position | Bare Uranium in 1. 79 W. R. P. | Bare Uranium in 1. 69 W. R. P. | Cd. Covered Uranium in 2. 94 W. R. P. | Cd. Fraction in 2. 94 W. R. P. | Bare Gold in 2. 94 W. R. P. |
| 0 | 4. 36 | 4. 58 | . 417 | . 897 | |
| 1 | | | . 507 | | |
| 3 | 3. 16 | 4. 01 | . 643 | . 703 | 2. 28 |
| 5 | 3. 48 | 4. 19 | . 705 | . 690 | 2. 44 |
| 6. 98 | 3. 45 | 4. 27 | | | |
| 7 | | | | | 2. 28 |
| 7. 15 | 3. 45 | | . 606 | | |
| 9 | 1. 60 | 1. 83 | . 451 | . 706 | 1. 63 |
| 13 | | | . 262 | | . 85 |
| 17 | . 371 | . 433 | . 136 | . 652 | . 42 |
| 21 | | | . 074 | | . 157 |
| Position | Cd. Covered Uranium in 1. 79 W. R. P. | Cd. Fraction in 1. 79 W. R. P. | | | |
| 0 | . 449 | . 896 | | | |
| 7. 15 | . 647 | . 813 | | | |
| 17 | . 113 | . 697 | | | |

TABLE 5. 14
AXIAL FLUX TRAVERSES WITH LAMINATED STEEL REFLECTOR -
CONTROL ROD C.

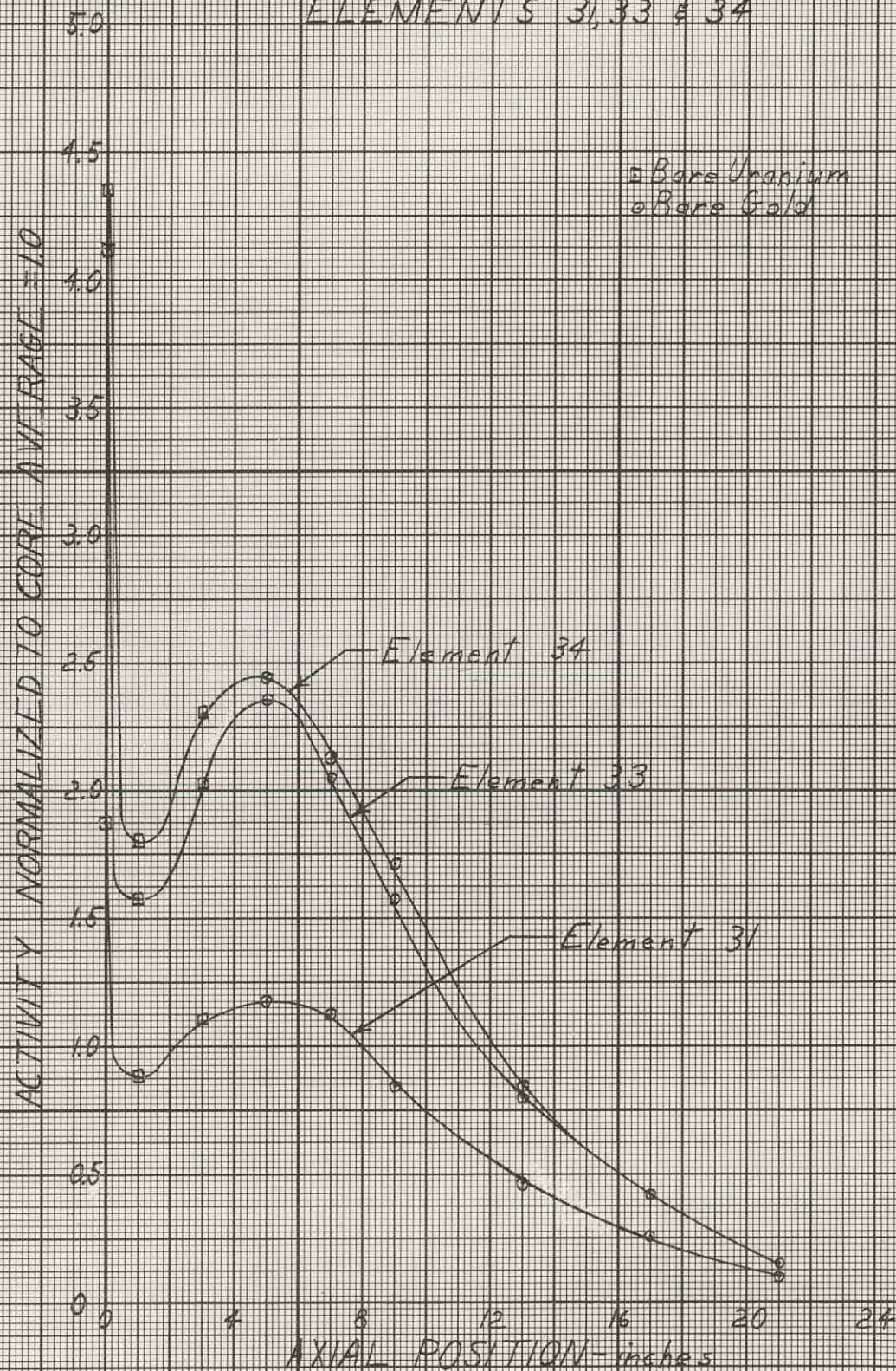
All Bare Uranium

| <u>Position</u> | <u>Activity in 1. 14 W. R. P.</u> | <u>Activity in 1. 04 W. R. P.</u> | <u>Activity in . 57 W. R. P.</u> | <u>Activity in Central R. P.</u> |
|-----------------|---------------------------------------|---------------------------------------|--------------------------------------|--------------------------------------|
| 6. 98 | 6. 45 | 6. 29 | 6. 43 | 6. 61 |
| 5 | 4. 27 | 3. 43 | | 2. 49 |
| 3 | 3. 97 | 3. 16 | | 2. 31 |
| 0 | 3. 07 | 2. 09 | | 1. 392 |

FIGURE 5.5

AXIAL TRAVERSES
WITH LAMINATED STEEL REFLECTOR

ELEMENTS 31, 33 & 34

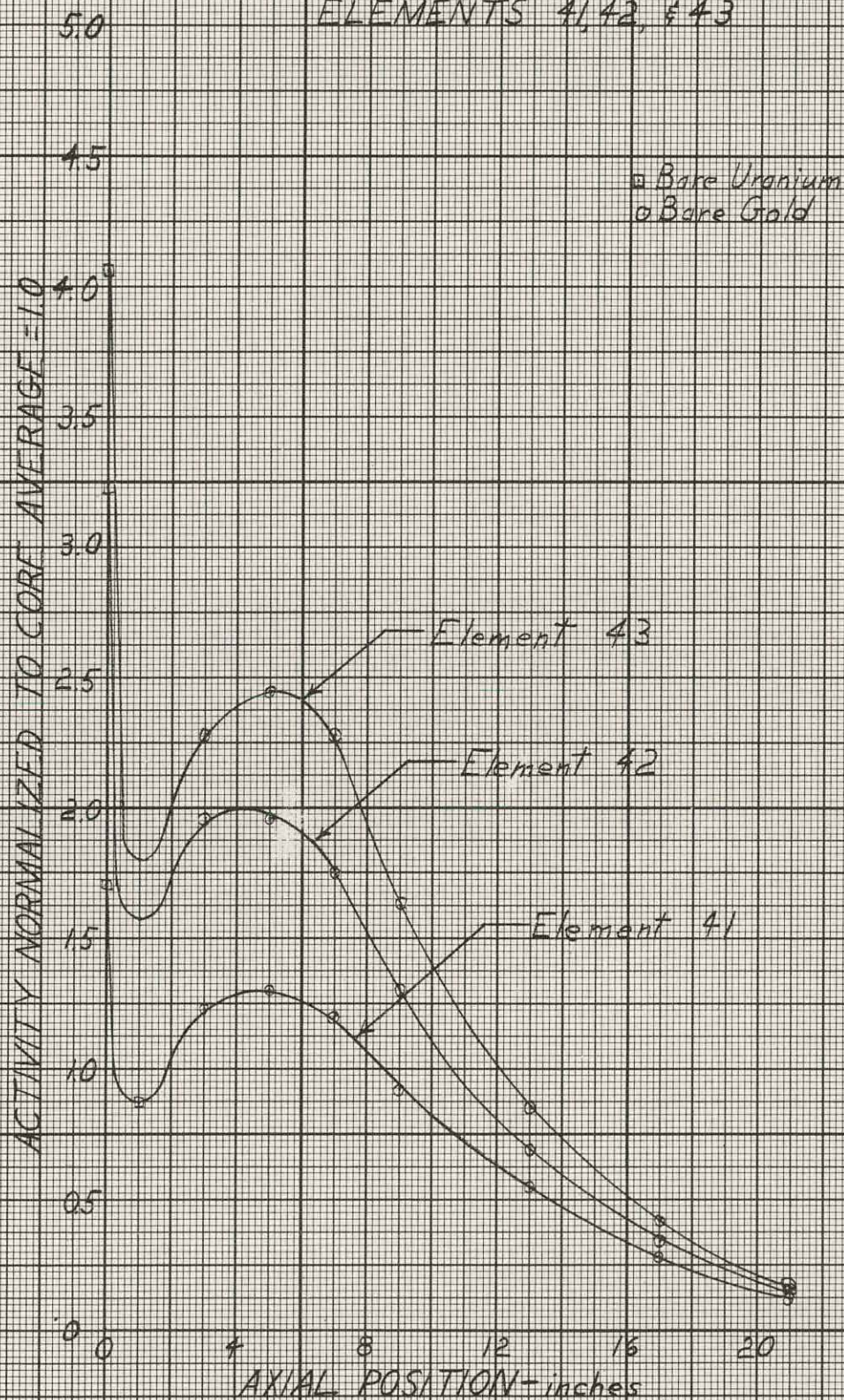


THIS PAGE
WAS INTENTIONALLY
LEFT BLANK

FIGURE 5.6

AXIAL TRAVERSES
WITH LAMINATED STEEL REFLECTOR

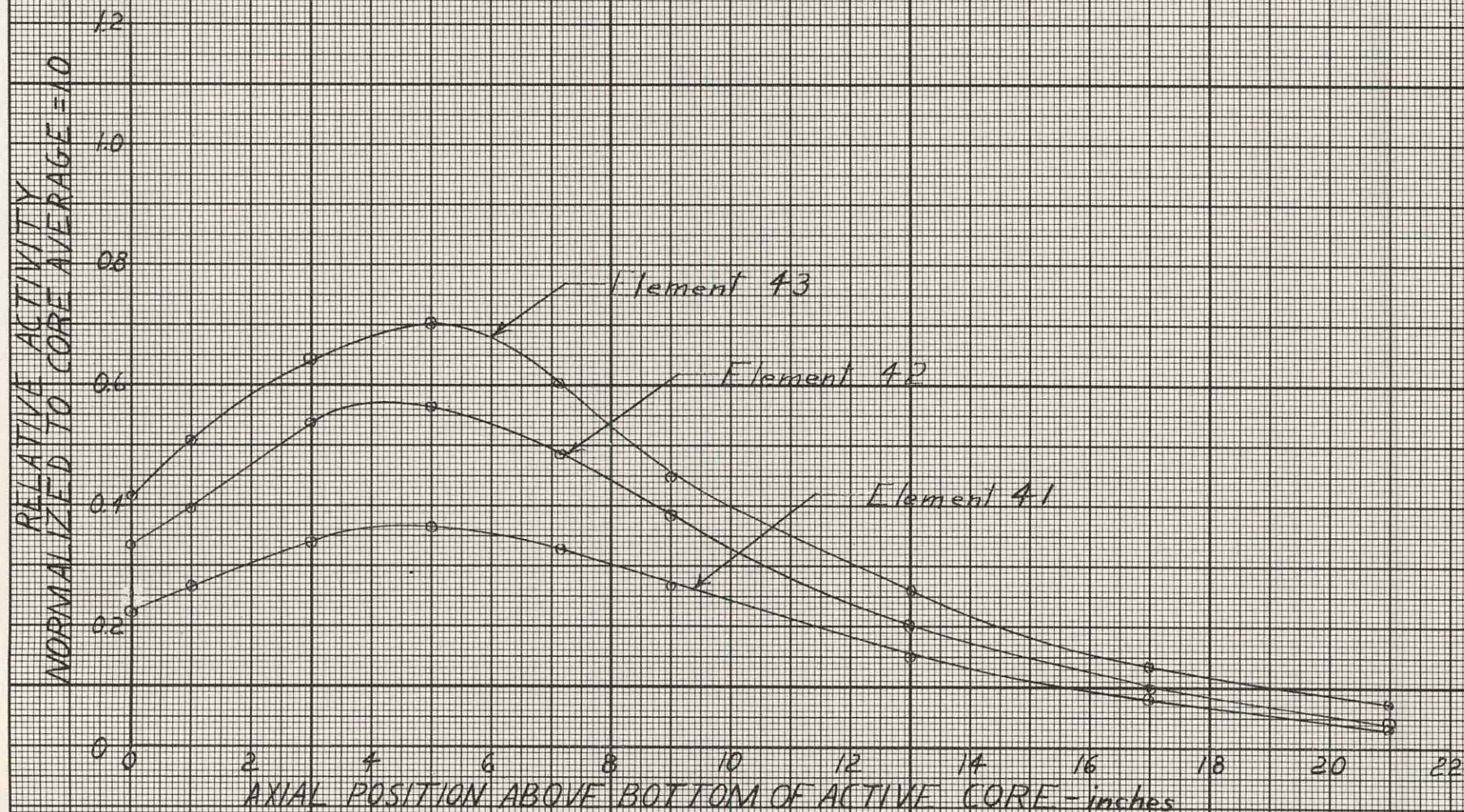
ELEMENTS 41, 42, & 43



THIS PAGE
WAS INTENTIONALLY
LEFT BLANK

FIGURE 5.7

AXIAL CADMIUM COVERED URANIUM TRAVERSES
WITH LAMINATED STEEL REFLECTOR

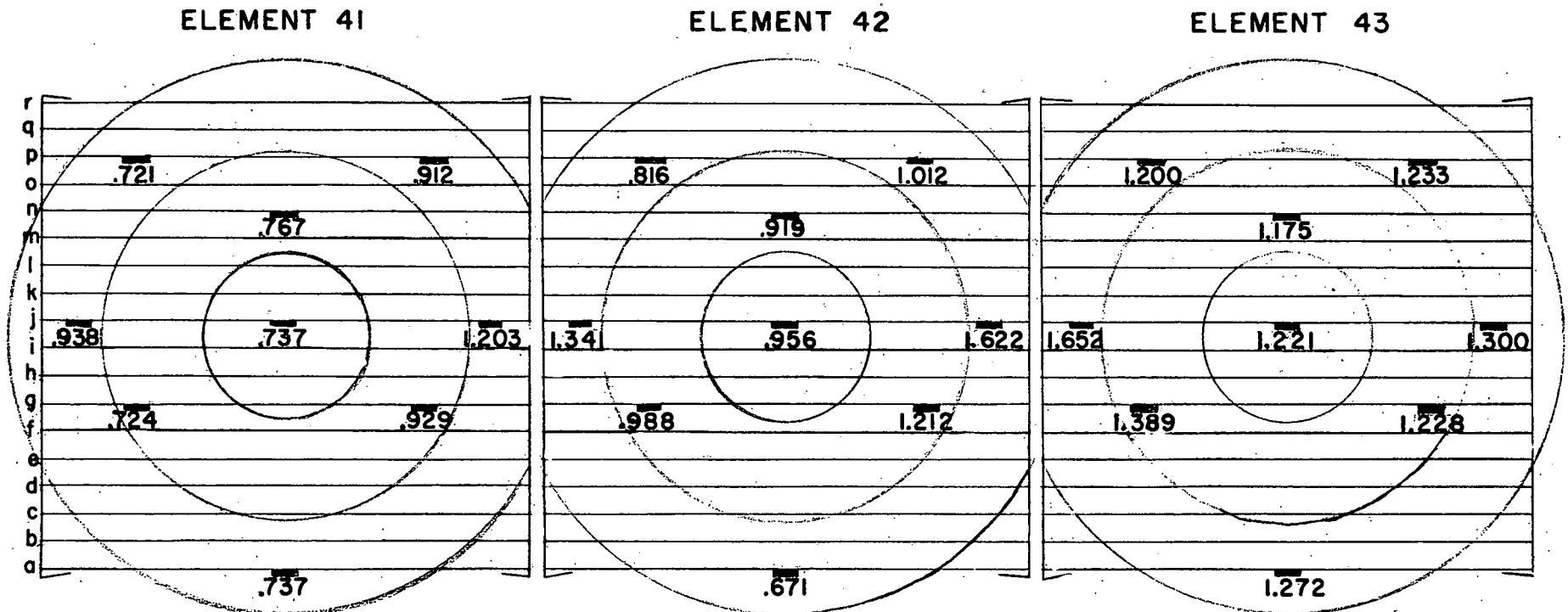


THIS PAGE
WAS INTENTIONALLY
LEFT BLANK

FIGURE 5.8

FUEL ELEMENT MAPPING

10.15 inch Axial Plan with Laminated Steel Reflector
Normalized to Core Average Equals 1.0



THIS PAGE
WAS INTENTIONALLY
LEFT BLANK

FIGURE 5.9
ELEMENT AVERAGES - RELATIVE TO
CORE AVERAGE EQUAL TO ONE

WATER REFLECTOR

| | | | | | | |
|-------|-------|-------|-------|-------|-------|-------|
| | 12 | 13 | 14 | 15 | 16 | |
| | 0.794 | 0.991 | 0.998 | 0.991 | 0.794 | |
| 21 | 22 | 23 | 24 | 25 | 26 | 27 |
| 0.743 | 0.940 | 1.051 | A | 1.051 | 0.940 | 0.743 |
| 31 | 32 | 33 | 34 | 35 | 36 | 37 |
| 0.875 | F | 1.230 | 1.371 | 1.230 | B | 0.875 |
| 41 | 42 | 43 | 44 | 45 | 46 | 47 |
| 0.933 | 1.110 | 1.349 | C | 1.349 | 1.110 | 0.933 |
| 51 | 52 | 53 | 54 | 55 | 56 | 57 |
| 0.875 | E | 1.230 | 1.371 | 1.230 | G | 0.875 |
| 61 | 62 | 63 | 64 | 65 | 66 | 67 |
| 0.743 | 0.940 | 1.051 | D | 1.051 | 0.940 | 0.743 |
| | 72 | 73 | 74 | 75 | 76 | |
| | 0.794 | 0.991 | 0.998 | 0.991 | 0.794 | |

THIS PAGE
WAS INTENTIONALLY
LEFT BLANK

FIGURE 5.10
ELEMENT AVERAGES-RELATIVE TO
CORE AVERAGE EQUAL TO ONE

LAMINATED STEEL REFLECTOR

| | | | | | | |
|-------|-------|-------|-------|-------|-------|-------|
| | 12 | 13 | 14 | 15 | 16 | |
| | 0.737 | 0.915 | 0.912 | 0.915 | 0.737 | |
| 21 | 22 | 23 | 24 | 25 | 26 | 27 |
| 0.661 | 1.048 | 1.157 | A | 1.157 | 1.048 | 0.661 |
| 31 | 32 | 33 | 34 | 35 | 36 | 37 |
| 0.786 | F | 1.318 | 1.382 | 1.318 | B | 0.786 |
| 41 | 42 | 43 | 44 | 45 | 46 | 47 |
| 0.827 | 1.244 | 1.378 | C | 1.378 | 1.244 | 0.827 |
| 51 | 52 | 53 | 54 | 55 | 56 | 57 |
| 0.786 | E | 1.318 | 1.382 | 1.318 | G | 0.786 |
| 61 | 62 | 63 | 64 | 65 | 66 | 67 |
| 0.661 | 1.048 | 1.157 | D | 1.157 | 1.048 | 0.661 |
| | 72 | 73 | 74 | 75 | 76 | |
| | 0.737 | 0.915 | 0.912 | 0.915 | 0.737 | |

THIS PAGE
WAS INTENTIONALLY
LEFT BLANK

5.4 Local Flux Distributions

5.4.1 Water Reflection

Figure 5.11 presents the bare uranium traverses across the center of elements 42, 43, and control rod C. It was obtained by cross-plotting data from Tables 5.4, 5.6 and 5.7 in the 3, 5, 7.15, and 9 inch axial planes. The seven rod bank was withdrawn to 7.14 inches.

5.4.2 Laminated Steel Reflection

Figure 5.12 shows the bare uranium traverses across the center of elements 42, 43, and control rod C, obtained by cross plotting from Tables 5.12, 5.13 and 5.14 in the 3, 5, 6.98 and 9 inch axial planes. The seven rod bank was withdrawn to 6.98 inches.

5.5 Core-Reflector Interface Flux Distribution

Figure 5.13 is a mapping of the girdle neutron flux with bare uranium foils for the water reflected core.

Figure 5.14 is a mapping of the girdle neutron flux with bare uranium foils for 1/8 inch of steel at the core boundary.

Figure 5.15 is a mapping of the girdle neutron flux with bare uranium foils for 1/4 inch of steel at the core boundary.

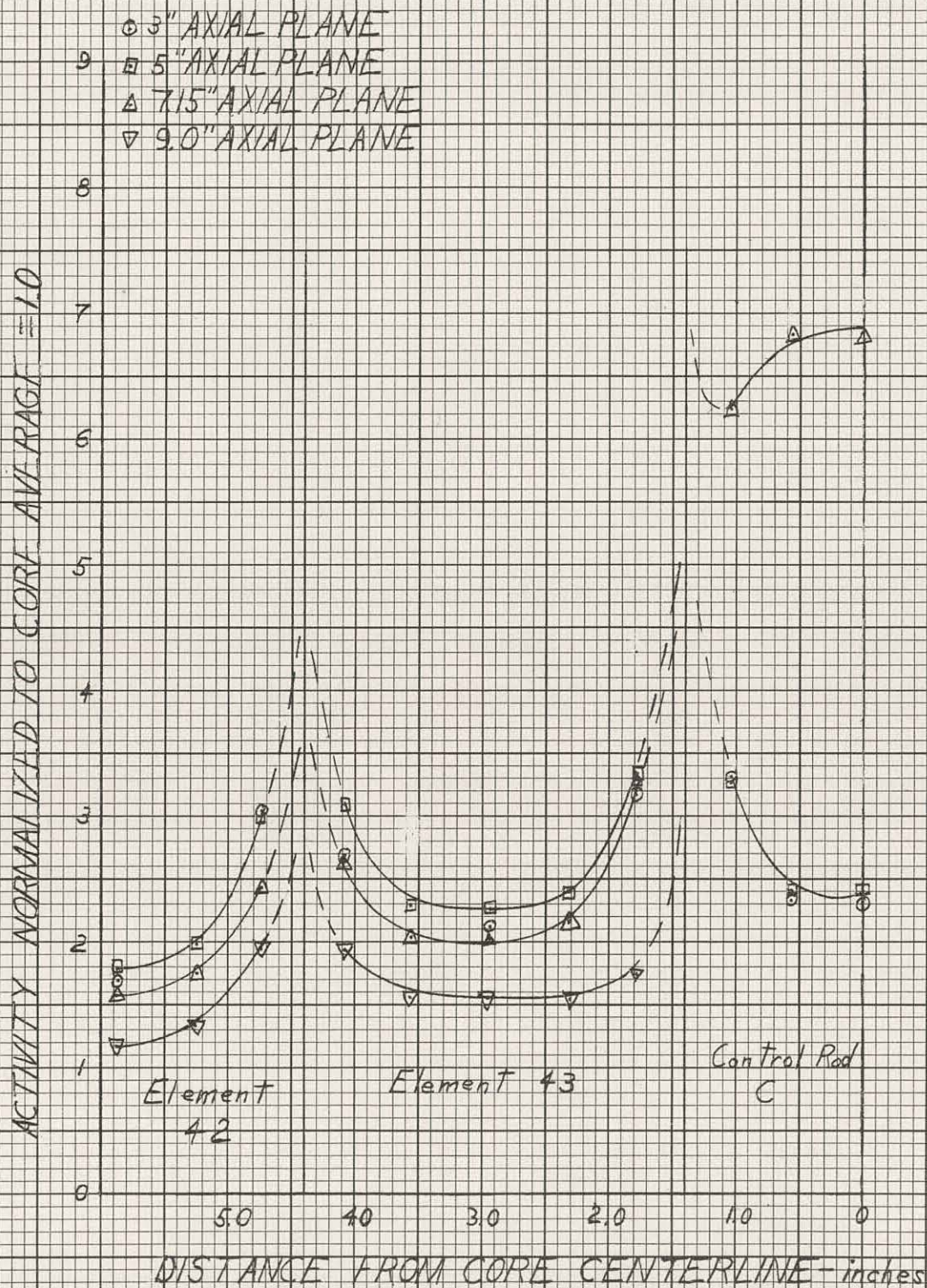
Figures 5.13, 5.14, and 5.15 indicate a satisfactory decrease in the neutron flux peaking as a function of steel skirt thickness.

5.6 Conclusions

Several serious flux peaks are evident, internal to the core, in the stationary elements surrounding control rod C. Certain of these peaks exceed values of four times the core average. Peaks at the leading edges of the control rod C fuel element are severe but will presumably be suppressed with internal poison loadings as previously recommended for the SM-1. (4) The large thermal peak at the bottom of the core may be due principally to the presence of control rod fuel penetration into this area concomitant with deep bank insertions. Since all activations reported here were taken at the initial 68°F core condition, they are undoubtedly quite pessimistic. It is therefore suggested that proper rod programming (control rod C initially fully inserted) should minimize, if not eliminate, the power peaking at the bottom of the control stationary elements and internally adjacent to control rod C.

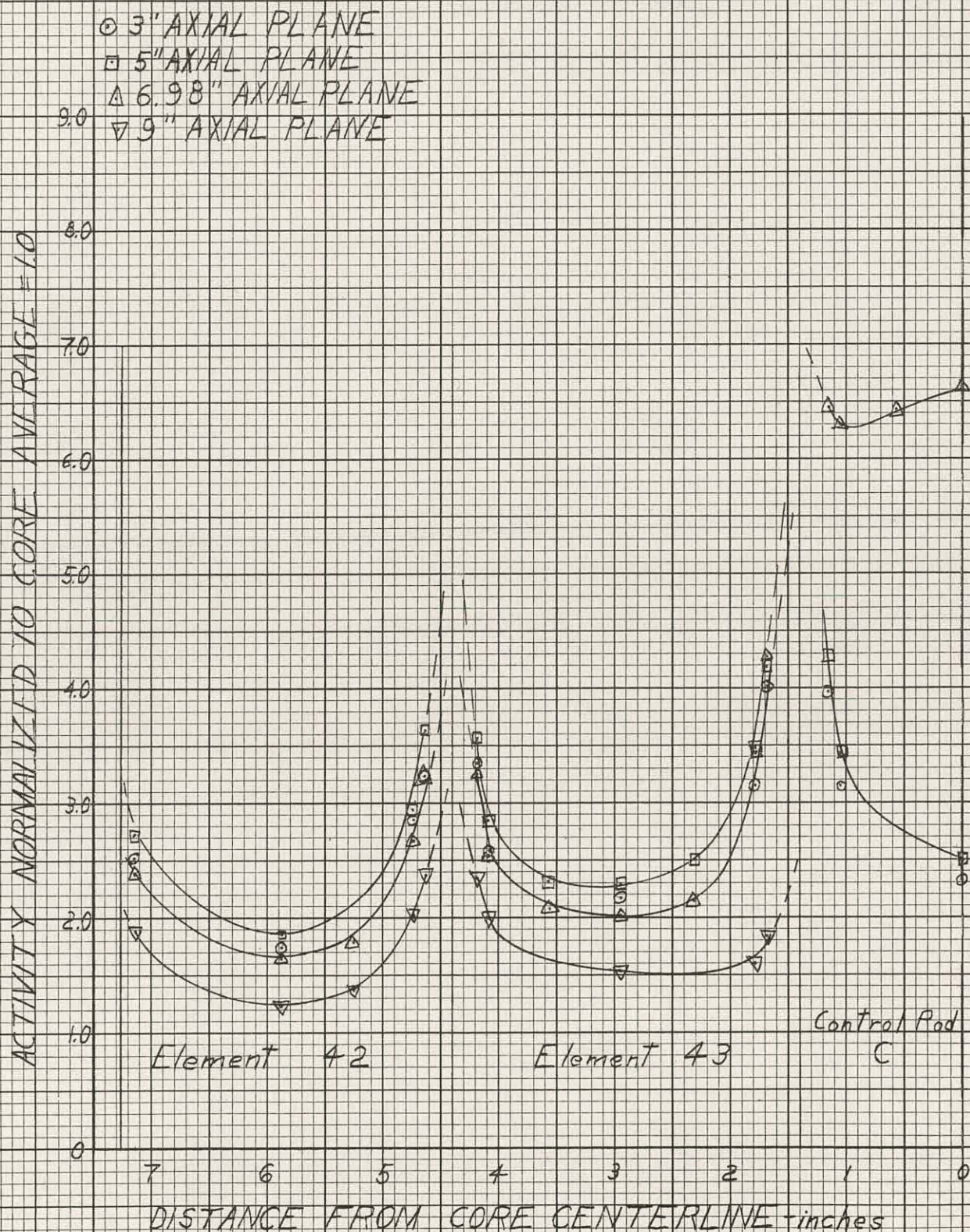
THIS PAGE
WAS INTENTIONALLY
LEFT BLANK

FIGURE 5.11
RADIAL BARE URANIUM TRAVERSES WITH WATER
REFLECTOR



THIS PAGE
WAS INTENTIONALLY
LEFT BLANK

FIGURE 5/2
RADIAL BARE URANIUM TRAVERSES WITH
LAMINATED STEEL REFLECTOR



THIS PAGE
WAS INTENTIONALLY
LEFT BLANK

Bare fission foils activated 5 inches above bottom of active core.
 Normalized to 1.0 at 2.884 inches radially in the 5 inch axial plane.

| | | | | |
|----|----------------|----------------|----------------|----------|
| 44 | 45 | 46 | 47 | |
| | 1.97 1.00 1.55 | 1.35 0.79 1.14 | 1.02 0.49 1.23 | Plate j |
| | C | | 1.13 | Plate a |
| 54 | 55 | 56 | 57 | |
| | | | 1.06 | Plate j |
| | | G | 1.10 | Plate a |
| 64 | 65 | 66 | 67 | |
| | | | 1.00 | Plate j |
| | D | | 1.19 0.94 1.37 | Plate a/ |
| 74 | 75 | 76 | 1.05 | Plate r |
| | | | 1.22 | Plate j |
| | | | 1.45 | Plate a |



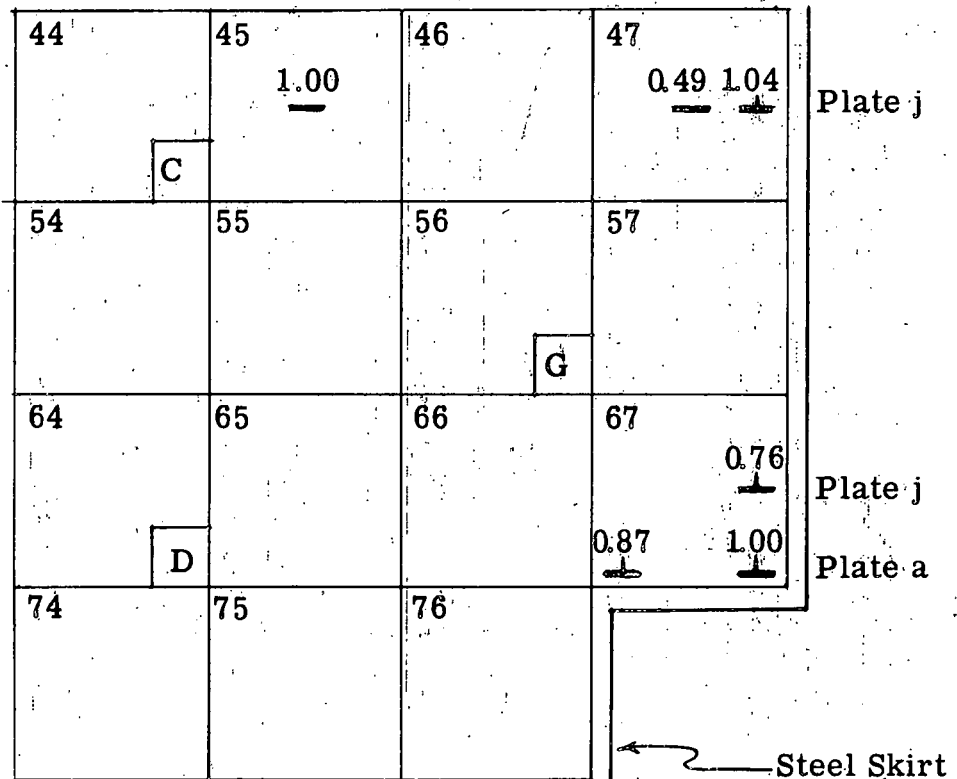
-  Foil located at center of meat.
 Foil located at edge of meat.

FIGURE 5.13
 GIRDLE NEUTRON FLUX-WATER REFLECTED

THIS PAGE
WAS INTENTIONALLY
LEFT BLANK

Bare fission foils activated 5 inches above bottom of active core.
 Normalized to 1.0 at 2.94 inches radially in the 5 inch axial plane.



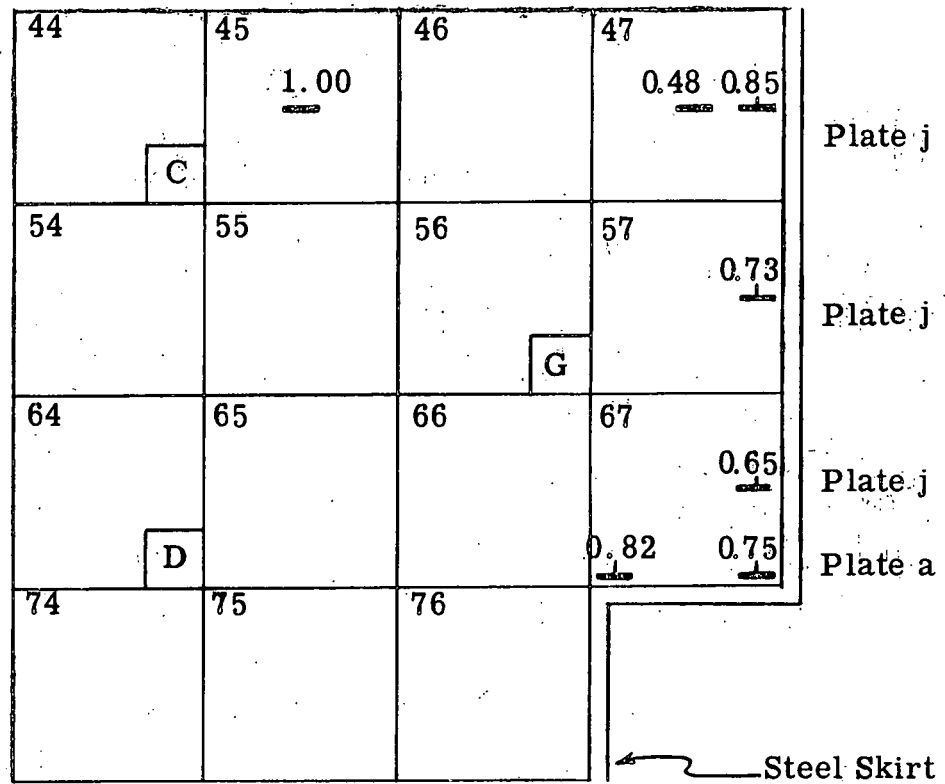
Foil located at Center of Meat.
 Foil located at Edge of Meat

Steel skirt located 0.060 inches from edge of side plate (0.015 inches from cell boundary).

FIGURE 5.14
 GIRDLE NEUTRON FLUX - 1/8 INCH SKIRT

THIS PAGE
WAS INTENTIONALLY
LEFT BLANK

Bare fission foils activated 5 inches above bottom of active core.
 Normalized to 1.0 at 2.94 inches radially in the 5 inch axial plane.



- Foil located at Center of Meat
- ⊥ Foil located at Edge of Meat

Steel skirt located 0.060 inches from edge of side plate (0.015 inches from cell boundary).

FIGURE 5.15
 GIRDLE NEUTRON FLUX - 1/4 INCH SKIRT

THIS PAGE
WAS INTENTIONALLY
LEFT BLANK

CHAPTER 6 - SM-2 MIDLIFE MOCKUP EXPERIMENTS

6.1 Introduction

The SM-2 midlife mockup composition was based on analytical calculations of the Alco Reactor Analysis Group. The 45 elements of the core were arranged into a series of 4 "rings" for the calculations. The concentrations of U^{235} and B^{10} at the calculated midlife were determined for both the stationary and control elements in these "rings." The xenon, samarium, and permanent poison buildup was accounted for by adjusting the amount of B^{10} calculated to be in each "ring" at the reactor midlife. Figure A. 5 in Appendix A shows the "ring" arrangement. The axial variation in the U^{235} and B^{10} burnup was of necessity ignored in both the calculations and the mockup. However, calculations indicate that ignoring the axial variations due to burnup is conservative from a reactivity standpoint, i. e., if the axial variations were accounted for, the 7 rod bank would be withdrawn more at criticality and thus more shutdown reactivity would be available.

Two midlife mockups were assembled in order to approach as closely as possible the determined SM-2 midlife loading. An element by element loading description is given in Appendix A for the preliminary and final mockups, loading references 49 and 52, respectively. Unless otherwise noted, the measurements were made with an infinite water reflector.

6.2 Preliminary SM-2 Midlife Mockup

The preliminary mockup was critical on the 7 rod bank at 4. 602 inches withdrawn. Several period measurements were made at the critical position to determine the 7 rod bank worth. The average 7 rod bank worth was 345 cents per inch at 4. 706 inches. Table 6. 1 presents the data.

TABLE 6. 1
7 ROD BANK CALIBRATION

| Average 7 Rod Bank Position, Inches | Bank Worth Cents/in. | % Deviation From Average |
|--|-------------------------|-----------------------------|
| 4. 690 | 347 \pm 3. 5 | +0. 58 |
| 4. 664 | 342 \pm 3. 5 | -0. 87 |
| 4. 723 | 342 \pm 3. 5 | -0. 87 |
| 4. 728 | 345 \pm 3. 5 | 0. 00 |
| 4. 726 | 349 \pm 3. 5 | +1. 16 |

Average worth 345 \pm 2 cents per inch at 4. 706 inches.

6.2.1 Flow Divider

The flow divider reactivity evaluation was made by inserting stainless steel sheets between the outer rings of elements. Figure 6.1 shows the flow divider location. Flow dividers of 18.1, 30.8, 49.0, and 67.1 mil thicknesses were mocked-up. An additional measurement was made for a 67.1 mil flow divider with a 2.5 in. laminated steel reflector. Table 6.2 presents the data obtained.

TABLE 6.2
FLOW DIVIDER MEASUREMENTS

| <u>Flow Divider Thickness, mils</u> | <u>ΔK_E Cents</u> |
|--|--|
| 18.1 | -24.8 |
| 30.8 | -41.6 |
| 49.0 | -63.3 |
| 67.1 | -81.5 |
| 67.1 (With 2.5 in. Reflector 4 sides and 4 corners) | -79.8 |

Figure 6.2 describes the effect on core reactivity of varying flow divider thickness. The extrapolated value for a flow divider of 0.095 inch thickness is -96.6 cents (ΔK_E). Since the mock-up does not allow the variation of center to center fuel element spacing, it was impractical to measure the effect of changing this spacing to accommodate the 0.093 inch flow divider and the proper water channels. It is assumed by linear extrapolation that the combined core alterations should not introduce a reactivity effect more negative than the -128 cents so obtained.

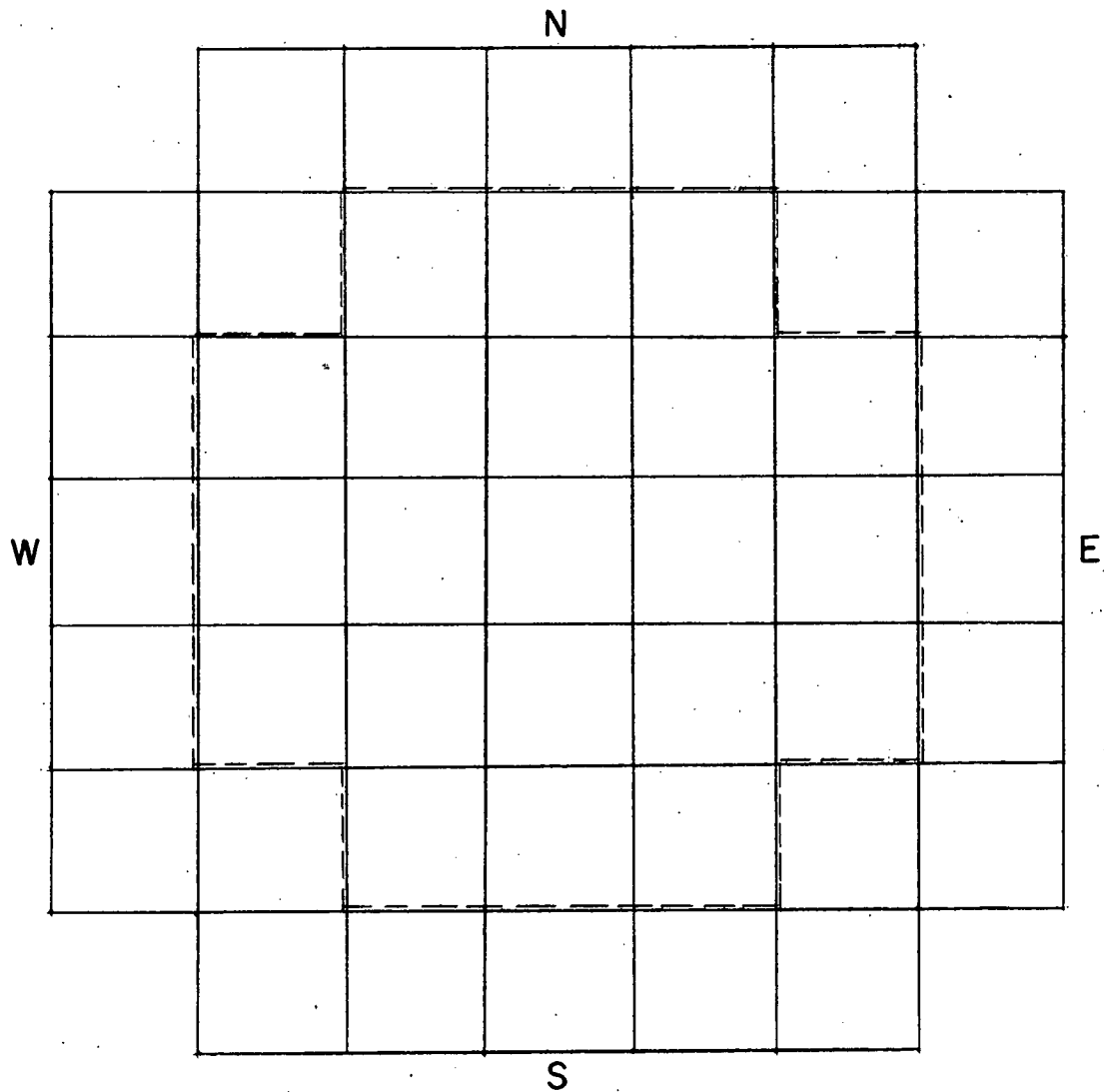
6.2.2 Reflector Measurements

The reflector measurements made during the cold clean SM-2 final mockup were repeated almost point by point for the SM-2 preliminary mid-life mockup. The same reflector assembly was used (Figure 4.11), and both 2 sided-2 cornered and 4 sided-4 cornered reflectors were measured as before. Figure 6.3 describes the reactivity effects of the laminated reflector for both 2 sided-2 cornered reflection and 4 sided-4 cornered reflection. Table 6.3 presents the data.

FIGURE 6.1

FLOW DIVIDER LOCATION

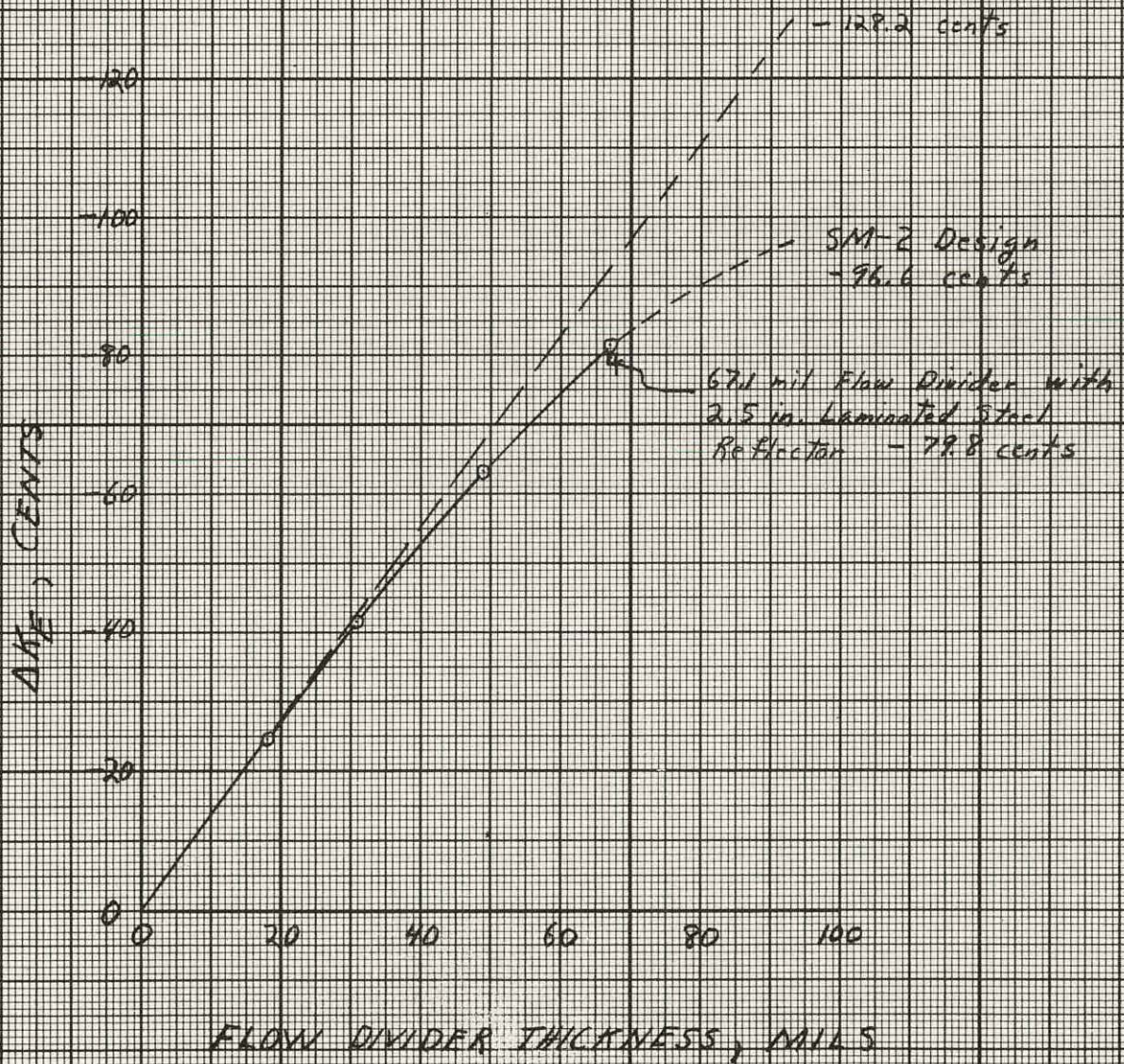
FLOW DIVIDER SHOWN BY DASHED LINES



THIS PAGE
WAS INTENTIONALLY
LEFT BLANK

FIGURE 6.2

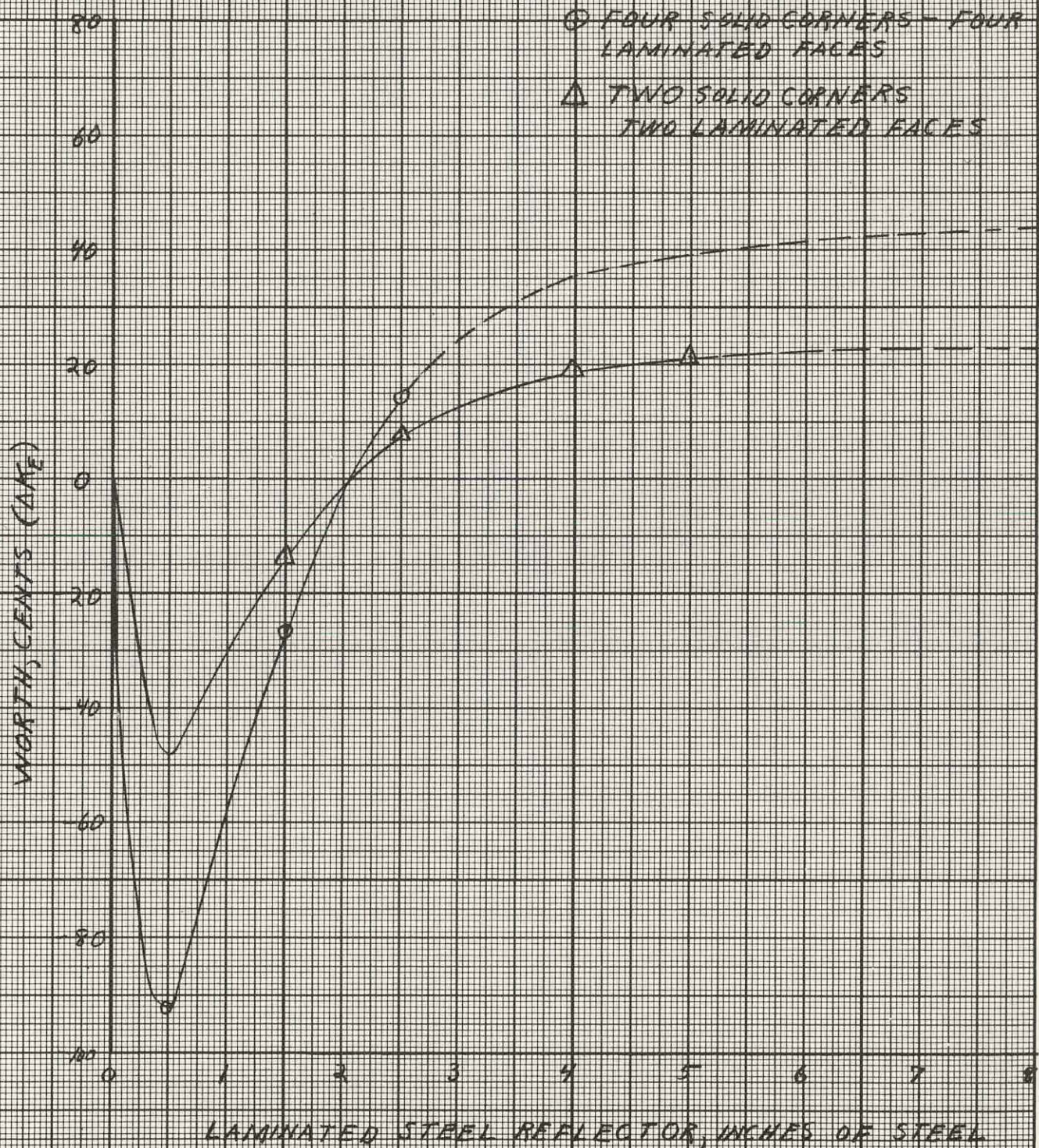
ΔK_E vs. FLOW DIVIDER THICKNESS



THIS PAGE
WAS INTENTIONALLY
LEFT BLANK

FIGURE 6.3

ΔK_E vs LAMINATED STEEL REFLECTOR THICKNESS



THIS PAGE
WAS INTENTIONALLY
LEFT BLANK

TABLE 6.3
 ΔK_E FOR VARIOUS LAMINATED STEEL REFLECTORS

| <u>Inches of Steel</u> | <u>ΔK_E - Cents</u> <u>4 Sides, 4 Corners</u> | <u>ΔK_E - Cents</u> <u>2 Sides, 2 Corners</u> |
|------------------------|---|---|
| .5 | -92.2 | |
| 1.5 | -26.5 | -13.8 |
| 2.5 | 14.1 | 7.6 |
| 4.0 | | 18.9 |
| 5.0 | | 21.3 |

The data overlap indicates a ratio of almost a factor of two in the reactivity effect of the 4 sided-4 cornered reflector to the 2 sided-2 cornered reflector. This factor was used to extrapolate the 4 sided-4 cornered reflector worth curve, and resulted in a laminated reflector worth not exceeding + 44 cents for the SM-2 midlife mockup.

A comparison of the midlife reflector data with the clean SM-2 reflector data reveals that the worth of a thick laminated stainless steel reflector is only about half that for the midlife mockup. Also, the reactivity "break-even point" occurs for a thinner reflector for the clean SM-2 than for the midlife mockup.

6.2.3 Critical Rod Configurations

The critical rod measurements were obtained by bring the reactor critical two control rods at a time. The other five rods were fully inserted. These measurements were made with a 67.1 mil flow divider and 2-1/2 inch reflector (4 sides, 4 corners). The following tabulation (Table 6.4) presents several critical rod configurations relevant to the determination of suitable "stuck rod criteria."

TABLE 6.4
PRELIMINARY SM-2 MIDLIFE CRITICAL ROD CONFIGURATIONS
ROD POSITIONS - INCHES WITHDRAWN

| Core | A | B | C | D | E | F | G |
|------|--------|--------|--------|---|--------|--------|---|
| 1 | 8.438 | 0 | 12.500 | 0 | 0 | 0 | 0 |
| 2 | 9.240 | 0 | 11.400 | 0 | 0 | 0 | 0 |
| 3 | 10.239 | 0 | 10.238 | 0 | 0 | 0 | 0 |
| 4 | 11.400 | 0 | 9.181 | 0 | 0 | 0 | 0 |
| 5 | 5.600 | 0 | 21.600 | 0 | 0 | 0 | 0 |
| 6 | 0 | 9.164 | 12.500 | 0 | 0 | 0 | 0 |
| 7 | 0 | 10.263 | 11.400 | 0 | 0 | 0 | 0 |
| 8 | 0 | 10.887 | 10.885 | 0 | 0 | 0 | 0 |
| 9 | 0 | 11.400 | 10.494 | 0 | 0 | 0 | 0 |
| 10 | 0 | 5.469 | 21.600 | 0 | 0 | 0 | 0 |
| 11 | 10.138 | 0 | 0 | 0 | 0 | 12.500 | 0 |
| 12 | 11.140 | 0 | 0 | 0 | 0 | 11.136 | 0 |
| 13 | 11.400 | 0 | 0 | 0 | 0 | 10.819 | 0 |
| 14 | 7.658 | 0 | 0 | 0 | 0 | 21.600 | 0 |
| 15 | 0 | 0 | 0 | 0 | 12.500 | 10.828 | 0 |
| 16 | 0 | 0 | 0 | 0 | 11.169 | 11.169 | 0 |
| 17 | 0 | 0 | 0 | 0 | 21.600 | 7.914 | 0 |

6.2.4 Flux Measurements

During the preliminary mockup, only a few flux measurements were made. The flux measurements were made in symmetric elements, numbers 43 and 45. Bare fission foils were used in element 45 and cadmium covered fission foils in element 43. Two foils were placed in each element five inches above the bottom of the active core, one at the inner edge and one at the center of the center fuel plate. The activities were normalized to 1.00 at 2.94 inches radially in the five inch axial plane. The reactor configurations included a 67.1 mil flow divider and a 2-1/2 inch reflector on all four sides with corners.

Since element 43 and 45 are symmetric it is possible to calculate the cadmium fraction for the positions measured. The cadmium fraction at the center of the center fuel plate of element 45 or 43 is 0.79 and the cadmium fraction at the edge of the center fuel plate nearest control element C is 0.88.

The worth of these measurements is doubtful due to the mockup limitations. It was therefore decided that further detailed flux mapping of the SM-2 final midlife mockup would be essentially meaningless.

6.3 Final SM-2 Midlife Mockup

The final mockup was critical on the 7 rod bank at 4.946 inches withdrawn. A calibration of the 7 rod bank was determined to be 341 cents per inch at 4.975 inches. Since the preliminary and final SM-2 midlife mockup critical positions differed by only about one-third of an inch the reflector and flow divider worth measurements were not repeated.

6.3.1 Critical Rod Configurations

Table 6.5 presents additional critical rod configurations determined for use in the evaluation of "stuck rod criteria."

TABLE 6.5
SM-2 MIDLIFE FINAL MOCKUP CRITICAL ROD CONFIGURATIONS
ROD POSITIONS - INCHES WITHDRAWN

| <u>Case</u> | <u>A</u> | <u>B</u> | <u>C</u> | <u>D</u> | <u>E</u> | <u>F</u> | <u>G</u> |
|-------------|----------|----------|----------|----------|----------|----------|----------|
| 1 | 2.734 | 2.732 | 21.6 | 2.734 | 0 | 2.737 | 2.735 |
| 2 | 0 | 0 | 10.669 | 10.669 | 0 | 0 | 0.005 |
| 3 | 0 | 0 | 12.190 | 0 | 0 | 0 | 12.193 |
| 4 | 0 | 0 | 0 | 11.344 | 0 | 0 | 11.342 |
| 5 | 0 | 12.037 | 0 | 0.006 | 0 | 0 | 12.037 |
| 6 | 0 | 16.885 | 0 | 0.006 | 0 | 16.888 | 0 |
| 7 | 0 | 0 | 0 | 14.726 | 0 | 14.727 | 0 |
| 8 | 14.692 | 0 | 0 | 14.691 | 0 | 0 | 0 |

Table 6.6 presents the worth in cents per inch of the rods on which criticality was attained.

TABLE 6. 6
CALIBRATION OF CONTROL RODS

| Case | Rod Bank Calibrated | Average Position in Inches | Worth of Rod Bank Cents/Inch |
|------|---------------------|-------------------------------|---------------------------------|
| 1 | A, B, D, E, F, G, | 2. 777 | 171 |
| 2 | C, D | 10. 759 | 116 |
| 3 | C, G | 12. 297 | 91 |
| 4 | D, G | 11. 423 | 107 |
| 5 | B, G | 12. 145 | 113 |
| 6 | B, F | 17. 200 | 34. 5 |
| 7 | D, F | 14. 898 | 53. 5 |
| 8 | A, D | 14. 847 | 53. 1 |

By using symmetry conditions, information for rod E can also be obtained from Tables 6. 5 and 6. 6.

REFERENCES

1. Noaks, J. W., "The Alco Products, Inc. Criticality Facility - Description and Operation," APAE No. 36.
2. Noaks, J. W., "Hazards Summary Report for the SM-2 Critical Experiments," APAE No. 36 Supplement 1.
3. Fairbanks, F. B., Gallagher, J. G., "APPR-1 Control Rod Experiments and Calculations," APAE Memo 92.
4. Noaks, J. W., Johnson, W. R., "APPR Zero Power Experiments - ZPE-1," APAE No. 8.
5. Noaks, J. W., et al, "Extended Zero Power Experiments on the APPR-ZPE-2," APAE No. 21.
6. Williamson, T. G., et al, "Reactor Analysis APPR-1 Core II," APAE No. 32.
7. MND-E-1718, "A Boron Determination for the APPR-1" Issued May 25, 1959.
8. Williams, D. V. P., et al, "Army Package Power Reactor Critical Experiments," ORNL-2128.

APPENDIX A
CORE LOADING COMPOSITIONS

THIS PAGE
WAS INTENTIONALLY
LEFT BLANK

A.1 Fuel Element Data

A.1.1 Fuel Plate Data

| | <u>Stationary</u> | <u>Control Rod</u> |
|----------------------------|---------------------|---------------------|
| Plate Width (in.) | 2.77 \pm .005 | 2.554 \pm .005 |
| Plate Thickness (in.) | 0.0408 \pm .0001 | 0.0401 \pm .0001 |
| Plate Length (in.) | 22-15/16 \pm 1/32 | 22-15/16 \pm 1/32 |
| Meat Width (in.) | 2.51 \pm .04 | 2.32 \pm .04 |
| Meat Thickness (in.) | 0.031 \pm .001 | 0.030 \pm .001 |
| Meat Length (in.) | 21.6 \pm .2 | 22.0 \pm .2 |
| Mass UO ₂ (gm) | 56.64 \pm .01 | 51.72 \pm .001 |
| Mass U ²³⁵ (gm) | 46.30 | 42.24 |
| Enrichment (%) | 93.33 \pm .02 | 93.12 \pm .01 |
| Mass Matrix Steel (gm) | 157.35 | 141.53 \pm .09 |
| Steel Clad Thickness (in.) | 0.005 \pm .001 | 0.005 \pm .001 |

A.1.2 Basic Side Plate Data

| <u>Ref. Loading No.</u> | <u>Dimension</u> | <u>Stationary</u> | <u>Control Rod</u> |
|-------------------------|------------------|-------------------|---------------------|
| 1-32, 34-48 | Width (in.) | 2.848 | 2.621 |
| | Thickness (in.) | 0.0245 | 0.0239 |
| Dimensions actual | Length (in.) | 27-1/4 \pm 1/16 | 24-13/16 \pm 1/16 |
| | Mass (gm) | 239.8 \pm .6 | 199.94 \pm .03 |
| 33 | Width (in.) | 2.863 | 2.619 |
| Plate width of SM-2 | Thickness (in.) | 0.0244 | 0.0239 |
| specified-mass | Length (in.) | 27-1/4 \pm 1/16 | 24-13/16 \pm 1/16 |
| equivalent thickness | Mass (gm) | 239.8 \pm .6 | 199.94 \pm .03 |
| 49-53 | Width (in.) | 2.863 | 2.619 |
| Side plates with | Thickness (in.) | 0.0327 | 0.0306 |
| channels. Plate | Length (in.) | 27-1/4 \pm 1/32 | 24-15/16 \pm 1/32 |
| width of SM-2 speci- | Mass (gm) | 328.0 \pm .5 | 256.3 \pm .2 |
| fied mass equivalent | | | |
| thickness | | | |

A. 1.3 Polystyrene Grooves Data

| | <u>Stationary</u> | <u>Control Rod</u> |
|-------------------------------|-------------------|--------------------|
| Volume (cm ³) | 61.5 + .3 | 58.9 + .5 |
| Mass (gm) | 64.0 + .3 | 61.2 + .4 |
| Density (gm/cm ³) | 1.040 | 1.038 |
| Ridge Width (in.) | 0.100 + .002 | 0.009 + .002 |
| Groove Width (in.) | 0.048 + .003 | 0.058 + .003 |
| Ridge Height (in.) | 0.150 | 0.150 |
| Web thickness (in.) | 0.015 | 0.015 |
| Number of Ridges | 17 | 15 |

A. 1.4 Additional Clad Data

| | <u>Stationary</u> | <u>Control Rod</u> |
|-----------------|-------------------|--------------------|
| Thickness (in.) | 0.0102 + .0001 | 0.0102 + .0001 |
| Width (in.) | 2.777 + .005 | 2.554 + .005 |
| Length (in.) | 23 + 1/32 | 23 + 1/32 |
| Mass (gm) | 82.9 + .1 | 77.22 + .02 |
| Thickness (in.) | --- | 0.0051 + .0001 |
| Width (in.) | --- | 2.554 + .005 |
| Length (in.) | --- | 23 + 1/32 |
| Mass | --- | 37.8 + .1 |

A. 2 Control Rod Data

A. 2.1 Control Rod Basket - Type 304 S. S.

Thickness - 0.054 in. Density - 7.85 + .06 gm/cm³

Outside Diameter - 2.797 in. square

Inside Diameter - 2.689 in. square

A. 2.2 Control Rod Absorber Data:

56.4 gm B¹⁰ - 4 plates - 2.620 in. square

Absorber Plate:

| | |
|---|--------------|
| Plate Length | 26-1/16 in. |
| Plate Width | 2.464 in. |
| Plate Thickness | 0.156 in. |
| Meat Length | 20-13/16 in. |
| Meat Thickness | 0.090 in. |
| Clad Thickness | 0.033 in. |
| Min. Inactive edge | 0.035 in. |
| Max. Inactive edge | 0.125 in. |
| Distance between meat and bottom of plate | 1/4 in. |

A. 3 Core Array - Reference Figures A. 1 and A. 2

Cell Size - 2.9375 in.
Core Diameter - 20.5625 in.
Active Core Length - $21.6 \pm .2$ in.

A. 4 Fuel Plate Orientation - Reference Figures A. 3 and A. 4

A. 5 Reflector Data

A. 5.1 Side Reflector Plate Data

26-7/8 in. x 14-7/8 in. x 1/2 in.

A. 5.2 Corner Reflector Data

Right Isosceles Triangle, hypotenuse = 6-15/16 in.
26-7/8 in. length

A. 6 Core Loading Compositions

A. 6.1 Reference Loading Number i:

Eight fuel elements grouped around rod C
No boron

Stationary Elements: 33, 34, 35, 43, 45, 53, 54 & 55
18 Fuel Plates - 833.40 gm U²³⁵/element
6667.20 gm U²³⁵

Control Element C
16 Fuel Plates - 675.84 gm U²³⁵

A. 6.2 Reference Loading Number ii:

Six fuel elements and rod C in open seven control rod array.
No boron

Stationary Elements: 23, 25, 42, 46, 63, and 65
18 Fuel Plates - 833.40 gm U²³⁵/element
5000.40 gm U²³⁵

Control Element C
16 Fuel Plates - 675.84 gm U²³⁵

Core Lattice Designations

Open Seven Control Rod Array

Control Rods A, B, C, D, E, F, G

| | | | | | | |
|---|----|----|----|----|----|----|
| | | | N | | | |
| | 12 | 13 | 14 | 15 | 16 | |
| | 21 | 22 | 23 | 24 | 25 | 26 |
| | | | A | | | 27 |
| | 31 | 32 | 33 | 34 | 35 | 36 |
| | | F | | | B | 37 |
| W | 41 | 42 | 43 | 44 | 45 | 46 |
| | | | C | | | 47 |
| | 51 | 52 | 53 | 54 | 55 | 56 |
| | | E | | | G | 57 |
| | 61 | 62 | 63 | 64 | 65 | 66 |
| | | | D | | | 67 |
| | 72 | 73 | 74 | 75 | 76 | |
| | | | | | | |
| | | | S | | | |

FIGURE A. 1

Closed Seven Control Rod Array

Control Rods A, B, C, D, E, F, G

| | | | | | | |
|---|----|----|----|----|----|----|
| | | | N | | | |
| | 12 | 13 | 14 | 15 | 16 | |
| | 21 | 22 | 23 | 24 | 25 | 26 |
| | | | A | | | 27 |
| | 31 | 32 | 33 | 34 | 35 | 36 |
| | | F | | | | 37 |
| W | 41 | 42 | 43 | 44 | 45 | 46 |
| | | E | | C | | B |
| | 51 | 52 | 53 | 54 | 55 | 56 |
| | | | | G | | 57 |
| | 61 | 62 | 63 | 64 | 65 | 66 |
| | | | D | | | 67 |
| | 72 | 73 | 74 | 75 | 76 | |
| | | | | | | |
| | | | S | | | |

FIGURE A. 2

Stationary Element Fuel Plate Arrangement

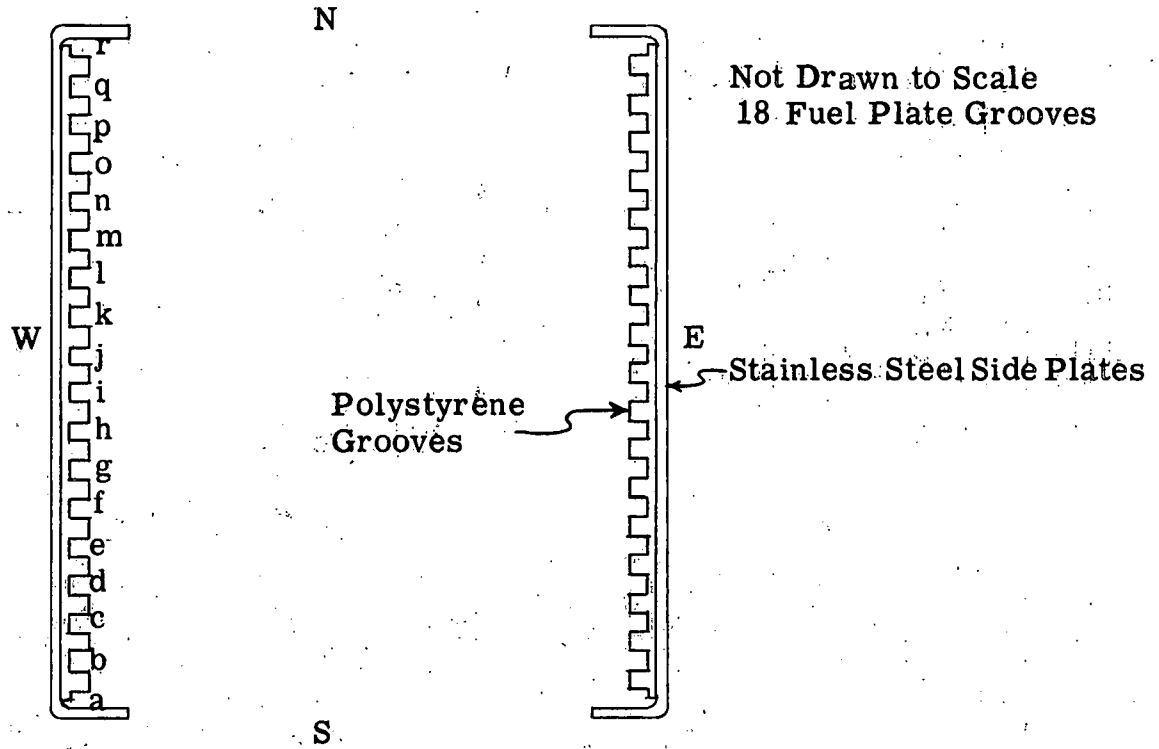


FIGURE A. 3

Control Rod Element Fuel Plate Arrangement

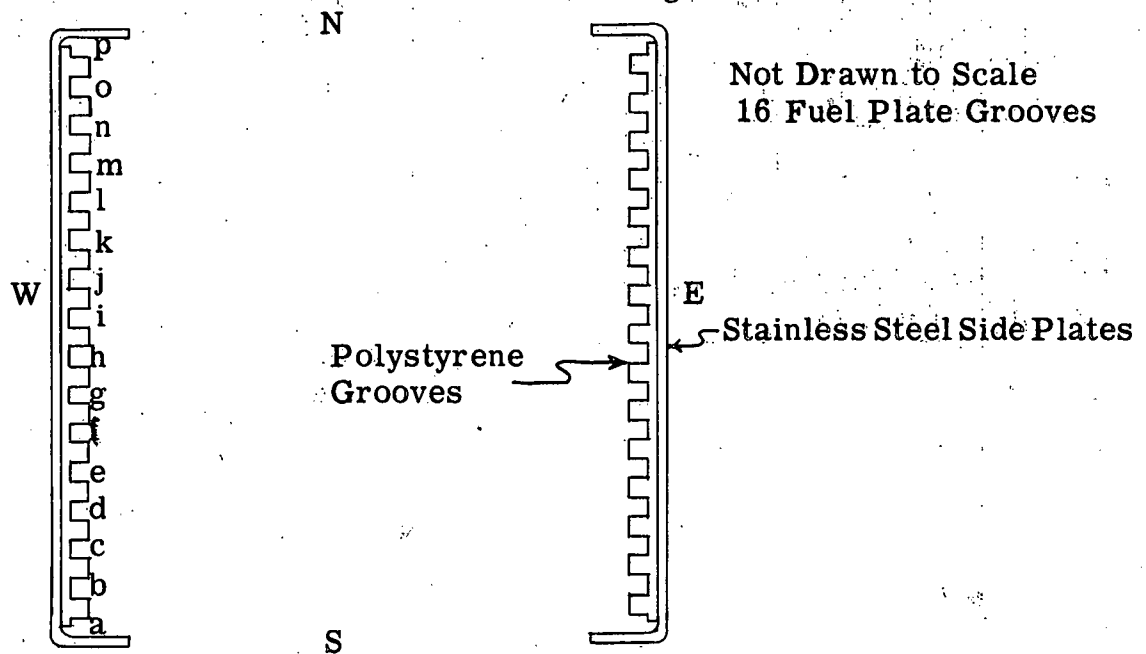


FIGURE A. 4

THIS PAGE
WAS INTENTIONALLY
LEFT BLANK

A.6.3 Core Loading Compositions

The underscored figures are not "significant figures", but are only to be taken as indicative.

| Reference Loading Number | Comments | Loaded Mass U ²³⁵ -Stationary Elements - (gm) | Loaded Mass U ²³⁵ Control Elements-(gm) | Total Mass* U ²³⁵ in Active Core-(gm) | Loaded Mass B ¹⁰ Stationary Elements-(gm) | Loaded Mass B ¹⁰ Control Elements-(gm) | Total Mass* B ¹⁰ in Active Core-(gm) | Loaded Mass Stainless Steel - Stationary Element-(gm) | Loaded Mass Stainless Steel - Control Element-(gm) | Total Mass* Stainless Steel in Active Core-(gm) |
|--------------------------|----------------|--|--|--|--|---|---|---|--|---|
| 1 | Sub-critical | | | | | | | | | |
| 2 | Open 7 Array | 5278.20 | 1182.72 | 6240 + 10 | 0 | 0 | 0 | 43780 + 320 | 20490 + 970 | 62700 + 1000 |
| 3 | Open 7 Array | 5648.60 | 1182.72 | 6433.2 + 8.6 | 0 | 0 | 0 | 45840 + 340 | 20490 + 970 | 63400 + 1000 |
| 4 | Open 7 Array | 6019.00 | 1182.72 | 6691.4 + 7.5 | 0 | 0 | 0 | 47900 + 350 | 20490 + 970 | 64600 + 1000 |
| 5 | Open 7 Array | 6389.40 | 1182.72 | 6971.0 + 6.7 | 0 | 0 | 0 | 49960 + 370 | 20490 + 970 | 66000 + 1000 |
| 6 | Open 7 Array | 6713.50 | 1182.72 | 7240.4 + 6.3 | 0 | 0 | 0 | 51760 + 390 | 20490 + 970 | 67400 + 1000 |
| 7 | Open 7 Array | 7037.60 | 1182.72 | 7523.8 + 5.9 | 0 | 0 | 0 | 53560 + 410 | 20490 + 970 | 68800 + 1000 |
| 8 | Open 7 Array | 7037.60 | 1478.40 | 7596.4 + 7.0 | 0 | 0 | 0 | 53560 + 410 | 22130 + 970 | 69200 + 1000 |
| 9 | Open 7 Array | 7408.00 | 1478.40 | 7930.2 + 6.7 | 0 | 0 | 0 | 55620 + 430 | 22130 + 970 | 71000 + 1100 |
| 10 | Open 7 Array | 7778.40 | 1478.40 | 8264.6 + 6.5 | 0 | 0 | 0 | 57680 + 450 | 22130 + 970 | 72800 + 1100 |
| 11 | Open 7 Array | 8148.80 | 1478.40 | 8599.7 + 6.2 | 0 | 0 | 0 | 59740 + 470 | 22130 + 970 | 74600 + 1100 |
| 12 | Open 7 Array | 8472.90 | 1478.40 | 8897.6 + 6.0 | 0 | 0 | 0 | 61540 + 490 | 22130 + 970 | 76200 + 1100 |
| 13 | Open 7 Array | 8797.00 | 1478.40 | 9201.4 + 5.9 | 0 | 0 | 0 | 63380 + 500 | 22130 + 970 | 77800 + 1100 |
| 14 | Open 7 Array | 9167.40 | 1478.40 | 9546.7 + 5.7 | 0 | 0 | 0 | 65400 + 520 | 22130 + 970 | 79700 + 1100 |
| 15 | Open 7 Array | 9537.80 | 1478.40 | 9895.3 + 5.5 | 0 | 0 | 0 | 67450 + 540 | 22130 + 970 | 81600 + 1100 |
| 16 | Open 7 Array | 9908.20 | 1478.40 | 10243.0 + 5.4 | 0 | 0 | 0 | 69510 + 560 | 22130 + 970 | 83400 + 1100 |
| 17 | Open 7 Array | 10232.30 | 1478.40 | 10549.5 + 5.3 | 0 | 0 | 0 | 71310 + 580 | 22130 + 970 | 85200 + 1100 |
| 18 | Open 7 Array | 10556.40 | 1774.08 | 10905.7 + 6.2 | 0 | 0 | 0 | 73120 + 600 | 23760 + 970 | 87100 + 1100 |
| 19 | Open 7 Array | 11667.60 | 1774.08 | 11971.6 + 5.9 | 0 | 0 | 0 | 79290 + 660 | 23760 + 970 | 92900 + 1200 |
| 20 | Open 7 Array | 12315.80 | 2069.76 | 12629.7 + 6.7 | 0 | 0 | 0 | 82890 + 700 | 25390 + 980 | 96600 + 1200 |
| 21 | Open 7 Array | 13427.00 | 2069.76 | 13674.6 + 6.4 | 0 | 0 | 0 | 89070 + 760 | 25390 + 980 | 102300 + 1200 |
| 22 | Open 7 Array | 14075.20 | 2365.44 | 14317.2 + 7.2 | 0 | 0 | 0 | 92670 + 790 | 27020 + 980 | 105800 + 1200 |
| 23 | Open 7 Array | 15834.60 | 2365.44 | 15451.7 + 6.9 | 0 | 0 | 0 | 102450 + 890 | 27020 + 980 | 114800 + 1300 |
| 24 | Open 7 Array | 10556.40 | 1774.08 | 11421 + 10 | 13.74 + .30 | 2.352 + .054 | 14.89 + .30 | 73120 + 600 | 23760 + 970 | 90700 + 1100 |
| 25 | Not Completed | | | | | | | | | |
| 26 | Open 7 Array | 9537.80 | 1774.08 | 10538 + 11 | 12.42 + .27 | 2.352 + .054 | 13.74 + .27 | 67450 + 540 | 23760 + 970 | 86000 + 1100 |
| 27 | Open 7 Array | 8148.80 | 1478.40 | 9409 + 13 | 10.61 + .23 | 1.960 + .046 | 12.28 + .23 | 59740 + 470 | 22130 + 970 | 80500 + 1100 |
| 28 | Open 7 Array | 12315.80 | 2069.76 | 13168 + 10 | 16.04 + .34 | 2.744 + .064 | 17.17 + .34 | 82890 + 700 | 25390 + 980 | 100200 + 1200 |
| 29 | Open 7 Array | 14075.20 | 2365.44 | 14922 + 11 | 18.33 + .40 | 3.136 + .073 | 19.45 + .40 | 92670 + 790 | 27020 + 980 | 109800 + 1300 |
| 30 | Open 7 Array | 17594.00 | 2956.80 | 18511 + 12 | 22.91 + .49 | 3.920 + .091 | 24.13 + .50 | 112220 + 990 | 30290 + 990 | 129700 + 1400 |
| 31 | Open 7 Array | 21112.80 | 3548.16 | 22117 + 14 | 27.50 + .59 | 4.70 + .11 | 28.83 + .59 | 131800 + 1200 | 33600 + 1000 | 149700 + 1500 |
| 32 | Open 7 Array | 24631.60 | 4139.52 | 25740 + 16 | 32.08 + .69 | 5.49 + .13 | 33.54 + .69 | 151300 + 1400 | 36800 + 1000 | 169800 + 1700 |
| 33** | Open 7 Array | 31669.20 | 4730.88 | 32916 + 18 | 41.24 + .89 | 6.27 + .14 | 42.90 + .89 | 190400 + 1800 | 40100 + 1000 | 209600 + 2000 |
| 34 | Closed 7 Array | 31669.20 | 4730.88 | 32891 + 18 | 41.24 + .89 | 6.27 + .14 | 42.86 + .89 | 190400 + 1800 | 40100 + 1000 | 209500 + 2000 |
| 35 | Same as No. 33 | | | | | | | | | |
| 36 | Subcritical | | | | | | | | | |
| 37 | Open 7 Array | 21112.80 | 3548.16 | 23871 + 29 | 55.0 + 1.2 | 9.41 + .22 | 62.3 + 1.2 | 131800 + 1200 | 33600 + 1000 | 160700 + 1500 |

THIS PAGE
WAS INTENTIONALLY
LEFT BLANK

A. 6. 3 Core Loading Compositions (Cont'd)

| Reference Loading Number | Comments | Loaded Mass U ²³⁵ -Stationary Elements-(gm) | Loaded Mass U ²³⁵ Control Elements-(gm) | Total Mass* U ²³⁵ in Active Core-(gm) | Loaded Mass B ¹⁰ Stationary Elements-(gm) | Loaded Mass B ¹⁰ Control Elements-(gm) | Total Mass* B ¹⁰ in Active Core-(gm) | Loaded Mass Stainless Steel - Stationary Element-(gm) | Loaded Mass Stainless Steel - Control Element-(gm) | Total Mass* Stainless Steel in Active Core-(gm) |
|--------------------------------|--------------|--|--|--|--|---|---|---|--|---|
| 38 | Open 7 Array | 24631.60 | 4139.52 | 27586 + 32 | 64.2 + 1.4 | 10.98 + .25 | 72.0 + 1.4 | 151300 + 1400 | 36800 + 1000 | 181200 + 1700 |
| 39 | Open 7 Array | 28150.40 | 4730.88 | 31436 + 36 | 73.3 + 1.6 | 12.54 + .29 | 82.0 + 1.6 | 170900 + 1600 | 40100 + 1000 | 202600 + 1900 |
| 40 | Open 7 Array | 31669.20 | 4730.88 | 34937 + 35 | 82.4 + 1.8 | 12.54 + .29 | 91.2 + 1.8 | 190400 + 1800 | 40100 + 1000 | 222100 + 2000 |
| 41 | Open 7 Array | 19353.40 | 3252.48 | 22292 + 31 | 50.4 + 1.1 | 8.62 + .20 | 58.2 + 1.1 | 122000 + 1100 | 31920 + 990 | 152300 + 1500 |
| 42 | Open 7 Array | 7037.60 | 1182.72 | 7702.4 + 7.4 | 3.207 + .076 | 0.549 + .014 | 3.516 + .076 | 53560 + 410 | 20490 + 970 | 70200 + 1000 |
| 43 | Open 7 Array | 10556.40 | 1774.08 | 11041.1 + 7.0 | 4.81 + .11 | 0.823 + .021 | 5.04 + .11 | 73120 + 600 | 23760 + 970 | 88000 + 1100 |
| 44 | Open 7 Array | 14075.20 | 2365.44 | 14522.9 + 8.1 | 6.41 + .15 | 1.098 + .028 | 6.62 + .15 | 92670 + 790 | 27020 + 980 | 107200 + 1200 |
| 45 | Open 7 Array | 17594.00 | 2956.80 | 18033.8 + 9.5 | 8.02 + .19 | 1.372 + .035 | 8.22 + .19 | 112220 + 990 | 30290 + 990 | 126600 + 1400 |
| 46 | Open 7 Array | 21112.80 | 3548.16 | 21536 + 11 | 9.62 + .23 | 1.646 + .042 | 9.82 + .23 | 131800 + 1200 | 33600 + 1000 | 146000 + 1500 |
| 47 | Open 7 Array | 24631.60 | 4139.52 | 25048 + 13 | 11.23 + .27 | 1.921 + .049 | 11.42 + .27 | 151300 + 1400 | 36800 + 1000 | 165400 + 1700 |
| 48 | Open 7 Array | 31669.20 | 4730.88 | 32114 + 14 | 14.43 + .34 | 2.195 + .056 | 14.64 + .34 | 190400 + 1800 | 40100 + 1000 | 204700 + 2000 |

* Total Masses in Active Core Account for Position of Control Rod Bank.

** Preliminary SM-2 cold-clean mockup.

THIS PAGE
WAS INTENTIONALLY
LEFT BLANK

A. 6. 4 - Reference Loading Number 49 - Preliminary SM-2 Midlife Mockup

Total Loaded Masses: - 28693.12 gm U²³⁵ 16.1 gm B¹⁰

Open Seven Control Rod Array

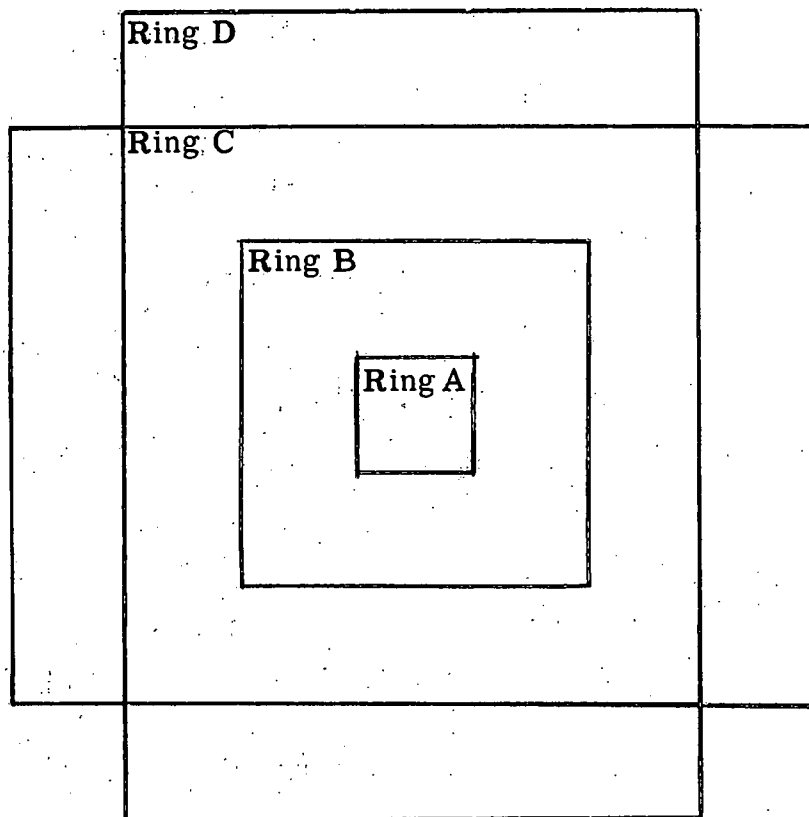


FIGURE A. 5

Ring D: Stationary Elements 12, 13, 14, 15, 16, 21, 27, 31, 37, 41, 47, 51, 57, 61, 67, 72, 73, 74, 75, 76

15 Fuel Plates - 694.50 gm U²³⁵/ element

24 Boron tapes - 0.506 gm B¹⁰/element

0.1224 in. additional steel plates

Fuel Plate Arrangement (numbered as in Figure A. 3)

Boron tape on North side of fuel plate.

- a. 1 fuel plate - 46.30 gm U²³⁵, 1 layer boron tape (0.0211 + .0005 gm B¹⁰/tape) - 0.0211 gm B¹⁰
- b. 1 fuel plate - 46.30 gm U²³⁵, 2 layers boron tape (0.0211 + .0005 gm B¹⁰/tape) - 0.0422 gm B¹⁰
- c. 4 0.0102 in. steel plates - 0.0408 in.
- d. 1 fuel plate - 46.30 gm U²³⁵, 2 layers boron tape (0.0211 + .0005 gm B¹⁰/tape) - 0.0422 gm B¹⁰

- e. 1 fuel plate - 46.30 gm U^{235} , 1 layer boron tape (0.0211 \pm .0005 gm B^{10} /tape) - 0.0211 gm B^{10}
- f. 1 fuel plate - 46.30 gm U^{235} , 2 layers boron tape (0.0211 \pm .0005 gm B^{10} /tape) - 0.0422 gm B^{10}
- g. 1 fuel plate - 46.30 gm U^{235} , 2 layers boron tape (0.0211 \pm .0005 gm B^{10} /tape) - 0.0422 gm B^{10}
- h. 1 fuel plate - 46.30 gm U^{235} , 1 layer boron tape (0.0211 \pm .0005 gm B^{10} /tape) - 0.0211 gm B^{10}
- i. 4 0.0102 in. steel plates - 0.0408 in.
- j. 1 fuel plate - 46.30 gm U^{235} , 1 layer boron tape (0.0211 \pm .0005 gm B^{10} /tape) - 0.0211 gm B^{10}
- k. 1 fuel plate - 46.30 gm U^{235} , 2 layers boron tape (0.0211 \pm .0005 gm B^{10} /tape) - 0.0422 gm B^{10}
- l. 1 fuel plate - 46.30 gm U^{235} , 2 layers boron tape (0.0211 \pm .0005 gm B^{10} /tape) - 0.0422 gm B^{10}
- m. 1 fuel plate - 46.30 gm U^{235} , 1 layer boron tape (0.0211 \pm .0005 gm B^{10} /tape) - 0.0211 gm B^{10}
- n. 1 fuel plate - 46.30 gm U^{235} , 2 layers boron tape (0.0211 \pm .0005 gm B^{10} /tape) - 0.0422 gm B^{10}
- o. 4 0.0102 in. steel plates - 0.0408 in.
- p. 1 fuel plate 46.30 gm U^{235} , 2 layers boron tape (0.0211 \pm .0005 gm B^{10} /tape) - 0.0422 gm B^{10}
- q. 1 fuel plate 46.30 gm U^{235} , 2 layers boron tape (0.0211 \pm .0005 gm B^{10} /tape) - 0.0422 gm B^{10}
- r. 1 fuel plate 46.30 gm U^{235} , 1 layer boron tape (0.0211 \pm .0005 gm B^{10} /tape) - 0.0211 gm B^{10}

Ring C: Stationary Elements 22, 23, 25, 26, 42, 46, 62, 63, 65, 66

14 Fuel Plates - 648.20 gm U^{235} /element

14 Boron tapes - 0.295 gm B^{10} /element

0.1632 in. additional steel plates

Fuel Plate Arrangement (numbered as in Figure A. 3)

Boron tape on North side of fuel plate.

- a. 1 fuel plate - 46.30 gm U^{235} , 1 layer boron tape
(0.0211 \pm .0005 gm B^{10} /tape) - 0.0211 gm B^{10}
- b. 1 fuel plate - 46.30 gm U^{235} , 1 layer boron tape
(0.0211 \pm .0005 gm B^{10} /tape) - 0.0211 gm B^{10}
- c. 4 0.0102 in. steel plates - 0.0408 in.
- d. 1 fuel plate 46.30 gm U^{235} , 1 layer boron tape
(0.0211 gm B^{10} /tape) - 0.0211 gm B^{10}
- e. 1 fuel plate 46.30 gm U^{235} , 1 layer boron tape
(0.0211 gm B^{10} /tape) - 0.0211 gm B^{10}
- f. 1 fuel plate 46.30 gm U^{235} , 1 layer boron tape
(0.0211 gm B^{10} /tape) - 0.0211 gm B^{10}
- g. 4 0.0102 in. steel plates - 0.0408 in.
- h. 1 fuel plate - 46.30 gm U^{235} , 1 layer boron tape
(0.0211 gm B^{10} /tape) - 0.0211 gm B^{10}
- i. 1 fuel plate - 46.30 gm U^{235} , 1 layer boron tape
(0.0211 gm B^{10} /tape) - 0.0211 gm B^{10}
- j. 1 fuel plate - 46.30 gm U^{235} , 1 layer boron tape
(0.0211 gm B^{10} /tape) - 0.0211 gm B^{10}
- k. 1 fuel plate - 46.30 gm U^{235} , 1 layer boron tape
(0.0211 gm B^{10} /tape) - 0.0211 gm B^{10}
- l. 4 0.0102 in. steel plates - 0.0408 in.
- m. 1 fuel plate - 46.30 gm U^{235} , 1 layer boron tape
(0.0211 gm B^{10} /tape) - 0.0211 gm B^{10}
- n. 1 fuel plate - 46.30 gm U^{235} , 1 layer boron tape
(0.0211 gm B^{10} /tape) - 0.0211 gm B^{10}
- o. 1 fuel plate - 46.30 gm U^{235} , 1 layer boron tape
(0.0211 gm B^{10} /tape) - 0.0211 gm B^{10}
- p. 4 0.0102 in. steel plates - 0.0408 in.
- q. 1 fuel plate - 46.30 gm U^{235} , 1 layer boron tape
(0.0211 gm B^{10} /tape) - 0.0211 gm B^{10}
- r. 1 fuel plate - 46.30 gm U^{235} , 1 layer boron tape
(0.0211 gm B^{10} /tape) - 0.0211 gm B^{10}

Control Elements A, B, D, E, F, G

12 Fuel Plates - 506.88 gm U^{235} /element

12 Boron tapes - 0.235 gm B^{10} /element

0.1632 in. additional steel plates

Fuel Plate Arrangement (Numbered as in Figure A. 4)

Boron tape on North side of fuel plate

- a. 1 fuel plate - 42.24 gm U^{235} , 1 layer boron tape
(0.0196 \pm .0005 gm B^{10} /tape) - 0.0196 gm B^{10}
- b. 4 0.0102 in. steel plates - 0.0408 in.
- c. 1 fuel plate 42.24 gm U^{235} , 1 layer boron tape
(0.0196 \pm .0005 gm B^{10} /tape) - 0.0196 gm B^{10}
- d. 1 fuel plate 42.24 gm U^{235} , 1 layer boron tape
(0.0196 \pm .0005 gm B^{10} /tape) - 0.0196 gm B^{10}
- e. 1 fuel plate - 42.24 gm U^{235} , 1 layer boron tape
(0.0196 \pm .0005 gm B^{10} /tape) - 0.0196 gm B^{10}
- f. 4 0.0102 in. steel plates - 0.0408 in.
- g. 1 fuel plate - 42.24 gm U^{235} , 1 layer boron tape
(0.0196 \pm .0005 gm B^{10} /tape) - 0.0196 gm B^{10}
- h. 1 fuel plate - 42.24 gm U^{235} , 1 layer boron tape
(0.0196 \pm .0005 gm B^{10} /tape) - 0.0196 gm B^{10}
- i. 1 fuel plate - 42.24 gm U^{235} , 1 layer boron tape
(0.0196 \pm .0005 gm B^{10} /tape) - 0.0196 gm B^{10}
- j. 1 fuel plate - 42.24 gm U^{235} , 1 layer boron tape
(0.0196 \pm .0005 gm B^{10} /tape) - 0.0196 gm B^{10}
- k. 4 0.0102 in. steel plates - 0.0408 in.
- l. 1 fuel plate - 42.24 gm U^{235} , 1 layer boron tape
(0.0196 \pm .0005 gm B^{10} /tape) - 0.0196 gm B^{10}
- m. 1 fuel plate - 42.24 gm U^{235} , 1 layer boron tape
(0.0196 \pm .0005 gm B^{10} /tape) - 0.0196 gm B^{10}
- n. 1 fuel plate - 42.24 gm U^{235} , 1 layer boron tape
(0.0196 \pm .0005 gm B^{10} /tape) - 0.0196 gm B^{10}

o. 4 0.0102 in. steel plates - 0.0408 in.

p. 1 fuel plate 42.24 gm U^{235} , 1 layer boron tape
($0.0196 \pm .0005$ gm B^{10} /tape) - 0.0196 gm B^{10}

Ring B: Stationary Elements 33, 34, 35, 43, 45, 53, 54, 55

13 Fuel plates - 601.90 gm U^{235} /element

9 Boron tapes - 0.190 gm B^{10} /element

0.2040 in. additional steel plates

Fuel Plate Arrangement (Numbered as in Figure A. 3)

Boron tape on North side of fuel plate

a. 1 fuel plate - 46.30 gm U^{235} , 1 layer boron tape
($0.0211 \pm .0005$ gm B^{10} /tape) - 0.0211 gm B^{10}

b. 4 0.0102 in. steel plates - 0.0408 in.

c. 1 fuel plate - 46.30 gm U^{235}

d. 1 fuel plate - 46.30 gm U^{235} , 1 layer boron tape
($0.0211 \pm .0005$ gm B^{10} /tape) - 0.0211 gm B^{10}

e. 1 fuel plate - 46.30 gm U^{235} , 1 layer boron tape
($0.0211 \pm .0005$ gm B^{10} /tape) - 0.0211 gm B^{10}

f. 4 0.0102 in. steel plates - 0.0408 in.

g. 1 fuel plate - 46.30 gm U^{235}

h. 1 fuel plate - 46.30 gm U^{235} , 1 layer boron tape
($0.0211 \pm .0005$ gm B^{10} /tape) - 0.0211 gm B^{10}

i. 1 fuel plate - 46.30 gm U^{235} , 1 layer boron tape
($0.0211 \pm .0005$ gm B^{10} /tape) - 0.0211 gm B^{10}

j. 4 0.0102 in. steel plates - 0.0408 in.

k. 1 fuel plate - 46.30 gm U^{235} , 1 layer boron tape
($0.0211 \pm .0005$ gm B^{10} /tape) - 0.0211 gm B^{10}

l. 1 fuel plate - 46.30 gm U^{235}

m. 4 0.0102 in. steel plates - 0.0408 in.

n. 1 fuel plate - 46.30 gm U^{235} , 1 layer boron tape
($0.0211 \pm .0005$ gm B^{10} /tape) - 0.0211 gm B^{10}

- o. 1 fuel plate - 46.30 gm U^{235} , 1 layer boron tape
($0.0211 \pm .0005$ gm B^{10} /tape) - 0.0211 gm B^{10}
- p. 1 fuel plate - 46.30 gm U^{235}
- q. 4 0.0102 in. steel plates - 0.0408 in.
- r. 1 fuel plate - 46.30 gm U^{235} , 1 layer boron tape
($0.0211 \pm .0005$ gm B^{10} /tape) - 0.0211 gm B^{10}

Ring A: Control Element C

11 Fuel Plates - 464.64 gm U^{235}
 7 Boron tapes - 0.137 gm B^{10}
 0.2040 in. additional steel plates

Fuel Plate Arrangement (Numbered as in Figure A. 4)
 Boron tape on North side of fuel plate

- a. 1 fuel plate - 42.24 gm U^{235} , 1 layer boron tape
($0.0196 \pm .0005$ gm B^{10} /tape) - 0.0196 gm B^{10}
- b. 4 0.0102 in. steel plates - 0.0408 in.
- c. 1 fuel plate - 42.24 gm U^{235}
- d. 1 fuel plate - 42.24 gm U^{235} , 1 layer boron tape
($0.0196 \pm .0005$ gm B^{10} /tape) - 0.0196 gm B^{10}
- e. 4 0.0102 in. steel plates - 0.0408 in.
- f. 1 fuel plate - 42.24 gm U^{235}
- g. 1 fuel plate - 42.24 gm U^{235} , 1 layer boron tape
($0.0196 \pm .0005$ gm B^{10} /tape) - 0.0196 gm B^{10}
- h. 4 0.0102 in steel plates - 0.0408 in.
- i. 1 fuel plate - 42.24 gm U^{235} , 1 layer boron tape
($0.0196 \pm .0005$ gm B^{10} /tape) - 0.0196 gm B^{10}
- j. 1 fuel plate - 42.24 gm U^{235}
- k. 1 fuel plate - 42.24 gm U^{235} , 1 layer boron tape
($0.0196 \pm .0005$ gm B^{10} /tape) - 0.0196 gm B^{10}
- l. 4 0.0102 in. steel plates - 0.0408 in.

- m. 1 fuel plate - 42.24 gm U^{235} , 1 layer boron tape
(0.0196 \pm .0005 gm B^{10} /tape) - 0.0196 gm B^{10}
- n. 1 fuel plate - 42.24 gm U^{235}
- o. 4 0.0102 in. steel plates - 0.0408 in.
- p. 1 fuel plate - 42.24 gm U^{235} , 1 layer boron tape
(0.0196 \pm .0005 gm B^{10} /tape) - 0.0196 gm B^{10}

A. 6. 5 Reference Loading Number 33 - Preliminary SM-2 Cold Clean Mockup

Total Loaded Masses - 36400.08 gm U^{235} 47.5 gm B^{10}
Open Seven Control Rod Array

All Stationary Elements:

- 18 Fuel Plates - 833.40 gm U^{235} /element
- 18 Boron tapes - 1.085 gm B^{10} /element

Fuel Plate Arrangement (Numbered as in Figure A. 3)
Boron tape on North side of fuel plate

- a. 1 fuel plate - 46.30 gm U^{235} , 1 layer boron tape
(0.060 \pm .001 gm B^{10} /tape) - 0.060 gm B^{10}
- b. 1 fuel plate - 46.30 gm U^{235} , 1 layer boron tape
(0.060 \pm .001 gm B^{10} /tape) - 0.060 gm B^{10}
- c. 1 fuel plate - 46.30 gm U^{235} , 1 layer boron tape
(0.060 \pm .001 gm B^{10} /tape) - 0.060 gm B^{10}
- d. 1 fuel plate - 46.30 gm U^{235} , 1 layer boron tape
(0.060 \pm .001 gm B^{10} /tape) - 0.060 gm B^{10}
- e. 1 fuel plate - 46.30 gm U^{235} , 1 layer boron tape
(0.060 \pm .001 gm B^{10} /tape) - 0.060 gm B^{10}
- f. 1 fuel plate - 46.30 gm U^{235} , 1 layer boron tape
(0.060 \pm .001 gm B^{10} /tape) - 0.060 gm B^{10}
- g. 1 fuel plate - 46.30 gm U^{235} , 1 layer boron tape
(0.060 \pm .001 gm B^{10} /tape) - 0.060 gm B^{10}
- h. 1 fuel plate - 46.30 gm U^{235} , 1 layer boron tape
(0.060 \pm .001 gm B^{10} /tape) - 0.060 gm B^{10}

- i. 1 fuel plate - 46.30 gm U²³⁵, 1 layer boron tape
(0.060 \pm .001 gm B¹⁰/tape) - 0.060 gm B¹⁰
- j. 1 fuel plate - 46.30 gm U²³⁵, 1 layer boron tape
(0.060 \pm .001 gm B¹⁰/tape) - 0.060 gm B¹⁰
- k. 1 fuel plate - 46.30 gm U²³⁵, 1 layer boron tape
(0.060 \pm .001 gm B¹⁰/tape) - 0.060 gm B¹⁰
- l. 1 fuel plate - 46.30 gm U²³⁵, 1 layer boron tape
(0.060 \pm .001 gm B¹⁰/tape) - 0.060 gm B¹⁰
- m. 1 fuel plate - 46.30 gm U²³⁵, 1 layer boron tape
(0.060 \pm .001 gm B¹⁰/tape) - 0.060 gm B¹⁰
- n. 1 fuel plate - 46.30 gm U²³⁵, 1 layer boron tape
(0.060 \pm .001 gm B¹⁰/tape) - 0.060 gm B¹⁰
- o. 1 fuel plate - 46.30 gm U²³⁵, 1 layer boron tape
(0.060 \pm .001 gm B¹⁰/tape) - 0.060 gm B¹⁰
- p. 1 fuel plate - 46.30 gm U²³⁵, 1 layer boron tape
(0.060 \pm .001 gm B¹⁰/tape) - 0.060 gm B¹⁰
- q. 1 fuel plate - 46.30 gm U²³⁵, 1 layer boron tape
(0.060 \pm .001 gm B¹⁰/tape) - 0.060 gm B¹⁰
- r. 1 fuel plate - 46.30 gm U²³⁵, 1 layer boron tape
(0.060 \pm .001 gm B¹⁰/tape) - 0.060 gm B¹⁰

All Control Elements:

16 Fuel Plates - 675.84 gm U²³⁵/element
 16 Boron tapes - 0.896 gm B¹⁰/element

Fuel Plate Arrangement (Numbered as in Figure A.4)
 Boron tape on North side of fuel plate.

- a. 1 fuel plate - 42.24 gm U²³⁵, 1 layer boron tape
(0.056 \pm .001 gm B¹⁰/tape) - 0.056 gm B¹⁰
- b. 1 fuel plate - 42.24 gm U²³⁵, 1 layer boron tape
(0.056 \pm .001 gm B¹⁰/tape) - 0.056 gm B¹⁰
- c. 1 fuel plate - 42.24 gm U²³⁵, 1 layer boron tape
(0.056 \pm .001 gm B¹⁰/tape) - 0.056 gm B¹⁰

- d. 1 fuel plate - 42.24 gm U²³⁵, 1 layer boron tape
(0.056 ± .001 gm B¹⁰/tape) - 0.056 gm B¹⁰
- e. 1 fuel plate - 42.24 gm U²³⁵, 1 layer boron tape
(0.056 ± .001 gm B¹⁰/tape) - 0.056 gm B¹⁰
- f. 1 fuel plate - 42.24 gm U²³⁵, 1 layer boron tape
(0.056 ± .001 gm B¹⁰/tape) - 0.056 gm B¹⁰
- g. 1 fuel plate - 42.24 gm U²³⁵, 1 layer boron tape
(0.056 ± .001 gm B¹⁰/tape) - 0.056 gm B¹⁰
- h. 1 fuel plate - 42.24 gm U²³⁵, 1 layer boron tape
(0.056 ± .001 gm B¹⁰/tape) - 0.056 gm B¹⁰
- i. 1 fuel plate - 42.24 gm U²³⁵, 1 layer boron tape
(0.056 ± .001 gm B¹⁰/tape) - 0.056 gm B¹⁰
- j. 1 fuel plate - 42.24 gm U²³⁵, 1 layer boron tape
(0.056 ± .001 gm B¹⁰/tape) - 0.056 gm B¹⁰
- k. 1 fuel plate - 42.24 gm U²³⁵, 1 layer boron tape
(0.056 ± .001 gm B¹⁰/tape), - 0.056 gm B¹⁰
- l. 1 fuel plate - 42.24 gm U²³⁵, 1 layer boron tape
(0.056 ± .001 gm B¹⁰/tape) - 0.056 gm B¹⁰
- m. 1 fuel plate - 42.24 gm U²³⁵, 1 layer boron tape
(0.056 ± .001 gm B¹⁰/tape) - 0.056 gm B¹⁰
- n. 1 fuel plate - 42.24 gm U²³⁵, 1 layer boron tape
(0.056 ± .001 gm B¹⁰/tape) - 0.056 gm B¹⁰
- o. 1 fuel plate - 42.24 gm U²³⁵, 1 layer boron tape
(0.056 ± .001 gm B¹⁰/tape) - 0.056 gm B¹⁰
- p. 1 fuel plate - 42.24 gm U²³⁵, 1 layer boron tape
(0.056 ± .001 gm B¹⁰/tape) - 0.056 gm B¹⁰

A. 6. 6 Reference Loading Number 50 - SM-1 Mockup No. 1

Closed Seven Control Rod Array

| | |
|--|---------------|
| Loaded Mass U ²³⁵ , Stationary Elements | 19353.40 gm |
| Loaded Mass U ²³⁵ , Control Elements | 2956.80 gm |
| Total Mass U ²³⁵ in Active Core | 20346 ± 13 gm |

| | |
|---|------------------|
| Loaded Mass B ¹⁰ , Stationary Elements | 8.82 + .21 gm |
| Loaded Mass B ¹⁰ , Control Elements | 1.372 + .035 gm |
| Total Mass B ¹⁰ in Active Core | 9.28 + .21 gm |
| Loaded Mass Stainless Steel, Stationary Elements | 165800 + 1100 gm |
| Loaded Mass Stainless Steel Control Elements | 34760 + 990 gm |
| Total Mass Stainless Steel in Active Core | 183900 + 1500 gm |

All Stationary Elements: *

- 11 Fuel Plates - 509.30 gm U²³⁵/element
- 11 Boron tapes - 0.232 gm B¹⁰/element

Fuel Plate Arrangement (Numbered as in Figure A. 3)
Boron tape on North side of fuel plate

- a. 1 fuel plate - 46.30 gm U²³⁵, 1 layer boron tape
(0.0211 + .0005 gm B¹⁰/tape) - 0.0211 gm B¹⁰
- b. 1 0.0102 in. steel plate - 0.0102 in.
- c. 1 fuel plate - 46.30 gm U²³⁵, 1 layer boron tape
(0.0211 + .0005 gm B¹⁰/tape) - 0.0211 gm B¹⁰
- d. 1 fuel plate - 46.30 gm U²³⁵, 1 layer boron tape
(0.0211 + .0005 gm B¹⁰/tape) - 0.0211 gm B¹⁰
- e. 2 0.0102 in steel plates - 0.0204 in.
- f. 1 fuel plate - 46.30 gm U²³⁵, 1 layer boron tape
(0.0211 + .0005 gm B¹⁰/tape) - 0.0211 gm B¹⁰
- g. 1 0.0102 in. steel plate - 0.0102 in.
- h. 1 fuel plate - 46.30 gm U²³⁵, 1 layer boron tape
(0.0211 + .0005 gm B¹⁰/tape) - 0.0211 gm B¹⁰
- i. 1 fuel plate - 46.30 gm U²³⁵, 1 layer boron tape
(0.0211 + .0005 gm B¹⁰/tape) - 0.0211 gm B¹⁰
- j. 1 0.0102 in. steel plate - 0.0102 in.

* 0.0525 in. thick side plates by adding extra steel to basic side plates.

- k. 1 fuel plate - 46.30 gm U^{235} , 1 layer boron tape
(0.0211 \pm .0005 gm B^{10} /tape) - 0.0211 gm B^{10}
- l. 1 0.0102 in. steel plate - 0.0102 in.
- m. 1 fuel plate 46.30 gm U^{235} , 1 layer boron tape
(0.0211 \pm .0005 gm B^{10} /tape) - 0.0211 gm B^{10}
- n. 2 0.0102 in steel plates - 0.0204 in.
- o. 1 fuel plate - 46.30 gm U^{235} , 1 layer boron tape
(0.0211 \pm .0005 gm B^{10} /tape) - 0.0211 gm B^{10}
- p. 1 fuel plate - 46.30 gm U^{235} , 1 layer boron tape
(0.0211 \pm .0005 gm B^{10} /tape) - 0.0211 gm B^{10}
- q. 1 0.0102 in steel plate - 0.0102 in.
- r. 1 fuel plate - 46.30 gm U^{235} , 1 layer boron tape
(0.0211 \pm .0005 gm B^{10} /tape) - 0.0211 gm B^{10}

All Control Elements:

- 10 Fuel Plates - 422.40 gm U^{235} /element
- 10 Boron tapes - 0.196 gm B^{10} /element

Fuel Plate Arrangement (Numbered as in Figure A. 4)
Boron tape on North side of fuel plate.

- a. 1 fuel plate - 42.24 gm U^{235} , 1 layer boron tape
(0.0196 \pm .0005 gm B^{10} /tape) - 0.0196 gm B^{10}
- b. 1 0.0102 in steel plate - 0.0102 in.
- c. 1 fuel plate - 42.24 gm U^{235} , 1 layer boron tape
(0.0196 \pm .0005 gm B^{10} /tape) - 0.0196 gm B^{10}
- d. 1 fuel plate - 42.24 gm U^{235} , 1 layer boron tape
(0.0196 \pm .0005 gm B^{10} /tape) - 0.0196 gm B^{10}
- e. 2 0.0102 in. steel plates - 0.0204 in.
- f. 1 fuel plate - 42.24 gm U^{235} , 1 layer boron tape
(0.0196 \pm .0005 gm B^{10} /tape) - 0.0196 gm B^{10}

- g. 1 0.0102 in steel plate - 0.0102 in.
- h. 1 fuel plate - 42.24 gm U²³⁵, 1 layer boron tape
(0.0196 \pm .0005 gm B¹⁰/tape) - 0.0196 gm B¹⁰
- i. 1 fuel plate - 42.24 gm U²³⁵, 1 layer boron tape
(0.0196 \pm .0005 gm B¹⁰/tape) - 0.0196 gm B¹⁰
- j. 1 0.0102 in. steel plate - 0.0102 in.
- k. 1 fuel plate - 42.24 gm U²³⁵, 1 layer boron tape
(0.0196 \pm .0005 gm B¹⁰/tape) - 0.0196 gm B¹⁰
- l. 1 0.0102 in. steel plate + 1 0.0051 in. steel plate - 0.0153 in.
- m. 1 fuel plate - 42.24 gm U²³⁵, 1 layer boron tape
(0.0196 \pm .0005 gm B¹⁰/tape) - 0.0196 gm B¹⁰
- n. 1 fuel plate - 42.24 gm U²³⁵, 1 layer boron tape
(0.0196 \pm .0005 gm B¹⁰/tape) - 0.0196 gm B¹⁰
- o. 1 0.0102 in. steel plate - 0.0102 in.
- p. 1 fuel plate - 42.24 gm U²³⁵, 1 layer boron tape
(0.0196 \pm .0005 gm B¹⁰/tape) - 0.0196 gm B¹⁰

A. 6.7 Reference Loading Number 51 - SM-1 Mockup No. 2

Closed Seven Control Rod Array

| | |
|---|----------------------|
| Loaded Mass U ²³⁵ , Stationary Elements | 19353.40 gm |
| Loaded Mass U ²³⁵ , Control Elements | 2956.80 gm |
| Total Mass U ²³⁵ in Active Core | 20494 \pm 14 gm |
| Loaded Mass B ¹⁰ , Stationary Elements | 13.18 \pm .26 gm |
| Loaded Mass B ¹⁰ , Control Elements | 1.984 \pm .042 gm |
| Total Mass B ¹⁰ in Active Core | 13.94 \pm .26 gm |
| Loaded Mass Stainless Steel, Stationary Elements | 165800 \pm 1100 gm |
| Loaded Mass Stainless Steel, Control Elements | 34760 \pm 990 gm |
| Total Mass Stainless Steel in Active Core | 184900 \pm 1500 gm |

All Stationary Elements:*

- 11 Fuel Plates - 509.30 gm U^{235} /element
- 17 Boron Tapes - 0.347 gm B^{10} /element

Fuel Plate Arrangement (Numbered as in Figure A. 3)
Boron tape on North side of fuel plate

- a. 1 fuel plate - 46.30 gm U^{235} , 2 layers boron tape
(0.0204 \pm .0004 gm B^{10} /tape) - 0.0408 gm B^{10}
- b. 1 0.0102 in. Steel plate - 0.0102 in.
- c. 1 fuel plate - 46.30 gm U^{235} , 1 layer boron tape
(0.0204 \pm .0004 gm B^{10} /tape) - 0.0204 gm B^{10}
- d. 1 fuel plate - 46.30 gm U^{235} , 2 layers boron tape
(0.0204 \pm .0004 gm B^{10} /tape) - 0.0408 gm B^{10}
- e. 2 0.0102 in. Steel Plates - 0.0204 in.
- f. 1 fuel plate - 46.30 gm U^{235} , 1 layer boron tape
(0.0204 \pm .0004 gm B^{10} /tape) - 0.0204 gm B^{10}
- g. 1 0.0102 in. steel plate - 0.0102 in.
- h. 1 fuel plate - 46.30 gm U^{235} , 2 layers boron tape
(0.0204 \pm .0004 gm B^{10} /tape) - 0.0408 gm B^{10}
- i. 1 fuel plate - 46.30 gm U^{235} , 1 layer boron tape
(0.0204 \pm .0004 gm B^{10} /tape) - 0.0204 gm B^{10}
- j. 1 0.0102 in. steel plate - 0.0102 in.
- k. 1 fuel plate - 46.30 gm U^{235} , 2 layers boron tape
(0.0204 \pm .0004 gm B^{10} /tape) - 0.0408 gm B^{10}
- l. 1 0.0102 in. steel plate - 0.0102 in.
- m. 1 fuel plate - 46.30 gm U^{235} , 1 layer boron tape
(0.0204 \pm .0004 gm B^{10} /tape) - 0.0204 gm B^{10}
- n. 2 0.0102 in. steel plates - 0.0204 in.
- o. 1 fuel plate - 46.30 gm U^{235} , 2 layers boron tape
(0.0204 \pm .0004 gm B^{10} /tape) - 0.0408 gm B^{10}

* 0.0525 in. thick side plates by adding extra steel to basic side plates.

- p. 1 fuel plate - 46.30 gm U^{235} , 1 layer boron tape
($0.0204 \pm .0004$ gm B^{10} /tape) - 0.0204 gm B^{10}
- q. 1 0.0102 in. steel plate - 0.0102 in.
- r. 1 fuel plate - 46.30 gm U^{235} , 2 layers boron tape ($0.0204 \pm .0004$ gm B^{10} /tape) - 0.0408 gm B^{10}

All Control Elements:

- 10 Fuel Plates - 422.40 gm U^{235} /element
- 15 Boron tapes - 0.284 gm B^{10} /element

Fuel Plate Arrangement (Numbered as in Figure A. 4)
Boron tape on North side of fuel plate

- a. 1 fuel plate - 42.24 gm U^{235} , 1 layer boron tape
($0.0189 \pm .0004$ gm B^{10} /tape) - 0.0189 gm B^{10}
- b. 1 0.0102 in. steel plate - 0.0102 in.
- c. 1 fuel plate - 42.24 gm U^{235} , 2 layers boron tape
($0.0189 \pm .0004$ gm B^{10} /tape) - 0.0378 gm B^{10}
- d. 1 fuel plate - 42.24 gm U^{235} , 1 layer boron tape
($0.0189 \pm .0004$ gm B^{10} /tape) - 0.0189 gm B^{10}
- e. 2 0.0102 in. steel plate - 0.0204 in.
- f. 1 fuel plate - 42.24 gm U^{235} , 2 layers boron tape
($0.0189 \pm .0004$ gm B^{10} /tape) - 0.0378 gm B^{10}
- g. 1 0.0102 in. steel plate - 0.0102 in.
- h. 1 fuel plate - 42.24 gm U^{235} , 1 layer boron tape
($0.0189 \pm .0004$ gm B^{10} /tape) - 0.0189 gm B^{10}
- i. 1 fuel plate - 42.24 gm U^{235} , 2 layers boron tape
($0.0189 \pm .0004$ gm B^{10} /tape) - 0.0378 gm B^{10}
- j. 1 0.0102 in. steel plate - 0.0102 in.
- k. 1 fuel plate - 42.24 gm U^{235} , 1 layer boron tape
($0.0189 \pm .0004$ gm B^{10} /tape) - 0.0189 gm B^{10}
- l. 1 0.0102 in. steel plate + 1 0.0051 in. steel plate - 0.0153 in.

- m. 1 fuel plate - 42.24 gm U^{235} , 2 layers boron tape
(0.0189 + .0004 gm B^{10} /tape) - 0.0378 gm B^{10}
- n. 1 fuel plate - 42.24 gm U^{235} , 1 layer boron tape
(0.0189 + .0004 gm B^{10} /tape) - 0.0189 gm B^{10}
- o. 1 0.0102 in. steel plate - 0.0102 in.
- p. 1 fuel plate - 42.24 gm U^{235} , 2 layers boron tape
(0.0189 + .0004 gm B^{10} /tape) - 0.0378 gm B^{10}

A. 6.8 Reference Loading Number 52 - SM-2 Midlife Mockup No. 2*

Total Loaded Masses - 29190.24 gm U^{235} 20.39 gm B^{10}

Open Seven Control Rod Array

Ring D: Stationary Elements 12, 14, 16, 21, 27, 41, 47, 61, 67, 72, 74, 76

15 Fuel Plates - 694.50 gm U^{235} /element
31 Boron Tapes - 0.632 gm B^{10} /element
0.1224 in. additional steel plates

Fuel Plate Arrangement (Numbered as in Figure A. 3):
Boron Tape on North side of fuel plate

- a. 1 fuel plate - 46.30 gm U^{235} , 2 layers boron tape
(0.0204 + .0004 gm B^{10} /tape) - 0.0408 gm B^{10}
- b. 1 fuel plate - 46.30 gm U^{235} , 2 layers boron tape
(0.0204 + .0004 gm B^{10} /tape) - 0.0408 gm B^{10}
- c. 1 fuel plate - 46.30 gm U^{235} , 2 layers boron tape
(0.0204 + .0004 gm B^{10} /tape) - 0.0408 gm B^{10}
- d. 4 0.0102 in. steel plates - 0.0408 in.
- e. 1 fuel plate - 46.30 gm U^{235} , 2 layers boron tape
(0.0204 + .0004 gm B^{10} /tape) - 0.0408 gm B^{10}
- f. 1 fuel plate - 46.30 gm U^{235} , 2 layers boron tape
(0.0204 + .0004 gm B^{10} /tape) - 0.0408 gm B^{10}
- g. 1 fuel plate - 46.30 gm U^{235} , 2 layers boron tape
(0.0204 + .0004 gm B^{10} /tape) - 0.0408 gm B^{10}

* Ring Notation as in Figure A. 5.

h. 1 fuel plate - 46.30 gm U²³⁵, 2 layers boron tape
(0.0204 \pm .0004 gm B¹⁰/tape) - 0.0408 gm B¹⁰

i. 1 fuel plate - 46.30 gm U²³⁵, 2 layers boron tape
(0.0204 \pm .0004 gm B¹⁰/tape) - 0.0408 gm B¹⁰

j. 4 0.0102 in. steel plates - 0.0408 in.

k. 1 fuel plate - 46.30 gm U²³⁵, 2 layers boron tape
(0.0204 \pm .0004 gm B¹⁰/tape) 0.0408 gm B¹⁰

l. 1 fuel plate - 46.30 gm U²³⁵, 2 layers boron tape
(0.0204 \pm .0004 gm B¹⁰/tape) - 0.0408 gm B¹⁰

m. 1 fuel plate - 46.30 gm U²³⁵, 2 layers boron tape
(0.0204 \pm .0004 gm B¹⁰/tape) - 0.0408 gm B¹⁰

n. 1 fuel plate - 46.30 gm U²³⁵, 3 layers boron tape
(0.0204 \pm .0004 gm B¹⁰/tape) - 0.0612 gm B¹⁰

o. 4 0.0102 in. steel plates - 0.0408 in.

p. 1 fuel plate - 46.30 gm U²³⁵, 2 layers boron tape
(0.0204 \pm .0004 gm B¹⁰/tapes) - 0.0408 gm B¹⁰

q. 1 fuel plate - 46.30 gm U²³⁵, 2 layers boron tape
(0.0204 \pm .0004 gm B¹⁰/tapes) - 0.0408 gm B¹⁰

r. 1 fuel plate - 46.30 gm U²³⁵, 2 layers boron tape
(0.0204 \pm .0004 gm B¹⁰/tapes) - 0.0408 gm B¹⁰

Stationary Elements 13, 15, 31, 37, 51, 57, 73, 75

16 Fuel Plates - 740.80 gm U²³⁵/element

32 Boron tapes - 0.653 gm B¹⁰/element

0.0816 in. additional steel plates

Fuel Plate Arrangement (Numbered as in Figure A. 3):

Boron tape on North side of fuel plate

a. 1 fuel plate - 46.30 gm U²³⁵, 2 layers boron tape
(0.0204 \pm .0004 gm B¹⁰/tape) - 0.0408 gm B¹⁰

b. 1 fuel plate - 46.30 gm U²³⁵, 2 layers boron tape
(0.0204 \pm .0004 gm B¹⁰/tape) - 0.0408 gm B¹⁰

- c. 1 fuel plate - 46.30 gm U^{235} , 2 layers boron tape
(0.0204 \pm .0004 gm B^{10} /tape) - 0.0408 gm B^{10}
- d. 4 0.0102 in. steel plates - 0.0408 in.
- e. 1 fuel plate - 46.30 gm U^{235} , 2 layers boron tape
(0.0204 \pm .0004 gm B^{10} /tape) 0.0408 gm B^{10}
- f. 1 fuel plate - 46.30 gm U^{235} , 2 layers boron tape
(0.0204 \pm .0004 gm B^{10} /tape) 0.0408 gm B^{10}
- g. 1 fuel plate - 46.30 gm U^{235} , 2 layers boron tape
(0.0204 \pm .0004 gm B^{10} /tape) 0.0408 gm B^{10}
- h. 1 fuel plate - 46.30 gm U^{235} , 2 layers boron tape
(0.0204 \pm .0004 gm B^{10} /tape) 0.0408 gm B^{10}
- i. 1 fuel plate - 46.30 gm U^{235} , 2 layers boron tape
(0.0204 \pm .0004 gm B^{10} /tape) 0.0408 gm B^{10}
- j. 1 fuel plate - 46.30 gm U^{235} , 2 layers boron tape
(0.0204 \pm .0004 gm B^{10} /tape) - 0.0408 gm B^{10}
- k. 1 fuel plate - 46.30 gm U^{235} , 2 layers boron tape
(0.0204 \pm .0004 gm B^{10} /tape) - 0.0408 gm B^{10}
- l. 1 fuel plate - 46.30 gm U^{235} , 2 layers boron tape
(0.0204 \pm .0004 gm B^{10} /tape) - 0.0408 gm B^{10}
- m. 1 fuel plate - 46.30 gm U^{235} , 2 layers boron tape
(0.0204 \pm .0004 gm B^{10} /tape) - 0.0408 gm B^{10}
- n. 1 fuel plate - 46.30 gm U^{235} , 2 layers boron tape
(0.0204 \pm .0004 gm B^{10} /tape) - 0.0408 gm B^{10}
- o. 4 0.0102 in. steel plates - 0.0408 in.
- p. 1 fuel plate - 46.30 gm U^{235} , 2 layers boron tape
(0.0204 \pm .0004 gm B^{10} /tape) - 0.0408 gm B^{10}
- q. 1 fuel plate - 46.30 gm U^{235} , 2 layers boron tape
(0.0204 \pm .0004 gm B^{10} /tape) - 0.0408 gm B^{10}
- r. 1 fuel plate - 46.30 gm U^{235} , 2 layers boron tape
(0.0204 \pm .0004 gm B^{10} /tape) 0.0408 gm B^{10}

Ring C: Stationary Elements 22, 23, 25, 26, 42, 46, 62, 63, 65, 66

14 Fuel Plates - 684.20 gm U^{235} /element
18 Boron tapes - 0.367 gm B^{10} /element
0.1632 in. additional steel plates

Fuel Plate arrangement (Numbered as in Figure A. 3):
Boron tape on North side of fuel plate.

- a. 1 fuel plate - 46.30 gm U^{235} , 1 layer boron tape
(0.0204 \pm .0004 gm B^{10} /tape) - 0.0204 gm B^{10}
- b. 1 fuel plate - 46.30 gm U^{235} , 1 layer boron tape
(0.0204 \pm .0004 gm B^{10} /tape) - 0.0204 gm B^{10}
- c. 1 fuel plate - 46.30 gm U^{235} , 1 layer boron tape
(0.0204 \pm .0004 gm B^{10} /tape) - 0.0204 gm B^{10}
- d. 4 0.0102 in. steel plates - 0.0408 in.
- e. 1 fuel plate - 46.30 gm U^{235} , 2 layers boron tape
(0.0204 \pm .0004 gm B^{10} /tape) - 0.0408 gm B^{10}
- f. 1 fuel plate - 46.30 gm U^{235} , 2 layers boron tape
(0.0204 \pm .0004 gm B^{10} /tape) - 0.0408 gm B^{10}
- g. 1 fuel plate - 46.30 gm U^{235} , 1 layer boron tape
(0.0204 \pm .0004 gm B^{10} /tape) - 0.0204 gm B^{10}
- h. 4 0.0102 in. steel plates - 0.0408 in.
- i. 1 fuel plate - 46.30 gm U^{235} , 1 layer boron tape
(0.0204 \pm .0004 gm B^{10} /tape) - 0.0204 gm B^{10}
- j. 1 fuel plate - 46.30 gm U^{235} , 1 layer boron tape
(0.0204 \pm .0004 gm B^{10} /tape) - 0.0204 gm B^{10}
- k. 4 0.0102 in. steel plates - 0.0408 in.
- l. 1 fuel plate - 46.30 gm U^{235} , 1 layer boron tape
(0.0204 \pm .0004 gm B^{10} /tape) - 0.0204 gm B^{10}
- m. 1 fuel plate - 46.30 gm U^{235} , 2 layers boron tape
(0.0204 \pm .0004 gm B^{10} /tape) - 0.0408 gm B^{10}
- n. 1 fuel plate - 46.30 gm U^{235} , 2 layers boron tape
(0.0204 \pm .0004 gm B^{10} /tape) - 0.0408 gm B^{10}

- o. 4 0.0102 in. steel plates - 0.0408 in.
- p. 1 fuel plate - 46.30 gm U^{235} , 1 layer boron tape
(0.0204 \pm .0004 gm B^{10} /tape) - 0.0204 gm B^{10}
- q. 1 fuel plate - 46.30 gm U^{235} , 1 layer boron tape
(0.0204 \pm .0004 gm B^{10} /tape) - 0.0204 gm B^{10}
- r. 1 fuel plate - 46.30 gm U^{235} , 1 layer boron tape
(0.0204 \pm .0004 gm B^{10} /tape) - 0.0204 gm B^{10}

Control Elements B, D, F

- 13 Fuel Plates - 549.12 gm U^{235} /element
- 15 Boron Tapes - 0.284 gm B^{10} /element
- 0.1224 in additional steel plates

Fuel Plate Arrangement (Numbered as in Figure A.4)
Boron tape on North side of fuel plate

- a. 1 fuel plate - 42.24 gm U^{235} , 1 layer boron tape
(0.0189 \pm .0004 gm B^{10} tape) - 0.0189 gm B^{10}
- b. 1 fuel plate - 42.24 gm U^{235} , 1 layer boron tape
(0.0189 \pm .0004 gm B^{10} tape) - 0.0189 gm B^{10}
- c. 1 fuel plate - 42.24 gm U^{235} , 1 layer boron tape
(0.0189 \pm .0004 gm B^{10} tape) - 0.0189 gm B^{10}
- d. 4 0.0102 in. steel plates - 0.0408 in.
- e. 1 fuel plate - 42.24 gm U^{235} , 1 layer boron tape
(0.0189 \pm .0004 gm B^{10} /tape) - 0.0189 gm B^{10}
- f. 1 fuel plate - 42.24 gm U^{235} , 2 layers boron tape
(0.0189 \pm .0004 gm B^{10} /tape) - 0.0378 gm B^{10}
- g. 1 fuel plate - 42.24 gm U^{235} , 1 layer boron tape
(0.0189 \pm .0004 gm B^{10} /tape) - 0.0189 gm B^{10}
- h. 1 fuel plate - 42.24 gm U^{235} , 1 layer boron tape
(0.0189 \pm .0004 gm B^{10} /tape) - 0.0189 gm B^{10}
- i. 4 0.0102 in. steel plates - 0.0408 in.

- j. 1 fuel plate - 42.24 gm U^{235} , 1 layer boron tape
(0.0189 \pm .0004 gm B^{10} /tape) - 0.0189 gm B^{10}
- k. 1 fuel plate - 42.24 gm U^{235} , 2 layers boron tape
(0.0189 \pm .0004 gm B^{10} /tape) - 0.0378 gm B^{10}
- l. 1 fuel plate - 42.24 gm U^{235} , 1 layer boron tape
(0.0189 \pm .0004 gm B^{10} /tape) - 0.0189 gm B^{10}
- m. 4 0.0102 in steel plates - 0.0408 in.
- n. 1 fuel plate - 42.24 gm U^{235} , 1 layer boron tape
(0.0189 \pm .0004 gm B^{10} /tape) 0.0189 gm B^{10}
- o. 1 fuel plate - 42.24 gm U^{235} , 1 layer boron tape
(0.0189 \pm .0004 gm B^{10} /tape) 0.0189 gm B^{10}
- p. 1 fuel plate - 42.24 gm U^{235} , 1 layer boron tape
(0.0189 \pm .0004 gm B^{10} /tape) 0.0189 gm B^{10}

Control Elements A, E, G

12 Fuel Plates - 506.88 gm U^{235} /element
 15 Boron tapes - 0.284 gm B^{10} /element
 0.1632 in. additional steel plates

Fuel Plate Arrangement (Numbered as in Figure A. 4) Boron tape on North side of fuel plate

- a. 1 fuel plate - 42.24 gm U^{235} , 1 layer boron tape
(0.0189 \pm .0004 gm B^{10} /tape) - 0.0187 gm B^{10}
- b. 1 fuel plate - 42.24 gm U^{235} , 1 layer boron tape
(0.0189 \pm .0004 gm B^{10} /tape) - 0.0187 gm B^{10}
- c. 1 fuel plate - 42.24 gm U^{235} , 1 layer boron tape
(0.0189 \pm .0004 gm B^{10} /tape) - 0.0187 gm B^{10}
- d. 4 0.0102 in. steel plates - 0.0408 in.
- e. 1 fuel plate - 42.24 gm U^{235} , 2 layers boron tape
(0.0189 \pm .0004 gm B^{10} /tape) - 0.0378 gm B^{10}
- f. 1 fuel plate - 42.24 gm U^{235} , 1 layer boron tape
(0.0189 \pm .0004 gm B^{10} /tape) - 0.0189 gm B^{10}

- g. 4 0.0102 in. steel plates - 0.0408 in.
- h. 1 fuel plate - 42.24 gm U^{235} , 2 layers boron tape
(0.0189 \pm .0004 gm B^{10} /tape) - 0.0378 gm B^{10}
- i. 1 fuel plate - 42.24 gm U^{235} , 1 layer boron tape
(0.0189 \pm .0004 gm B^{10} tape) - 0.0189 gm B^{10}
- j. 4 0.0102 in. steel plates - 0.0408 in.
- k. 1 fuel plate - 42.24 gm U^{235} , 1 layer boron tape
(0.0189 \pm .0004 gm B^{10} /tape) - 0.0189 gm B^{10}
- l. 1 fuel plate - 42.24 gm U^{235} , 2 layers boron tape
(0.0189 \pm .0004 gm B^{10} tape) - 0.0378 gm B^{10}
- m. 4 0.0102 in. steel plates - 0.0408 in.
- n. 1 fuel plate - 42.24 gm U^{235} , 1 layer boron tape
(0.0189 \pm .0004 gm B^{10} /tape) - 0.0189 gm B^{10}
- o. 1 fuel plate - 42.24 gm U^{235} , 1 layer boron tape
(0.0189 \pm .0004 gm B^{10} /tape) - 0.0189 gm B^{10}
- p. 1 fuel plate - 42.24 gm U^{235} , 1 layer boron tape
(0.0189 \pm .0004 gm B^{10} /tape) - 0.0189 gm B^{10}

Ring B: Stationary Elements 33, 35, 53, 55

13 Fuel Plates - 601.90 gm U^{235} /element
 13 Boron tapes - 0.265 gm B^{10} /element
 0.204 in additional steel plates

**Fuel Plate Arrangement (Numbered as in Figure A. 3)
 Boron tape on North side of fuel plate**

- a. 1 fuel plate - 46.30 gm U^{235} , 1 layer boron tape
(0.0204 \pm .0004 gm B^{10} /tape) - 0.0204 gm B^{10}
- b. 1 fuel plate - 46.30 gm U^{235} , 1 layer boron tape
(0.0204 \pm .0004 gm B^{10} /tape) - 0.0204 gm B^{10}
- c. 4 0.0102 in. steel plates - 0.0408 in.
- d. 1 fuel plate - 46.30 gm U^{235} , 1 layer boron tape
(0.0204 \pm .0004 gm B^{10} /tape) - 0.0204 gm B^{10}

- e. 1 fuel plate - 46.30 gm U²³⁵, 1 layer boron tape
(0.0204 \pm .0004 gm B¹⁰/tape) - 0.0204 gm B¹⁰
- f. 4 0.0102 in. steel plates - 0.0408 in.
- g. 1 fuel plate - 46.30 gm U²³⁵, 1 layer boron tape
(0.0204 \pm .0004 gm B¹⁰/tape) - 0.0204 gm B¹⁰
- h. 1 fuel plate - 46.30 gm U²³⁵, 1 layer boron tape
(0.0204 \pm .0004 gm B¹⁰/tape) - 0.0204 gm B¹⁰
- i. 4 0.0102 in. steel plates 0.0408 in.
- j. 1 fuel plate - 46.30 gm U²³⁵, 1 layer boron tape
(0.0204 \pm .0004 gm B¹⁰/tape) - 0.0204 gm B¹⁰
- k. 1 fuel plate 46.30 gm U²³⁵, 1 layer boron tape
(0.0204 \pm .0004 gm B¹⁰/tape) - 0.0204 gm B¹⁰
- l. 4 0.0102 in. steel plates - 0.0408 in.
- m. 1 fuel plate 46.30 gm U²³⁵, 1 layer boron tape
(0.0204 \pm .0004 gm B¹⁰/tape) - 0.0204 gm B¹⁰
- n. 1 fuel plate 46.30 gm U²³⁵, 1 layer boron tape
(0.0204 \pm .0004 gm B¹⁰/tape) - 0.0204 gm B¹⁰
- o. 1 fuel plate 46.30 gm U²³⁵, 1 layer boron tape
(0.0204 \pm .0004 gm B¹⁰/tape) - 0.0204 gm B¹⁰
- p. 4 0.0102 in. steel plates - 0.0408 in.
- q. 1 fuel plate - 46.30 gm U²³⁵, 1 layer boron tape
(0.0204 \pm .0004 gm B¹⁰/tape) - 0.0204 gm B¹⁰
- r. 1 fuel plate - 46.30 gm U²³⁵, 1 layer boron tape
(0.0204 \pm .0004 gm B¹⁰/tape) - 0.0204 gm B¹⁰

Stationary Elements 34, 43, 45, 54

13 Fuel Plates - 601.90 gm U²³⁵/element
 12 Boron Tapes - 0.245 gm B¹⁰/element
 0.2040 in. additional steel plates

Fuel Plate Arrangement (Numbered as in Figure A. 3)
 Boron tape on North side of fuel plate.

- a. 1 fuel plate - 46.30 gm U^{235} , 1 layer boron tape
 (0.0204 \pm .0004 gm B^{10} /tape) - 0.0204 gm B^{10}
- b. 1 fuel plate - 46.30 gm U^{235} , 1 layer boron tape
 (0.0204 \pm .0004 gm B^{10} /tape) - 0.0204 gm B^{10}
- c. 4 0.0102 in steel plates - 0.0408 in.
- d. 1 fuel plate - 46.30 gm U^{235} , 1 layer boron tape
 (0.0204 \pm .0004 gm B^{10} /tape) - 0.0204 gm B^{10}
- e. 1 fuel plate - 46.30 gm U^{235} , 1 layer boron tape
 (0.0204 \pm .0004 gm B^{10} /tape) - 0.0204 gm B^{10}
- f. 4 0.0102 in. steel plates - 0.0408 in.
- g. 1 fuel plate - 46.30 gm U^{235} , 1 layer boron tape
 (0.0204 \pm .0004 gm B^{10} /tape) - 0.0204 gm B^{10}
- h. 1 fuel plate - 46.30 gm U^{235} , 1 layer boron tape
 (0.0204 \pm .0004 gm B^{10} /tape) - 0.0204 gm B^{10}
- i. 4 0.0102 in. steel plates - 0.0408 in.
- j. 1 fuel plate - 46.30 gm U^{235} , 1 layer boron tape
 (0.0204 \pm .0004 gm B^{10} /tape) - 0.0204 gm B^{10}
- k. 1 fuel plate - 46.30 gm U^{235} , 1 layer boron tape
 (0.0204 \pm .0004 gm B^{10} /tape) - 0.0204 gm B^{10}
- l. 4 0.0102 in. steel plates - 0.0408 in.
- m. 1 fuel plate - 46.30 gm U^{235} , 1 layer boron tape
 (0.0204 \pm .0004 gm B^{10} /tape) 0.0204 gm B^{10}
- n. 1 fuel plate - 46.30 gm U^{235} , 1 layer boron tape
 (0.0204 \pm .0004 gm B^{10} /tape) - 0.0204 gm B^{10}
- o. 1 fuel plate - 46.30 gm U^{235}
- p. 4 0.0102 in. steel plates - 0.0408 in.

- q. 1 fuel plate - 46.30 gm U^{235} , 1 layer boron tape
(0.0204 \pm .0004 gm B^{10} /tape) - 0.0204 gm B^{10}
- r. 1 fuel plate - 46.30 gm U^{235} , 1 layer boron tape
(0.0204 \pm .0004 gm B^{10} /tape) - 0.0204 gm B^{10}

Ring A: Control Element C

11 Fuel Plates - 464.64 gm U^{235}
 9 Boron tapes - 0.170 gm B^{10}
 0.2040 in additional steel plates

Fuel Plate Arrangement (Numbered as in Figure A. 4)
 Boron tape on North side of fuel plate

- a. 1 fuel plate - 42.24 gm U^{235} , 1 layer boron tape
(0.0189 \pm .0004 gm B^{10} /tape) - 0.0189 gm B^{10}
- b. 1 fuel plate - 42.24 gm U^{235} , 1 layer boron tape
(0.0189 \pm .0004 gm B^{10} /tape) - 0.0189 gm B^{10}
- c. 4 0.0102 in. steel plates - 0.0408 in.
- d. 1 fuel plate 42.24 gm U^{235} , 1 layer boron tape
(0.0189 \pm .0004 gm B^{10} /tape) 0.0189 gm B^{10}
- e. 1 fuel plate 42.24 gm U^{235}
- f. 4 0.0102 in. steel plates - 0.0408 in.
- g. 1 fuel plate - 42.24 gm U^{235} , 1 layer boron tape
(0.0189 \pm .0004 gm B^{10} /tape) 0.0189 gm B^{10}
- h. 4 0.0102 in. steel plates - 0.0408 in.
- i. 1 fuel plate - 42.24 gm U^{235} , 1 layer boron tape
(0.0189 \pm .0004 gm B^{10} /tape) - 0.0189 gm B^{10}
- j. 1 fuel plate - 42.24 gm U^{235} , 1 layer boron tape
(0.0189 \pm .0004 gm B^{10} /tape) - 0.0189 gm B^{10}
- k. 4 0.0102 in steel plates - 0.0408 in.
- l. 1 fuel plate - 42.24 gm U^{235}
- m. 1 fuel plate 42.24 gm U^{235} , 1 layer boron tape
(0.0189 \pm .0004 gm B^{10} /tape) - 0.0189 gm B^{10}

n. 4 0.0102 in. steel plates - 0.0408 in.

o. 1 fuel plate 42.24 gm U²³⁵, 1 layer boron tape
(0.0189 \pm .0004 gm B¹⁰/tape) - 0.0189 gm B¹⁰

p. 1 fuel plate 42.24 gm U²³⁵, 1 layer boron tape
(0.0189 \pm .0004 gm B¹⁰/tape) - 0.0189 gm B¹⁰

A. 6.9. Reference Loading Numbers 53 - Final SM-2 Cold Clean Mockup

Total Loaded Masses - 36400.08 gm U²³⁵ - 60.9 gm B¹⁰

Open Seven Control Rod Array

Loaded Mass U²³⁵, Stationary Elements - 31669.20 gm

Loaded Mass U²³⁵, Control Elements - 4730.88 gm

Total Mass U²³⁵, in Active Core - 33205 \pm 20 gm

Loaded Mass B¹⁰, Stationary Elements - 53.0 gm

Loaded Mass B¹⁰, Control Elements - 7.94 gm

Total Mass B¹⁰ in Active Core - 55.6 gm

Loaded Mass Stainless Steel, Stationary Elements - 195700 \pm 1800 gm

Loaded Mass Stainless Steel, Control Elements - 40800 \pm 1000 gm

Total Mass Stainless Steel in Active Core - 216900 \pm 2000 gm

All Stationary Elements:

18 Fuel Plates - 833.40 gm U²³⁵/element

One fuel plate in each space (Figure A. 3)

Boron tape on North side of fuel plate

| Element | B ¹⁰ Loading(gm) | Element | B ¹⁰ Loading(gm) | Element | B ¹⁰ Loading(gm) |
|---------|-----------------------------|---------|-----------------------------|---------|-----------------------------|
| 12 | 1.398 | 23 | 1.374 | 35 | 1.353 |
| 13 | 1.391 | 25 | 1.332 | 37 | 1.416 |
| 14 | 1.401 | 26 | 1.368 | 41 | 1.375 |
| 15 | 1.371 | 27 | 1.400 | 42 | 1.359 |
| 16 | 1.410 | 31 | 1.407 | 43 | 1.359 |
| 21 | 1.339 | 33 | 1.381 | 45 | 1.321 |

| <u>Element</u> | <u>B¹⁰ Loading(gm)</u> | <u>Element</u> | <u>B¹⁰ Loading(gm)</u> | <u>Element</u> | <u>B¹⁰ Loading(gm)</u> |
|----------------|-----------------------------------|----------------|-----------------------------------|----------------|-----------------------------------|
| 22 | 1.345 | 34 | 1.371 | 46 | 1.384 |
| 47 | 1.434 | 62 | 1.417 | 74 | 1.469 |
| 51 | 1.389 | 63 | 1.399 | 75 | 1.431 |
| 53 | 1.397 | 65 | 1.374 | 76 | 1.469 |
| 54 | 1.354 | 66 | 1.405 | | |
| 55 | 1.373 | 67 | 1.469 | | |
| 57 | 1.385 | 72 | 1.469 | | |
| 61 | 1.414 | 73 | 1.534 | | |

All Control Elements:

16 Fuel Plates - 675.84 gm U²³⁵/element
 One fuel plate in each space (Figure A. 4)
 Boron tape on North side of fuel plate

| <u>Element</u> | <u>B¹⁰ Loading (gm)</u> |
|----------------|------------------------------------|
| A | 1.134 |
| B | 1.134 |
| C | 1.134 |
| D | 1.134 |
| E | 1.134 |
| F | 1.134 |
| G | 1.134 |

APPENDIX B

CHEMICAL ANALYSES OF CORE MATERIALS

THIS PAGE
WAS INTENTIONALLY
LEFT BLANK

Corner Reflector - Type 304 S. S.

| <u>Analysis</u> | <u>Wt. %</u> |
|-----------------|--------------|
| C | 0.06 |
| Mn | 1.28 |
| P | 0.034 |
| S | 0.017 |
| Si | 0.52 |
| Cr | 18.71 |
| Ni | 9.43 |
| Cu | 0.48 |
| Mo | 0.27 |
| Fe | Balance |

Side Reflector Plates - Type 304 S. S.

| <u>Analysis</u> | <u>Wt. %</u> |
|-----------------|--------------|
| C | 0.050 |
| Mn | 1.34 |
| P | 0.033 |
| S | 0.020 |
| Si | 0.57 |
| Cr | 19.00 |
| Ni | 9.62 |
| Fe | Balance |

Stationary Element End Box - Type 304 S. S.

| <u>Analysis</u> | <u>Wt. %</u> |
|-----------------|--------------|
| C | 0.050 |
| Mn | 1.70 |
| P | 0.031 |
| S | 0.016 |
| Si | 0.62 |
| Cr | 18.50 |
| Ni | 9.40 |
| Fe | Balance |

Stationary Element and Control Element 8 mil Side Plates - Type 302 S. S.

| <u>Analysis</u> | <u>Wt. %</u> |
|-----------------|--------------|
| C | 0.091 |
| Mn | 1.64 |
| P | 0.018 |
| S | 0.017 |
| Si | 0.56 |
| Cr | 17.54 |
| Ni | 8.50 |
| Cu | 0.21 |
| Mo | 0.17 |
| Fe | Balance |

Stationary Element and Control Element 15 mil Side Plates - Type 304 S. S.

| <u>Analysis</u> | <u>Wt. %</u> |
|-----------------|--------------|
| C | 0.059 |
| Mn | 1.14 |
| P | 0.026 |
| S | 0.015 |
| Si | 0.35 |
| Ni | 9.20 |
| Cr | 18.23 |
| Fe | Balance |

Stationary Element and Control Element 25 mil Side Plates - Type 304 S. S.

| <u>Analysis</u> | <u>Wt. %</u> |
|-----------------|--------------|
| C | 0.060 |
| Mn | 0.98 |
| P | 0.014 |
| S | 0.005 |
| Si | 0.48 |
| Ni | 9.25 |
| Cr | 18.35 |
| Fe | Balance |

Stationary Element 31 mil Side Plates - Type 304 S. S.

| <u>Analysis</u> | <u>Wt. %</u> |
|-----------------|--------------|
| C | 0.056 |
| Mn | 1.15 |
| P | 0.017 |
| S | 0.013 |
| Si | 0.29 |
| Ni | 9.53 |
| Cr | 19.80 |
| Fe | Balance |

Control Element 31 mil Side Plates - Type 304 S. S.

| <u>Analysis</u> | <u>Wt. %</u> |
|-----------------|--------------|
| C | 0.046 |
| Mn | 1.11 |
| P | 0.017 |
| S | 0.015 |
| Si | 0.71 |
| Ni | 8.72 |
| Cr | 18.72 |
| Fe | Balance |

Stationary Element and Control Element 25 mil Side Plate Channels -
Type 302 S. S.

| <u>Analysis</u> | <u>Wt. %</u> |
|-----------------|--------------|
| C | 0.092 |
| Mn | 1.23 |
| P | 0.026 |
| S | 0.013 |
| Si | 0.22 |
| Ni | 7.22 |
| Cr | 17.48 |
| Fe | Balance |

Fuel Plate Frame and Cover Plate - Type 304L S.S.

| <u>Analysis</u> | <u>Average Wt. %</u> |
|-----------------|----------------------|
| C | 0.024 |
| Mn | 1.23 |
| P | 0.023 |
| S | 0.019 |
| Si | 0.57 |
| Ni | 10.15 |
| Cr | 18.67 |
| Mo | 0.01 |
| Cu | 0.03 |
| Fe | Balance |

Absorber Frame and Cover Plate - Type 304L S.S.

| <u>Analysis</u> | <u>Average Wt. %</u> |
|-----------------|----------------------|
| C | 0.022 |
| Mn | 1.45 |
| P | 0.023 |
| S | 0.021 |
| Si | 0.60 |
| Ni | 9.77 |
| Cr | 18.77 |
| Fe | Balance |

Stationary Element and Control Element 10 mil Additional Clad -
Type 302 S.S.

| <u>Analysis</u> | <u>Wt. %</u> |
|-----------------|--------------|
| C | 0.10 |
| Mn | 0.64 |
| P | 0.026 |
| S | 0.011 |
| Si | 0.32 |
| Cr | 17.00 |
| Ni | 8.10 |
| Fe | Balance |

Stationary Element and Control Element 5 mil Additional Clad -
Type 302 S. S.

| <u>Analysis</u> | <u>Wt. %</u> |
|-----------------|--------------|
| C | 0.045 |
| Mn | 1.71 |
| P | 0.015 |
| S | 0.010 |
| Si | 0.53 |
| Cr | 17.78 |
| Ni | 0.12 |
| Cu | 0.13 |
| Fe | Balance |

Aluminum Strips - Type 1100 H14

| <u>Analysis</u> | <u>Wt. %</u> |
|-----------------|---------------------|
| Si | 1.00 |
| Cu | 0.20 |
| Mn | 0.05 |
| Zn | 0.10 |
| Others | 0.15 |
| Al | Balance (99.0 min.) |

Water Analysis

| | |
|--------------|--------------------|
| Total Solids | 250 ppm |
| PH | 7.8 |
| Chloride | 16.6 ppm |
| Iron | 1.1 ppm |
| Chromium | less than 0.06 ppm |
| Nickel | less than 0.1 ppm |

Boron Carbide - Chemical Analysis

| <u>Analysis Performed by</u> | <u>Total Boron - Wt. %</u> |
|------------------------------|----------------------------|
| New Brunswick Laboratory | 78.92 % |
| Lucius Pitkin, Inc. | 79.57 % |

NOTE: Standardized against natural boron in the form of reagent grade boric acid.

Boron-10 in Boron - Isotope Analysis by Mass Spectograph

| <u>Isotope</u> | <u>Atom %</u> |
|----------------------|---------------|
| B-10 | 20.0% + 0.2% |
| B-11 (by difference) | 80.0% |

NOTE: Analysis was performed on the New Brunswick sample.

APPENDIX C

PROBABLE ERROR ANALYSIS

THIS PAGE
WAS INTENTIONALLY
LEFT BLANK

C. 1 Theory of Errors

C. 1. 1 Introduction

There are four types of errors:

1. Constant or systematic errors (meter calibrations wrong; zero off; results influenced by some secondary phenomenon which has been neglected; etc.)
2. Personal Errors (setting cross hair to one particular side of center; actuating stop watch too soon; etc.). If the individual is consistent in these errors, they are merely a subdivision of the first type.
3. Mistakes (errors in reading a scale, i. e. 6.3 for 5.7; errors in recording data such as transposition, i. e. 165 for 156; etc.). If sufficient data have been taken, and the discrepancy of one observation with the mean is large enough to be certain, the observation can be legitimately rejected.
4. Accidental errors. These are errors due to the combined effect of a number of causes, each of which is just as likely to have a (+) effect as a (-) effect.

The first and second types are (in general) constant or systematic, the third type is erratic, the fourth statistical. The fourth is therefore the only type that can be treated mathematically.

A number of methods have appeared for the mathematical treatment of this fourth type of error. Of these, the only one which can be shown by experiment to conform with the actual behavior of nature is that of "least squares." Least squares obtains its name from the fact that it makes the sum of the squares of the "residuals," rather than the sum of the residuals, have the smallest possible value. A residual is the difference of any given observation from the value predicted by all the observations combined (i. e., the distance of a point from a curve; or the difference of a single observation from the average of all; etc.).

C. 1. 2 Probable Errors of Averages

There are two types of probable errors, namely external, R_e , and internal, R_i , that apply to the average, or mean, of several similar observations. The external p. e. (probable error) depends on the difference of each

of the similar observations from their mean. It is, in short, a measure of the consistency of the quantities entering into the mean value. If, however, each of the quantities which are averaged have known probable errors (which may be different for each quantity), then an internal p. e. of the mean can be computed which depends entirely on these individual probable errors (and is therefore independent of their consistency).

In expressing the p. e. of a mean, common practice is to be conservative and use the larger of the internal or external p. e. The ratio of the two probable errors R_e/R_i should be approximately unity. The deviation of this ratio to values above unity is a gauge of the presence of constant or systematic errors. To be specific: if n is five, a ratio of two is an indication, and a ratio of three almost certain evidence, of the presence of constant or systematic errors; while if n is 20, a ratio of 1.5 is an indication, and a ratio of two almost certain evidence of such errors.

Both the value of the mean and its p. e. are influenced by the relative weights, p , of the results entering into it. Obviously if one observation is considered twice as reliable as another, it should influence the result twice as much as the other. If the observations are all of equal reliability, we assign a weight of one to each. These observations are commonly referred to as "unweighted."

The residual, v , is simply the difference between an individual observation, x , and the mean, \bar{x} , of all the observations, i. e., $v = x - \bar{x}$.

The following cases are described:

1. The external p. e., R_e , of the weighted mean \bar{x} of n observations x_1, x_2, \dots, x_n having relative weights p_1, p_2, \dots, p_n .

The weighted mean is

$$\bar{x} = \frac{\sum (px)}{\sum p} \quad (1)$$

In Eq. (1) and in all the following equations, the summations run from one to n .

The external p. e. of the mean is

$$R_e = \pm 0.6745 \sqrt{\frac{\sum (pv^2)}{(n-1) \sum p}} \quad (2)$$

The result would then be expressed as

$$\bar{x} \pm R_e$$

The weights p used in these formulas may be assigned arbitrarily (from experimental conditions) or they may be from known probable errors as in Sec. 3, Eq. 5.

2. The external p. e., R_e , of the mean of n observations x_1, x_2, \dots, x_n having equal weights. Equations (1) and (2) become

$$\bar{x} = \frac{\sum x}{n}$$

$$R_e = \pm 0.6745 \sqrt{\frac{\sum (v^2)}{(n-1) \cdot n}} \quad (4)$$

3. The internal p. e., R_i , of the weighted mean \bar{x} of n observations x_1, x_2, \dots, x_n , the probable errors of which are r_1, r_2, \dots, r_n , and the weights of which are p_1, p_2, \dots, p_n . If the p. e. is known, the weight of a quantity is usually taken as proportional to the reciprocal of the square of its p. e., i. e.

$$P_j = \frac{c}{r_j^2}, \quad j = 1, 2, \dots, n \quad (5)$$

Here c is a purely arbitrary constant. It may be taken as unity, but is commonly chosen to make the arithmetical work as easy as possible. Its value does not affect the results.

The weighted mean is (same as Eq. (1))

$$\bar{x} = \frac{\sum (px)}{\sum p} \quad (6)$$

Its internal p. e. is

$$R_i = \pm \sqrt{\frac{c}{\sum p}} = \pm \sqrt{\frac{1}{\sum \left(\frac{1}{r^2}\right)}} \quad (7)$$

4. The internal p. e., R_i , of the mean \bar{x} of n observations x_1, x_2, \dots, x_n , the p. e. of which is the same, namely r .

Equations (6) and (7) became

$$\bar{x} = \frac{\sum x}{n} \quad (8)$$

$$R_i = \pm \frac{r}{\sqrt{n}} \quad (9)$$

It is to be emphasized that the probable errors r in both Sections 3 and 4 must be completely independent. In particular, they must not involve any error that is common to all of them.

C. 1. 3 Probable Errors of Functions

In general terms suppose

$$Z = f(z_1, z_2, z_3, \dots) \quad (10)$$

where z_1, z_2 , etc. are observed quantities with probable errors r_1, r_2 , etc. We desire to find the p. e. R of Z .

$$R = \pm \sqrt{\left(\frac{\partial Z}{\partial z_1}\right)^2 r_1^2 + \left(\frac{\partial Z}{\partial z_2}\right)^2 r_2^2 + \left(\frac{\partial Z}{\partial z_3}\right)^2 r_3^2 + \dots} \quad (11)$$

The results for several common functions are summarized in the accompanying table.

| Function | Probable Error R |
|-------------------------------|---|
| $Z = z_1 + z_2 + z_3 + \dots$ | $R = \pm \sqrt{r_1^2 + r_2^2 + r_3^2 + \dots}$ (12) |

| | |
|-----------|--------------------------------|
| $Z = z^n$ | $R = \pm Z n \frac{r}{z}$ (13) |
|-----------|--------------------------------|

| | |
|-------------------|--|
| $Z = z_1 z_2 z_3$ | $R = \pm Z \sqrt{\left(\frac{r_1}{z_1}\right)^2 + \left(\frac{r_2}{z_2}\right)^2 + \left(\frac{r_3}{z_3}\right)^2 + \dots}$ (14) |
|-------------------|--|

| | |
|-------------------------|--|
| $Z = z_1^a z_2^b z_3^c$ | $R = \pm Z \sqrt{\left(\frac{r_1}{z_1}\right)^2 a^2 + \left(\frac{r_2}{z_2}\right)^2 b^2 + \left(\frac{r_3}{z_3}\right)^2 c^2 + \dots}$ (15) |
|-------------------------|--|

| | |
|-----------|--------------------|
| $Z = a z$ | $R = \pm a r$ (16) |
|-----------|--------------------|

| | |
|----------------|----------------------------|
| $Z = \log_e z$ | $R = \pm \frac{r}{z}$ (17) |
|----------------|----------------------------|

| | |
|-------------------|-----------------------------------|
| $Z = \log_{10} z$ | $R = \pm 0.4343 \frac{r}{z}$ (18) |
|-------------------|-----------------------------------|

| | |
|----------------------------|---|
| $Z = a f(z_1, z_2, \dots)$ | $R = a \text{ times the p. e. of } f(z_1, z_2, \dots)$ (19) |
|----------------------------|---|

C. 1. 4 The Straight Line Function $y = a + b x$

Suppose a number of values of y have been observed for a range of x . A graphical statement of the problem is this: when the data are plotted on graph paper, what straight line gives the "best" possible fit and, when one is selected, what is the uncertainty in its slope and its intercept? A mathematical statement of the same problem is this: what are the "best" values of a and b indicated by the experimental data, and what are their respective uncertainties.

The graphical attack gives no definite answer to the problem, for no two people will agree as to the best line, and the uncertainties can only be guessed. The mathematical attack using least squares gives a unique answer and definite uncertainties.

The least squares formulas for a and b are respectively

$$a = \frac{(\sum py) (\sum p x^2) - (\sum px) (\sum pxy)}{D}, \quad (20)$$

$$b = \frac{(\sum p) (\sum pxy) - (\sum px) (\sum py)}{D}, \quad (21)$$

$$\text{where } D = (\sum p) (\sum p x^2) - (\sum px)^2, \quad (22)$$

and the weight of each observation of v is p . The value of p may vary for different y values because of changing experimental conditions; or it may be constant. These formulas require the calculation of six sums (made over n observations) of the experimental quantities x , y , and p .

The probable errors in a and b are respectively

$$r_a = r_e \sqrt{\frac{\sum (p x^2)}{D}} \quad (23)$$

$$r_b = r_e \sqrt{\frac{\sum p}{D}} \quad (24)$$

$$\text{where } r_e = 0.6745 \sqrt{\frac{\sum (p v^2)}{n-2}} \quad (25)$$

Here the residual v is the observed y minus the y calculated from

$$y = a + b x$$

If the p. e. in the y of Eq. (26) is desired at any particular value of x, say at $x = \epsilon$, then this is found from

$$r_{\epsilon} = r_e \sqrt{\frac{\sum [p(x-\epsilon)^2]}{D}} \quad (27)$$

C.1.5 Probable Errors of Counting Rate Determinations

The p. e. of a counting determination is

$$R = \pm 0.6745 \sqrt{n}$$

where n is the number of particles actually counted.

It is customary to describe the activity of a radioactive sample in rate terminology and thus if n particles were observed in t minutes, the counting rate, N, of the sample is

$$N = \frac{n}{t} \quad (29)$$

The p. e. in the determination of the counting rate would be

$$\begin{aligned} R &= \pm 0.6745 \frac{\sqrt{n}}{t} \\ &= \pm 0.6745 \frac{\sqrt{Nt}}{t} \\ R &= \pm 0.6745 \sqrt{\frac{N}{t}} \end{aligned} \quad (30)$$

The p. e. in the counting rate of an activated foil is a function of the observed counting rate (in counts per minute) with its p. e. minus the counting rate of the background (in counts per minute) with its p. e. Using equations (30) and (12), the p. e. in the counting rate of an activated foil is

$$R = \pm 0.6745 \sqrt{\frac{N_s}{t_s} + \frac{N_B}{t_B}} \quad (31)$$

where N_s is the counting rate of the foil including background, N_B is the counting rate due to background, t_s is the time during which the foil was counted, and t_B is the time during which background was counted.

C.2 Application of Error Analysis to Data

C. 2. 1 Notation - Core Composition and Bank Worth with Probable Errors

| | | |
|-------|--|-----|
| A | Number of stationary fuel plates | |
| B | Number of control fuel plates | |
| C | Mass of U^{235} per stationary fuel plate | gm |
| D | Mass of U^{235} per control fuel plate | gm |
| E | Loaded mass of U^{235} , stationary elements | gm |
| F | Loaded mass of U^{235} , control elements | gm |
| G | Average seven rod bank position | in. |
| G_1 | Probable error in G | in. |
| H | Control fuel plate meat length | in. |
| H_1 | Probable error in H | in. |
| J | Mass of U^{235} in active core, control rod bank | gm |
| J_1 | Probable error in J | gm |
| K | Total mass of U^{235} in active core | gm |
| K_1 | Probable error in K | gm |
| L | Number of stationary element side plates | |
| M | Stationary element side plate mass | gm |
| M_1 | Probable error in M | gm |
| N | Number of stationary element additional steel plates | |
| P | Mass per stationary element additional steel plate | gm |

| | | |
|-------|--|-----|
| P_1 | Probable error in P | gm |
| a | Steel mass in active core per stationary fuel plate | gm |
| a_1 | Probable error in a | gm |
| Q | Loaded mass of stainless steel, stationary elements | gm |
| Q_1 | Probable error in Q | gm |
| R | Number of control side plates | |
| S | Control element side plate mass | gm |
| S_1 | Probable error in S | gm |
| T | Number of control element additional steel plates | — |
| V | Mass per control element additional steel plate | gm |
| V_1 | Probable error in V | gm |
| b | Steel mass per control fuel plate | gm |
| b_1 | Probable error in b | gm |
| d | Number of control rods | |
| e | Control rod basket steel mass | gm |
| e_1 | Probable error in e | gm |
| W | Loaded mass of stainless steel, control elements | gm |
| W_1 | Probable error in W | gm |
| X | Active core length | in. |
| X_1 | Probable error in X | in. |
| Y | Mass of stainless steel in active core, control rod bank | gm |
| Y_1 | Probable error in Y | gm |

| | | |
|----------|---|-----------|
| Z | Total mass of stainless steel in active core | gm |
| Z_1 | Probable error in Z | gm |
| f | Strips of mylar tape per stationary fuel plate | |
| g | Strips of mylar tape per control fuel plate | |
| h | Mass of B^{10} per stationary tape | gm |
| h_1 | Probable error in h | gm |
| j | Mass of B^{10} per control tape | gm |
| j_1 | Probable error in j | gm |
| k | Loaded mass of B^{10} , stationary elements | gm |
| k_1 | Probable error in k | gm |
| ℓ | Loaded mass of B^{10} , control elements | gm |
| ℓ_1 | Probable error in ℓ | gm |
| m | Mass of B^{10} in active core, control rod bank | gm |
| m_1 | Probable error in m | gm |
| n | Total mass of B^{10} in active core | gm |
| n_1 | Probable error in n | gm |
| p | Reactivity in cents | cents |
| p_1 | Probable error in p | cents |
| q | Distance moved by seven rod bank | in. |
| q_1 | Probable error in q | in. |
| r | Seven rod bank worth | cents/in. |
| r_1 | Probable error in r | cents/in. |

C. 2. 2 Equations - Core Composition and Bank Worth with Probable Errors

1. Mass of U^{235} in Active Core, Control Rod Bank

$$J \pm J_1 = \frac{FG}{H} \pm \frac{FG}{H} \sqrt{\left(\frac{G_1}{G}\right)^2 + \left(\frac{H_1}{H}\right)^2}$$

2. Total Mass of U^{235} in Active Core

$$K \pm K_1 = (E \pm J) \pm J_1$$

3. Loaded Mass of Stainless Steel, Stationary Elements

$$Q \pm Q_1 = (Aa \pm LM \pm NP) \pm \sqrt{(Aa_1)^2 + (LM_1)^2 + (NP_1)^2}$$

4. Loaded Mass of Stainless Steel, Control Elements

$$W \pm W_1 = (Bb \pm RS \pm de \pm TV) \pm \sqrt{(Bb_1)^2 + (RS_1)^2 + (de_1)^2 + (TV_1)^2}$$

5. Mass of Stainless Steel in Active Core, Control Rod Bank

$$Y \pm Y_1 = \left[\frac{(Bb + RS)G}{x} \pm de \right] \pm \sqrt{(de_1)^2 + \left[\frac{(Bb + RS)G}{x} \sqrt{\left(\frac{G_1}{G}\right)^2 + \left(\frac{x_1}{x}\right)^2} \pm \left(\frac{\sqrt{(Bb_1)^2 + (RS_1)^2}}{Bb + RS} \right)^2 \right]^2}$$

6. Total Mass of Stainless Steel in Active Core

$$Z \pm Z_1 = (Q + Y) \pm \sqrt{(Q_1)^2 + (Y_1)^2}$$

7. Loaded Mass of B^{10} , Stationary Elements

$$k \pm k_1 = Afh \pm Afh_1$$

8. Loaded Mass of B^{10} , Control Elements

$$l \pm l_1 = Bg j \pm Bg j_1$$

9. Mass of B^{10} in Active Core, Control Rod Bank

$$m \pm m_1 = \frac{lG}{H} \pm \frac{lG}{H} \sqrt{\left(\frac{l_1}{l}\right)^2 + \left(\frac{G_1}{G}\right)^2 + \left(\frac{H_1}{H}\right)^2}$$

10. Total Mass of B^{10} in Active Core

$$n \pm n_1 = (k + m) \pm \sqrt{(k_1)^2 + (m_1)^2}$$

11. Seven Rod Bank Worth in cents/inch

$$r \pm r_1 = \frac{p}{q} \pm \frac{p}{q} \sqrt{\left(\frac{p_1}{p}\right)^2 + \left(\frac{q_1}{q}\right)^2}$$

Bar

2

+

C. 2. 3 Notation-Relative Neutron Flux with Probable Errors

| | |
|--------|--|
| S_1 | CPM of Standard in System I (Scintillation counter 1) |
| S_2 | CPM of Standard in System II (Scintillation counter 2) |
| B_1 | CPM of Background in System I |
| B_2 | CPM of Background in System II |
| F_1 | CPM of Foil in System I |
| F_2 | CPM of Foil in System II |
| A | Corrected Counts of Standard in System I |
| A_1 | Probable Error in A |
| A' | Corrected Counts of Standard in System II |
| A'_1 | Probable Error in A' |
| C | Corrected Counts of Foil in System I |
| C_1 | Probable Error in C |
| C' | Corrected Counts of Foil in System II |
| C'_1 | Probable Error in C' |
| R | Ratio of Counts of Foil in System I to Standard in System II |
| R_1 | Probable Error in R |
| R' | Ratio of Counts of Foil in System II to Standard in System I |
| R'_1 | Probable Error in R' |
| M | Product of Two Ratios (above) |
| M_1 | Probable Error in M |
| P | Square Root of Product of Two Ratios |
| P_1 | Probable Error in P |
| t_F | Foil Counting Time |
| t_B | Background Counting Time |

C. 2. 4 Equations-Relative Neutron Flux with Probable Errors

1. Corrected Counts of Standard in System I

$$A \pm A_1 = (S_1 - B_1) \pm 0.6745 \sqrt{\frac{S_1}{t_F} + \frac{B_1}{t_B}}$$

2. Corrected Counts of Standard in System II

$$A' \pm A'_1 = (S_2 - B_2) \pm 0.6745 \sqrt{\frac{S_2}{t_F} + \frac{B_2}{t_B}}$$

3. Corrected Counts of Foil in System I

$$C \pm C_1 = (F_1 - B_1) \pm 0.6745 \sqrt{\frac{F_1}{t_F} + \frac{B_1}{t_B}}$$

4. Corrected Counts of Foil in System II

$$C' \pm C'_1 = (F_2 - B_2) \pm 0.6745 \sqrt{\frac{F_2}{t_F} + \frac{B_2}{t_B}}$$

5. Ratio of Counts of Foil in System I to Standard in System II

$$R \pm R_1 = \frac{C}{A'} \pm \frac{C}{A'} \sqrt{\left(\frac{A'_1}{A'}\right)^2 + \left(\frac{C_1}{C}\right)^2}$$

6. Ratio of Counts of Foil in System II to Standard in System I

$$R' \pm R'_1 = \frac{C'}{A} \pm \frac{C'}{A} \sqrt{\left(\frac{A_1}{A}\right)^2 + \left(\frac{C'_1}{C'}\right)^2}$$

7. Product of the Two Ratios

$$M \pm M_1 = RR' \pm RR' \sqrt{\left(\frac{R_1}{R}\right)^2 + \left(\frac{R'_1}{R'}\right)^2}$$

8. Square Root of Product of Two Ratios

$$P \pm P_1 = \sqrt{M} \pm \frac{1}{2} \left(\frac{M_1}{M}\right) \sqrt{M}$$

APPENDIX D

**EFFECT OF DELAYED NEUTRON UNCERTAINTIES ON
REACTIVITY REPORTED IN DOLLARS AND CENTS**

THIS PAGE
WAS INTENTIONALLY
LEFT BLANK

D.1 Introduction

The availability of delayed neutron yield and half-life data with probable errors (ANL-5800, "Reactor Physics Constants") has prompted a re-evaluation of reactivity determined by the inhour equation. This re-evaluation is presented here, with a probable error analysis for the conversion of reactor periods to reactivity in cents.

It is shown in this analysis that previous reactivity values reported in cents, using early delayed neutron data (Glasstone and Edlund, "The Elements of Nuclear Reactor Theory," 1952) are affected only slightly by this re-evaluation.

All reactivity data described in this report were calculated by the inhour equation plotted in cents as a function of reactor period for a β of 0.0064.

D.2 Procedure

The following inhour equation was used to calculate reactivity:

$$\rho = \frac{l}{T K_{\text{eff}}} + \sum_{i=1}^n \frac{\beta_i}{1 + \lambda_i T} \quad (1)$$

where:

- l = neutron lifetime (about 5×10^{-5} sec)
- T = period in seconds
- K_{eff} = effective multiplication factor (assumed to be unity)
- β_i = delayed neutron fraction of i^{th} group
- $\beta_i = a_i \beta$
- β = total delayed neutron fraction
- a_i = relative abundance of the i^{th} group
- λ_i = delay constant of the i^{th} group

The above equation, although the one customarily used, is not completely exact. The exact equation is

$$\rho = \frac{l}{T K_{\text{eff}}} + \sum_{i=1}^n \frac{\gamma_i \beta_i}{1 + \lambda_i T} \quad (2)$$

where

γ_i = effectiveness of i^{th} group delayed neutrons compared with prompt neutrons.

However, it is always assumed because of lack of data the $\gamma_j = \gamma_i$

and hence $\gamma_i = \frac{\beta_{\text{eff}}}{\beta}$ Where β_{eff} equals the effective total delayed neutron fraction.

Assuming $\gamma_i = \frac{\beta_{\text{eff}}}{\beta}$ equation (2)

reduced to:

$$\rho = \frac{\lambda}{T K_{\text{eff}}} + \beta_{\text{eff}} \sum_{i=1}^n \frac{a_i}{1 + \lambda_i T} \quad (3)$$

Because β_{eff} is not usually experimentally determined, experimental facilities usually report reactivity changes in cents. Therefore in order to get an equation of cents as a function of the reactor period, by definition, equation (3) is divided by β_{eff} . The result is:

$$\frac{\rho}{\beta_{\text{eff}}} = \frac{\lambda}{T K_{\text{eff}} \beta_{\text{eff}}} + \sum_{i=1}^n \frac{a_i}{1 + \lambda_i T} \quad (4)$$

Equation (4) gives the reactivity in dollars as a function of the reactor period. By definition one dollar = 100 cents. It will be noticed that essentially the same result could have been obtained by dividing equation (1) by β . The following probable error analysis will show that the value of β or β_{eff} does not affect the reactivity value in cents corresponding to a given period unless the period is very short (< 2 sec) and short reactor periods are generally avoided:

D.3 Probable Errors:

In general terms, if

$$Z = f(z_1, z_2, z_3, \dots)$$

Then the probable error associated with Z is

$$R = \pm \sqrt{\left(\frac{\partial Z}{\partial z_1}\right)^2 \gamma_1^2 + \left(\frac{\partial Z}{\partial z_2}\right)^2 \gamma_2^2 + \dots}$$

where Z_1, Z_2, Z_3 , etc. are observed quantities with probable errors δ_1, δ_2 , etc. Hence it follows that the probable error of ρ/β_{eff} is

$$\text{P. E. } \left(\frac{\rho}{\beta_{\text{eff}}} \right) = \sqrt{\left(\frac{d\ell}{\beta_{\text{eff}} T K_{\text{eff}}} \right)^2 + \left(\frac{\ell d\beta_{\text{eff}}}{T \beta_{\text{eff}}^2 K_{\text{eff}}} \right)^2 + \sum_{i=1}^n \left(\frac{da_i}{1 + \lambda_i T} \right)^2 + \sum_{i=1}^n \left(\frac{a_i T d\lambda_i}{(1 + \lambda_i T)^2} \right)^2}$$

Table D.1 gives the values used in the calculations. They were taken from ANL-5800 except for the values of ℓ and $d\ell$. β was used instead of β_{eff} .

TABLE D.1

| | |
|----------------------------|---------------------------|
| $d\ell = 2 \times 10^{-5}$ | $\ell = 2 \times 10^{-5}$ |
| $d\beta = 0.0003$ | $\beta = .0064$ |
| $da_1 = .003$ | $a_1 = .033$ |
| $da_2 = .009$ | $a_2 = .219$ |
| $da_3 = .022$ | $a_3 = .916$ |
| $da_4 = .011$ | $a_4 = .395$ |
| $da_5 = .009$ | $a_5 = .115$ |
| $da_6 = .008$ | $a_6 = .042$ |
| $d\lambda_1 = .0003$ | $\lambda_1 = .0124$ |
| $d\lambda_2 = .0010$ | $\lambda_2 = .0305$ |
| $d\lambda_3 = .004$ | $\lambda_3 = .111$ |
| $d\lambda_4 = .012$ | $\lambda_4 = .301$ |
| $d\lambda_5 = 0.15$ | $\lambda_5 = 1.13$ |
| $d\lambda_6 = 0.33$ | $\lambda_6 = 3.00$ |

Table D.2 gives a breakdown of the probable error in the reactivity in cents using a 20 second period.

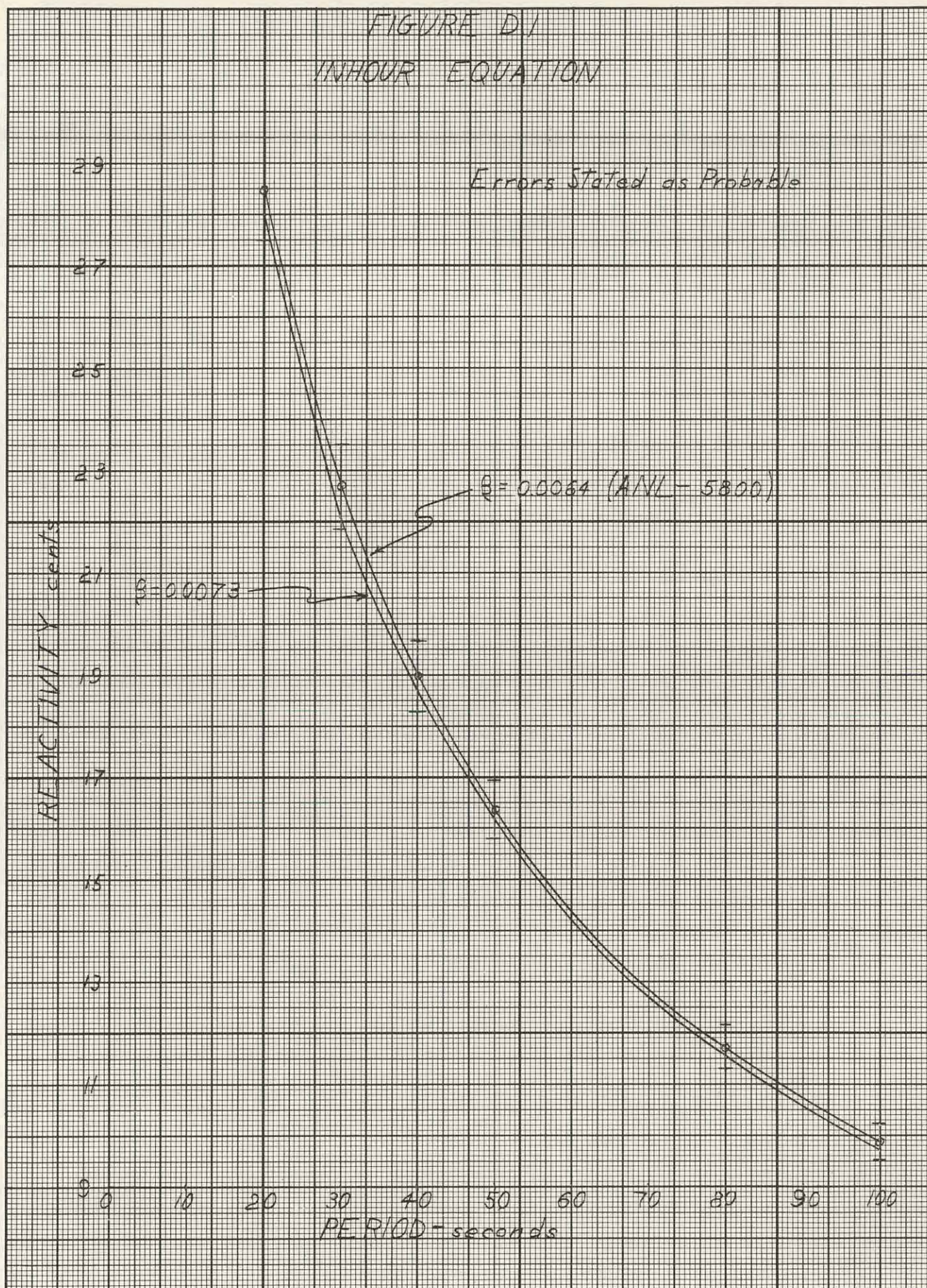
TABLE D.2

Probable error breakdown for 20 second period

$$\left(\frac{d\ell}{\beta T K_{\text{eff}}} \right)^2 = 2.44 \times 10^{-8}; \quad \left(\frac{\ell d\beta}{T \beta^2 K_{\text{eff}}} \right)^2 = 5.38 \times 10^{-11}$$

THIS PAGE
WAS INTENTIONALLY
LEFT BLANK

FIGURE D.1
INHOUR EQUATION



THIS PAGE
WAS INTENTIONALLY
LEFT BLANK

$$\sum_{i=1}^4 \left(\frac{da_i}{1 + \lambda_i T} \right)^2 = 8.618 \times 10^{-5}; \quad \sum_{i=5}^6 \left(\frac{da_i}{1 + \lambda_i T} \right)^2 = 1.627 \times 10^{-7}$$

$$\sum_{i=1}^6 \left(\frac{a_i T d\lambda_i}{(1 + \lambda_i T)^2} \right)^2 = 9.249 \times 10^{-6}; \quad \text{P. E. } \left(\frac{\rho}{\beta} \right)^2 = 9.5616 \times 10^{-5}$$

An inspection of Table D-2 shows that the effect of the uncertainties in λ and β or β_{eff} is negligible in calculating the probable error of the reactivity in cents for a 20 second period. For longer periods the probable errors in λ and β would be even less important. The uncertainties in the abundances of the first 4 delayed neutron groups account for most of the probable error.

Figure D. 1 is a curve of reactivity in cents versus period in seconds.

D. 4 Discussion of Results:

An inspection of Figure D. 1 shows that the previous reactivity versus period curve used does not differ appreciably from the one calculated with the new data. Also the probable error analysis shows that even though β_{eff} probably does differ from 0.0064 it is not important when reporting reactivity data in cents.